INTERNATIONAL GEOSYNTHETICS SOCIETY

SIMSG ISSMGE

Proceedings of the
Technical Workshop on Soil Reinforcement

7-9 July 2026
Reggio Calabria, Italy

Organized by:

Technical Committee on Soil Reinforcement (TC-R)
International Geosynthetics Society (IGS)

Technical Committee on Reinforced Fill Structures (TC-218)
Int. Society for Soil Mechanics and Geotechnical Engineering (ISSMGE)

SIMSG ISSMGE

igs Reinforcement

Venue and co-organized by:

"Mediterranea" University of Reggio Calabria
Department of Civil, Energy, Environmental and Material Engineering (DICEAM)
via Zehender 1, Località Feo di Vito, 89122 Reggio Calabria, Italy

Sponsored by:

Edited by Ivan P. Damians and Aníbal Moncada,
Internacional Geosynthetics Society (IGS) - 2026.

Table of contents

MECHANICAL AND DYNAMIC BEHAVIOUR OF FIBER–REINFORCED SOILS AT VERY SMALL STRAINS

Ioannis N. Markou, Konstantinos E. Bantralexis and Evangelos D. Evangelou

Department of Civil Engineering, Democritus University of Thrace,
University Campus Kimmeria, GR-67150 Xanthi, Greece
E-mail: imarkou@civil.duth.gr

Keywords: Fiber-reinforced soil, Mechanical behaviour, Triaxial compression test, Dynamic properties, Wave propagation, Bender element test

Abstract. *Improvement of the engineering properties of soils by reinforcing them with fibers, at an appropriate percentage of the weight of dry soil, is frequently selected to ensure the safe construction and operation of many structures. Toward this end, the mechanical behaviour and the dynamic properties of fiber-reinforced soils at very small strains are investigated experimentally in this research effort by conducting Unconsolidated Undrained triaxial compression and Bender Element tests under different confining pressures. Five soils ranging from "excellent" to "poor" materials for use in earthwork structures were tested in combination with five types of polypropylene fibers having lengths ranging from 9 to 50 mm. The tests were conducted on specimens at their "as-compacted" water content, with fiber contents ranging from 0.5 to 2% by weight of dry soil. Fiber reinforcement reduces the stiffness and increases the deformability of the soil. A Mohr–Coulomb type linear failure criterion satisfactorily describes the shear strength behaviour of fiber-reinforced soils in total stress terms. The cohesion values of the fiber-reinforced soils range between 61 kPa and 301 kPa and increase up to seven times in comparison with the cohesion values of the unreinforced soils. The variations of the angle of internal friction of soils due to fiber reinforcement are generally limited to ±25%. The results also indicate that the dynamic and the small strain stiffness parameters of fiber-reinforced soils increase with increasing confining pressure, while also being affected by the soil type and the fiber type and content. Although fiber inclusion resulted generally in reduction of the dynamic properties of soils, increases ranging from 5% to 55% were observed in certain soil – fiber combinations in comparison with the unreinforced soils.*

1 INTRODUCTION

Soil reinforcement with geogrids, geotextiles, metal strips, fibers, etc., is an efficient and trustworthy technique for improving the mechanical behaviour of soil in several applications, including retaining structures, embankments, foundations, slopes and pavements. However, as fiber inclusions bring several technical, economic and environmental benefits, a great deal of interest has recently emerged worldwide regarding the potential applications of fibers within the soils and other similar materials, such as coal ashes and mine tailings. Although natural fibers, mainly from different plants, are used in countries where they are in abundance, synthetic polymer fibers are preferred because they are standardized industrial products exhibiting better mechanical behaviour and durability than natural fibers. The fiber-reinforced soils in applications such as embankments and pavements are usually unsaturated both at the construction and operation stages. It is therefore practical for the design of these structures to investigate the mechanical behaviour of fiber-reinforced soils by conducting unconsolidated undrained (UU) triaxial compression tests on specimens at their "as-compacted" water content and to analyze the obtained results in terms of total stresses. Although the documentation of the effectiveness of fibers for soil reinforcement has been the objective of several research efforts based on UU triaxial compression testing, the effects of soil and fiber type on the mechanical behaviour of fiber-reinforced soils have not been methodically examined in the past under these conditions, and the effects of fiber length and content on the shear strength parameters of fiber-reinforced soils need further experimental documentation.

The study of the behaviour of fiber-reinforced soils under dynamic or seismic loading conditions is also a field of major importance to research. The Bender Elements method is a non-destructive laboratory practice based on the emission and detection of shear waves (S-waves) and primary waves (P-waves) with piezoceramic elements placed at the edges of the soil specimen. By utilizing this method, it is possible to measure the wave propagation velocities (V_s and V_p) within the soil specimen and, as a result, to calculate the initial shear modulus (G_0) and the initial Young's modulus (E_0) of the soil at very small strains. However, the investigation of the response of fiber-reinforced soils in Bender Element tests is extremely limited. Taking into consideration this noticeable lack of sufficient experimental evidence, the present study aims at a better understanding of the mechanical and dynamic behaviour of fiber-reinforced soils at very small strains by conducting UU triaxial compression and Bender Element tests in various soil specimens containing polypropylene fibers of different types.

2 MATERIALS AND PROCEDURES

The five soils tested in this study include a poorly graded sand (SP) with negligible fine-grained fraction and four composite soils (CS1-CS4) produced by mixing this sand with a lean clay (CL), by weight, using the proportions shown in Table 1. Characteristic grain sizes, the values of Atterberg limits (liquid limit, LL, and plastic limit, PL) and the classification of all soils are also shown in Table 1. The tested soils cover a wide variety of specimens that can be used in earthwork structures with SP, CS1 and CS2 characterized as "excellent to good" soils and CS3 and CS4 characterized as "fair to poor" soils for that purpose. The specimens in this study were prepared by compacting the soils, either in dry condition (SP soil) or with the optimum water content (CS1-CS4 soils), to obtain the maximum dry unit weight determined by the compaction test conducted in accordance with the ASTM Standard D 698.

Table 1: Characteristics and classification of soils

Soil Designation	Mixing Proportions SP – CL (%)	Characteristic Grain Sizes			Atterberg Limits LL – PL	Soil Classification USCS (AASHTO)
		D_{90} (mm)	D_{50} (mm)	D_{10} (mm)		
SP	100 – 0	2.620	0.892	0.303	-----	SP (A-1-b)
CL	0 – 100	0.039	0.004	< 0.0014	46 – 21	CL (A-7-6)
CS1	85 – 15	2.308	0.699	0.007	26 – 17	SC (A-2-4)
CS2	70 – 30	1.961	0.513	0.0014	29 – 17	SC (A-2-6)
CS3	50 – 50	1.666	0.131	< 0.0014	37 – 19	SC (A-6)
CS4	25 – 75	1.057	0.010	< 0.0014	45 – 20	CL (A-7-6)

The soils were reinforced with polypropylene fibers of five different types having densities equal to 905 kg/m^3 and melting points at 165^{o}C. More specifically, monofilament fibers of circular cross-section, two tapes of different width and hollow and fibrillated fibers, with dimensions and relevant properties presented in Table 2, were used for soil reinforcement. These fibers are designated as M, T1, T2, H and F, respectively. Four different fiber lengths (9 mm, 18 mm, 30 mm and 50 mm) were used in the experimental measurements and their concentrations in the soil-fiber mixtures ranged from 0.5% to 2.0% by weight of dry soil, to investigate the effect of fiber length and content on the mechanical and dynamic behaviour of fiber-reinforced soils.

Table 2: Fiber characteristics

Fiber Type	Designation	Diameter/ Thickness (μm)	Width (mm)	Length (mm)	Tensile Stress at Failure (N/mm^2)	Elongation at Failure (%)
Monofilament	M	35	-----	9, 18, 30, 50	570	20.2
Tape 1	T1	43	1.13	9, 18, 30, 50	541	23.3
Tape 2	T2	38	2.78	18	556	27.0
Hollow	H	45	-----	18	513	54.2
Fibrillated	F	42	2.78	30	416	12.1

The cylindrical specimens prepared for testing, had a diameter of 50 mm and a height of 110 mm. The UU triaxial compression tests were performed in accordance with the ASTM Standard D 2850-15, and the specimens were tested under confining pressures of 50, 100, 200 and 400 kPa, at an axial strain rate equal to 0.715 mm/min (0.65%/min). The tests were completed when either the maximum deviator stress was obtained or the axial strain reached the limit of 15%, as set by the ASTM Standard D 2850-15. The Bender Elements tests were conducted at confining pressures (σ_3) equal to 0 kPa, 50 kPa, 100 kPa, 200 kPa, and 400 kPa in accordance with the provisions of the ASTM D8295-19 standard.

3 MECHANICAL BEHAVIOUR

The results obtained from the UU triaxial compression tests are presented and discussed in detail by Evangelou et al. (2023). The main findings of this investigation are summarized in this section. The stress–strain curves of soils reinforced with low contents of fibers of small length (9 mm) more often exhibit a strain-softening behavior. As the fiber length and content increase, the stress–strain behavior of fiber-reinforced soils becomes strain-hardening. The deformability parameters of fiber-reinforced soils exhibit a wide range of values and are not consistently affected by the factors examined in the present study. The failure deformation values range from 3.52% to 15.00% and the values of the initial and the secant modulus of elasticity range from 6.2 MPa to 89.0 MPa and from 6.1 MPa to 86.7 MPa, respectively. Fiber reinforcement reduces the stiffness and increases the deformability of the soil. The fiber-reinforced soil exhibits a more ductile behavior in comparison with the unreinforced soil. The stiffness of the fiber-reinforced soil is generally superior in the initial part of the stress–strain curve but, in several cases, it remains invariable up to the point where the deviator stress is equal to 50% of its maximum value.

A Mohr–Coulomb type linear failure criterion satisfactorily describes the shear strength behavior of fiber-reinforced soils, in total stress terms, as obtained through UU triaxial compression tests. The cohesion values of the fiber-reinforced soils obtained in the present study range between 61 kPa and 301 kPa and the values of their angle of internal friction range between 10° and 46.5°. The angle of internal friction of fiber-reinforced soils is not significantly affected by the factors examined in the present study. Although increases in the angle of internal friction reaching 40% were observed in some cases, the variations of the angle of internal friction of soils due to fiber reinforcement are generally limited to ±25%. Fiber reinforcement contributes to the shear strength improvement in soils by adding cohesion ranging between 84 kPa and 124 kPa to the clean sand and by increasing the cohesion of cohesive soils up to seven times. The cohesion improvement due to fiber reinforcement is increased with increasing fiber content and fiber length up to 30 mm, is increased when monofilament (M) and tape 1 (T1) fibers are used and is inversely proportional to the fine-grained fraction and the cohesion of the unreinforced soil.

4 DYNAMIC BEHAVIOUR AT VERY SMALL STRAINS

The results obtained from the Bender Element tests are presented and discussed in detail by Bantralexis et al. (2026). The main findings of this investigation are summarized in this section. The increase of confining pressure is accompanied by a clear and systematic, significant increase in the propagation velocities of shear (V_s) and primary waves (V_p) indicating better activation of stress transfer mechanisms through fiber-reinforced soils. For the cohesive soils tested in this investigation, this tendency is generally accompanied by an improvement of V_s and V_p velocities of fiber-reinforced soil compared to those of unreinforced soil. The values of dynamic and small strain stiffness parameters obtained by applying the first arrival method are generally greater than those obtained with the peak-to-peak method for the cohesive soils (sand – clay mixtures). On the contrary, the values of dynamic and small strain stiffness parameters obtained by applying both methods to the clean sand (SP soil) are comparable.

The effect of fiber length on the dynamic properties of monofilament fiber-reinforced soils depends on soil type. For CS2 soil (70% sand – 30% clay), longer fiber lengths (30 mm and 50 mm) contributed to an increase in dynamic parameters ranging from 7% to 55% compared to those of the unreinforced soil, indicating a favorable interaction between long fiber lengths and this specific soil structure. The dynamic parameters of monofilament fiber-reinforced soils decrease with increasing fiber content. This behavior can possibly be attributed to the reduction of compaction effectiveness due to the increased quantity of fibers in the composite material. Reinforced CS2 soil with fiber contents up to 1.5% exhibits generally larger values of dynamic and small strain stiffness parameters (range: 5% - 32%) than the unreinforced soil. The types of soil and fiber significantly affect the dynamic and small strain stiffness parameters of fiber-reinforced soils at very small strains and result in specific soil – fiber combinations presenting optimum performance. The best overall performance is achieved by the CS2 soil reinforced with monofilament fiber exhibiting generally maximum values of dynamic and small strain stiffness parameters in comparison with all the other soil – fiber combinations and, in many cases, greater values of dynamic and small strain stiffness parameters than those of the unreinforced soil. Also, the CS4 soil (25% sand – 75% clay) reinforced with all fiber types presents an increase of V_s and G_0 values ranging from 4% to 54% in comparison with those of the unreinforced soil.

REFERENCES

Bantralexis, K.E., Boura, E.S., Markou, I.N., and Evangelou, E.D.; 2026. Dynamic parameters of fiber-reinforced soils at very small strains. Fibers 14(7): 77. https://doi.org/10.3390/fib14070077

Evangelou, E.D., Markou, I.N., Verykaki, S.E., and Bantralexis, K.E.; 2023. Mechanical behavior of fiber-reinforced soils under undrained triaxial loading conditions. Geotechnics 3(3): 874-893. https://doi.org/10.3390/geotechnics3030047

MODAL ANALYSES METHODS FOR THE SEISMIC RESPONSE OF REINFORCED SOIL WALLS

Pietro Rimoldi

Civil Engineering Consultant
Via Perini 18, 20157 Milano, Italy
E-mail: pietro.rimoldi@gmail.com

Key words: Reinforced soil walls, Seismic response, Modal analysis

Abstract. *The paper presents an overview of the modal analysis methods, that is advanced mathematical models aimed to simulate the dynamic response of geogrid reinforced soil walls to any seismic ground motion. These methods use both time and frequency domain models to analyse the unreinforced and reinforced soil walls response to a given time history of the horizontal seismic motion applied at the bedrock; through a mathematical procedure it is possible to evaluate the spectra of acceleration, velocity and displacement along the height of the reinforced soil structure, the inertia and dynamic forces.*

1 MODAL ANALYSES METHOD

Carotti and Rimoldi introduced advanced mathematical models in the late 1990s, aimed to simulate the dynamic response of geogrid reinforced soil walls to any seismic ground motion.

In the mathematical method (Carotti and Rimoldi, 1997 and 1998), the soil structure is modelled as a stack of layers with a lumped mass scheme (Fig. 1). The interactions between two adjacent masses is described in terms of two interlayer force fields (Fig. 1): a conservative elastic field, which models the increase of the inherent stiffness of the wall, including the interlayer stiffness due to geogrid layers; and a viscous type field, which models the increase of the inherent damping of a wall, including the interlayer viscous damping and the interlayer Coulomb-type damping (friction) due to the geogrid layers. The unreinforced and reinforced soil wall responses to a given time history of the horizontal seismic motion applied at the bedrock are analysed using both time and frequency domain models.

This multi degree-of-freedom (multi-DOF) Newtonian discrete model yields the linear seismic dynamics of an unreinforced soil wall and the non-linear seismic dynamics of geogrid reinforced soil walls.

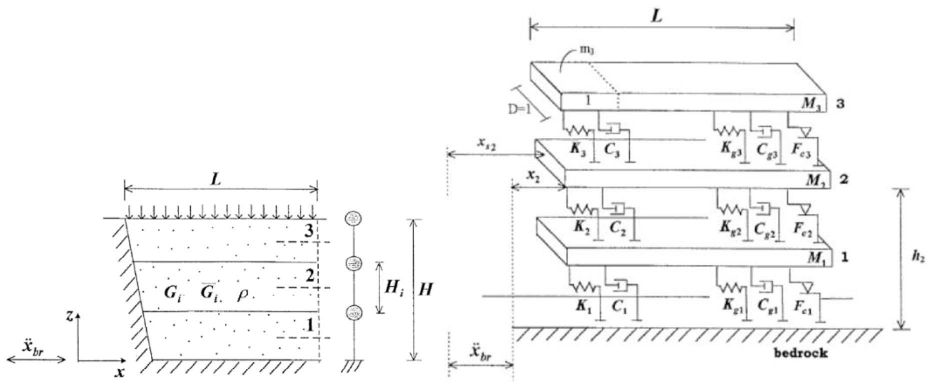

Fig. 1. The mathematical model [Carotti and Rimoldi, 1997 and 1998): scheme of the soil structure as a stack of layers and the lumped mass model for a 3 DOF system, showing all the interaction parameters

It is possible to perform a modal analysis of the dynamic wall response, with reference to the shear modal shapes shown in Fig. 2 left.

Assuming that the Kelvin-Voigt constitutive model is valid, there are two interlayer forces between two soil masses: conservative, elastic forces; and viscous-type, dissipative forces; for a mass of height H_i and a unit cross section ($D = L = 1$), the mass per unit area m_i, the interlayer stiffness k_i, and the interlayer viscous damping c_i (Fig. 2 center) are expressed as:

$$m_i = \frac{1}{2}\left(\varrho_{i+1} H_{i+1} + \varrho_i H_i\right) \qquad k_i = \frac{\tau}{\epsilon H_i} = \frac{G}{H_i} \qquad c_i = \frac{\tau}{\dot{\epsilon} H_i} = \frac{\overline{G}}{H_i} \tag{1}$$

where ρ is the soil density, G is the elastic shear modulus of the soil and $\overline{G}$ the coefficient of viscous shear damping (proportional to the shear strain velocity).

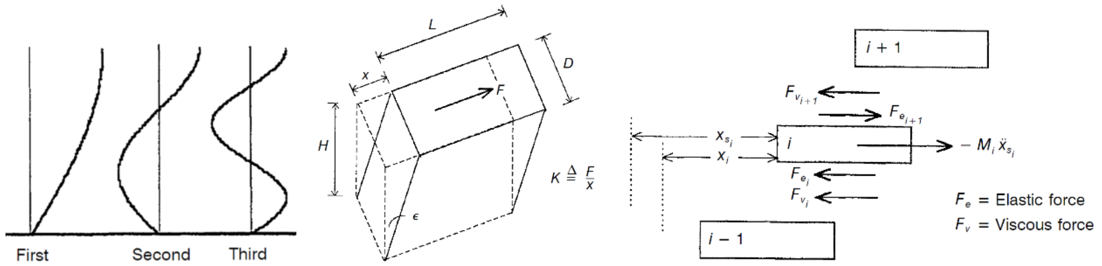

Fig. 2. Left: Three shear modal shapes used in the modal analysis of the dynamic wall response; center: schematic of the model for the evaluation of the interlayer stiffness and viscous damping; right: schematic of the model forces acting on a soil layer during second modal vibration.

Setting M_i, K_i, and C_i equal to m_i, c_i, and k_i, but referring to a soil element of generic length L and unit width ($D = 1$), in the case of a generic number of soil layers, n, the Newtonian equation of motion for the i^{th} layer is:

$$M_i \ddot{x}_i - K_i x_{i-1} + (K_i + K_{i+1}) x_i - K_{i+1} x_{i+1} - C_i \dot{x}_{i-1} + (C_i + C_{i+1}) \dot{x}_i - C_{i+1} \dot{x}_{i+1} = -M_i \ddot{x}_{br} \tag{2}$$

The first and second parameters in Eq. 1 represent the elastic and viscous boundary forces from the lower soil layer, respectively, while the third and fourth parameters represent the same boundary forces from the upper layer; the absolute acceleration of the ith layer, x_{si}, is broken down into the components of acceleration relative to the bedrock, x_i, and the bedrock acceleration, x_{br}.

If L_g is the geogrid length in the direction of the seismic acceleration, F is the tensile force applied to the geogrid, and Δl the geogrid elongation, it is postulated that, for the condition of geogrid-soil interlock the interlayer stiffness is expressed in Eq. 3 left.

The interlayer viscous damping force increases by the inherent viscous damping of the geogrid; from sinusoidal cyclic tensile tests and from the examination of an average elliptical cycle, the average viscous force, F_{visc} (the velocity counterphase force when there is no displacement), can be obtained, together with the value of the peak velocity (product of the peak displacement obtained from the test plot, and angular frequency, $\omega = 2\pi f$, of the test); from the force-velocity ratio, the coefficient of damping is obtained as in Eq. 3 right, where ω is the angular frequency of the motion and Δl is the differential interlayer displacement, ($x_i - x_{i-1}$), when perfect geogrid-soil interlock is assumed:

$$K_{g_i} = \frac{F}{\Delta l} = \frac{F}{\epsilon_{gI} L_g} \qquad C_{g_i} = \frac{F_{visc}}{\Delta l\, \omega} = \frac{F_{visc}}{\epsilon_g L_g\, \omega} \tag{3}$$

The Newtonian equation of motion for the multi-DOF nonlinear model with N soil layers and N geogrid layers (Fig. 1) can be obtained from Eqs. 1, 2 and 3, taking into account the elastic stiffness, K_{gi}, the viscous damping, C_{gi}, and the Coulomb-type friction force, F_{ci}, induced by the geogrid layers. As a result, the system of forces acting on a soil layer is obtained for each modal shape, as shown in Fig. 2 right.

The interlayer damping increases due to the geogrid-soil Coulomb friction F_{ci} under the weight of the soil above; if φ_{sg} is the soil-geogrid interface friction angle, it is:

$$F_{c_i} = -tg\,\phi_{sg}\,g \sum_{k=i}^{n} M_k \,\mathrm{sign}(\dot{x}_k) \tag{4}$$

where the direction of the opposing frictional force is determined by the sign of $(\dot{x}_k)$.

If $\hat{M}$ is the equivalent mass of the distributed load on top of the wall, then, in the case of a generic number of soil layers, n, the Newtonian equation of motion for the i^{th} layer is:

$$\begin{aligned} M_i \ddot{x}_i &- K_i(x_{i-1} - x_i) - C_i(\dot{x}_{i-1} - \dot{x}_i) + K_{i+1}(x_i - x_{i+1}) + C_{i+1}(\dot{x}_i - \dot{x}_{i+1}) \\ &- K_{g_i}(x_{i-1} - x_i) - C_{g_i}(\dot{x}_{i-1} - \dot{x}_i) + K_{g_{i+1}}(x_i - x_{i+1}) + C_{g_{i+1}}(\dot{x}_i - \dot{x}_{i+1}) \\ &+ tg\,\phi_{sg}\,g\left(\sum_{j=i}^{n} M_j + \hat{M}\right)\mathrm{sign}(\dot{x}_i) - tg\,\phi_{sg}\,g\left(\sum_{j=i+1}^{n} M_j + \hat{M}\right)\mathrm{sign}(\dot{x}_{i+1}) \\ &= -M_i \ddot{x}_{br} \end{aligned} \tag{5}$$

Note that by incorporating the Coulomb-type friction force from Eq. 4 the system defined by Eq. 5 becomes nonlinear.

Hence the model requires the solution of a system of differential equations, and can provide kinematic and mechanical information, including the spectral values of the active earth pressure coefficient K_{agE} in seismic conditions:

$$k_{agE} = \frac{2 \cdot P_{agE}}{\gamma \cdot H^2} \qquad P_{agE_i} = F_{IN_i} + T_{g_i}; \qquad F_{IN_i} = -M_i \cdot \ddot{x}_{si} \tag{6}$$

where F_{IN_i} is the overall inertia force and T_{g_i} is the tensile strength in the i^{th} geogrid.

2 NUMERICAL SIMULATION

Numerical simulations have been performed using a step-by-step integration algorithm to solve Eq. 5 (Carotti and Rimoldi, 1998); the mathematical model has been validated by comparing the simulation results of two geodynamic systems with experimental results described in the literature; here the simulation is reported for a reduced-scale, geogrid-reinforced model sand wall constructed on a shaking table and subjected to a nonstationary sinusoidal excitation (Fig. 3, from Murata et al, 1994). For the simulations, only the three main geogrid layers, that span the entire width of the wall, were considered. Full details are reported in Carotti and Rimoldi (1998).

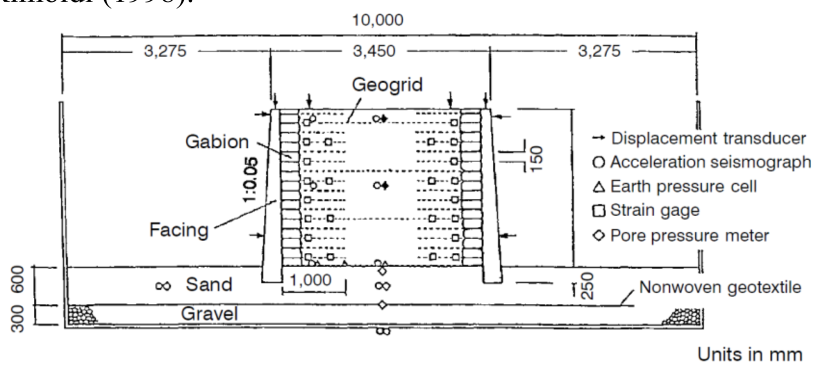

Fig. 3. Reduced-scale, geogrid-reinforced sand wall model (from Murata et al, 1994)

The results presented by Murata et al. (1994) indicate that there is a strong acceleration amplification at the top of the wall with respect to the seismic input acceleration at the bedrock. The monofrequency, sinusoidal input acceleration with a peak acceleration of 5 m/s^2 at a frequency of 3.4 Hz was used in the numerical simulation. Fig. 5a gives the amplification ratio, AR, which is the ratio of the peak absolute acceleration of the soil layers to the peak bedrock acceleration, and Fig. 5b gives the relative displacement of the soil layers for the simulations of the reduced-scale model wall. Comparison of cases with and without geogrid reinforcement is not possible; however, it is worth noting that the AR value decreases from 4.7 to 1.5 at the top of the geogrid-reinforced wall, and the relative displacement decreases from 42 to 7 mm. These acceleration amplification and displacement values for the unreinforced wall correspond very well with results reported by Murata et al. (1994).

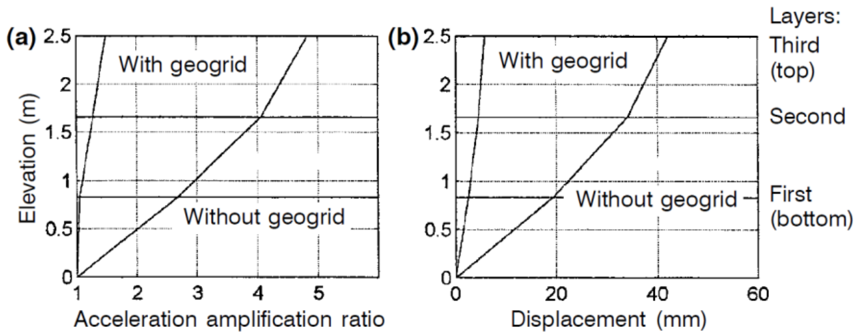

Fig. 5. Simulated response of the walls in Fig. 4 with and without geogrid reinforcement (with peak input acceleration of 5 m/s^2 at a frequency of 3.4 Hz): (a) acceleration amplification ratio with respect to the peak base input acceleration; (b) displacement relative to the base of the structure (from Carotti and Rimoldi, 1998)

3 CONCLUSIONS

From the dynamic equations of motion of a wall or embankment under kinematic bedrock excitation, the structure can be modeled as a multi-DOF, lumped-mass system. This technique provides advantages for the description of interlayer interactions, particularly for geogrid-reinforced walls, and the interpretation of the phenomena through modal decoupling of the seismic dynamic response. Based on this scheme, soil-geogrid interaction is described as a local increase of both stiffness and damping; thus, a nonlinear Newtonian model of reinforced wall dynamics is obtained. Predictions based on the proposed model have been compared with limited available experimental data; the model can then be utilized to extrapolate the behaviour of reinforced walls of different geometries under various excitations.

REFERENCES

A. Carotti, P. Rimoldi; 1997. Time and frequency domain models for the seismic analysis of geogrid reinforced soil walls. Proc. Geosynthetics '97 Conf., Long Beach, USA (1997)

A. Carotti, P. Rimoldi; 1998. A nonlinear model for the seismic response analysis of geosynthetic reinforced soil structures. Geosynthetics International, Vol. 5, Nos. 1-2, pp 189-223. 1998

Murata, O., Tateyama, M., and Tatsuoka, F., 1994. Shaking Table Tests on a Large Geosynthetic-Reinforced Soil Retaining Wall Model. In Recent Case Histories of Permanent Geosynthetic-Reinforced Soil Retaining Walls, Balkema, Proceedings of Seiken Symposium No. 11, Tokyo, Japan, 1994.

THE INFLUENCE OF SOIL AND REINFORCEMENT STIFFNESS ON THE SEISMIC RESPONSE OF MSE WALLS: A TIME HISTORY DYNAMIC ANALYSIS

Oltion Korini

Geoquest Company,
280 avenue Napoleon Bonaparte, 92500 Rueil-Malmaison, France
E-mail: oltion.korini@geoquest-group.com, web page: https://www.geoquest-group.com/

Key words: Time history analysis, Seismic load, Reinforced fill structures, Flac2D software

Abstract. *A MSE wall of 10.5 m height is subjected to a dynamic excitation, and the effect of the reinforcement stiffness and soil stiffness on the response is studied. Three soil stiffnesses are considered: max variable with depth, min variable with depth, and constant (usual Young modulus). Three reinforcement stiffnesses are considered, the usual Geostrap design, double Geostrap design, and steel strips. So, in total, there are 9 analysis cases. The deformed shape of the wall and the strips tension is compared between the cases.*

1 INTRODUCTION

Seismic design of MSE walls is typically done using pseudostatic analysis. This type of analysis uses a constant force to represent seismic excitation which may have variable intensity, frequence and duration. It was also tested using finite difference software (FDM) that beyond an acceleration of 0.4g a MSE wall becomes unstable for a typical design. In some sites, the PGA may significantly exceed this value, thus making pseudostatic analysis inappropriate. Time history analysis applies the true seismic motion at the base of the model and accounts for all its characteristics including duration. Shaking table tests on MSE walls have shown that these structures can resist motions with significant PGA values (Ling et al., 2005; Panah and Ramezani, 2024; Safaee, 2022). This was also observed after real earthquakes (Bathurst et al., 2002; Koseki et al., 2006; Tatsuoka et al., 1997). With the emergence of advanced numerical tools, the determination of the performance of MSE walls under a specific earthquake motion is starting to get popular. In this article, several time-history analyses are performed using Flac2D software for studying the influence of the soil and reinforcement stiffnesses in the response of the MSE walls.

2 METHODOLOGY

The response of a MSE wall depends on both soil and reinforcement properties. In this study the soil is modeled using Mohr-Coulomb model in three cases, one with the usual constant Young modulus and two cases with variable stiffness in function of confining pressure according to Seed formula (Seed et al., 1986). It is chosen to use k2 = 30 and k2 = 80 for minimal and maximal Young modulus variations. Typical values are chosen for the constant modulus case: 100 MPa for reinforced fill, 70 MPa for general fill and 80 MPa for the foundation.

The reinforcement design is done using the coherent gravity analytical method for both geosynthetic strips (Geostrap) and steel strips. To these cases it is added one where the Geostrap design is doubled in order to check its influence in the results. The seismic motion is a record from Loma-Prieta earthquake with PGA = 0.46g (Fig. 1). In the analytical method PGA = 0.23g is used for considering the reduction factor due to the wall flexibility as per design standards.

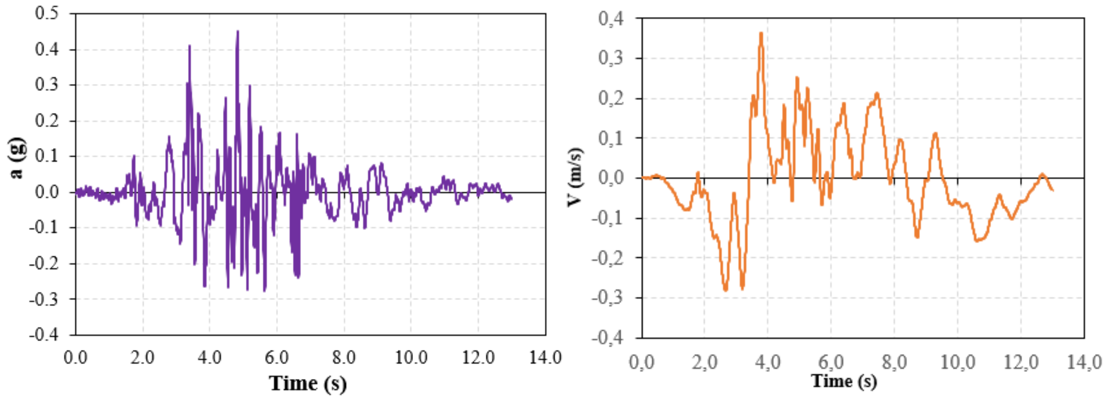

Figure 1: Acceleration (left) and integrated speed (right) of Loma Prieta earthquake.

A MSE wall of 10.5 m high is modelled for this parametric study (Fig. 2). The foundation thickness is kept 2 m because it is aimed to investigate mainly the internal stability and to limit seismic signal amplification effects.

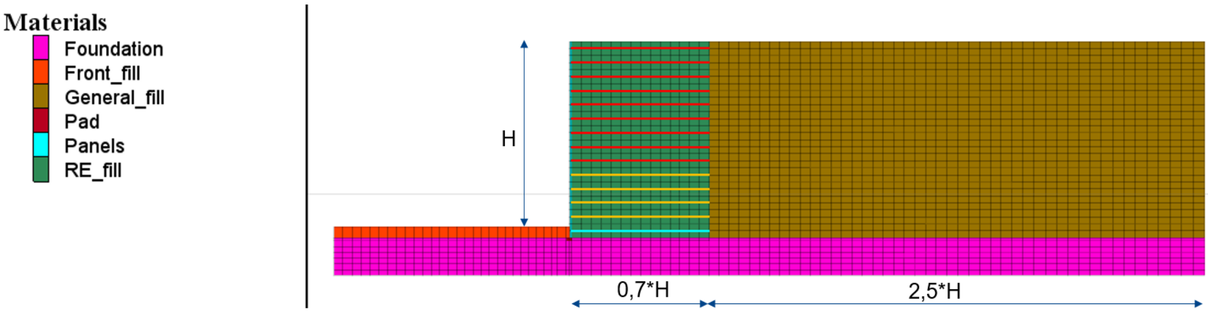

Figure 2: Model layout in Flac2D

3 RESULTS

All the cases were run with the same seismic load and boundary conditions. For the cases with the steel strip reinforcement, the analysis could not be completed due to premature failure of the strips. For k2min and constant E the analysis with the steel strips after 10 seconds, while for k2max ended at 4 seconds. The latter results are incomplete.

3.1 Facing's displacements

The facing's displacements are important when comparing the performance of the analyzed cases. The results for all the cases are presented in Fig. 3. It is remarkable that the variation of soil stiffness has very little effect for the cases that use geosynthetic strips. On the other hand, the steel strips seem more sensitive to the variation of soil stiffness. The steel strips mobilize faster than geosynthetic strips and therefore can absorb more load during a dynamic event. In addition, the steel strips have less interaction area compared to geosynthetic strips for a similar design, which could be the reason of the higher displacement observed at the former ones.

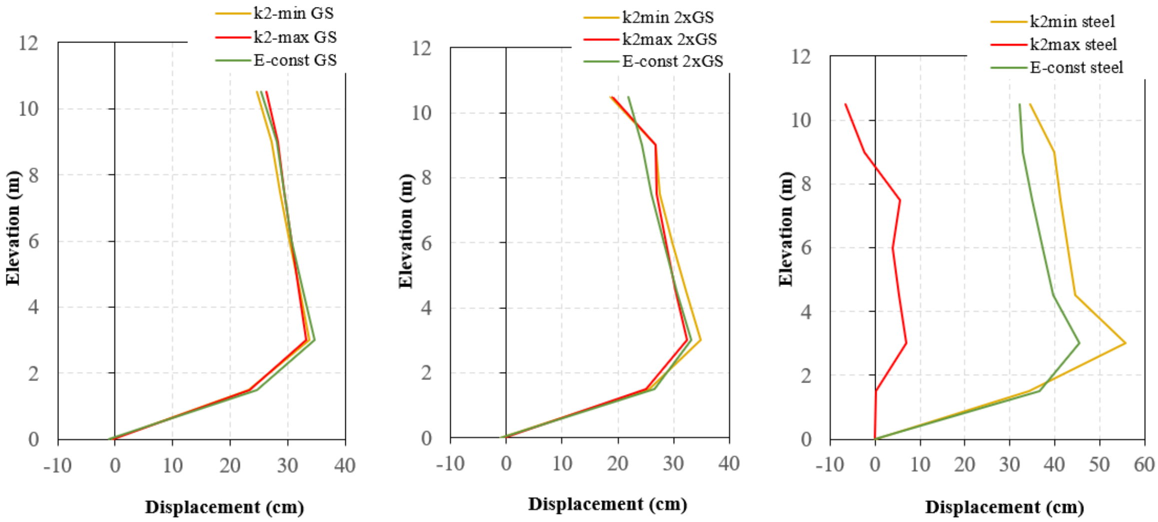

Figure 3: Displacements of front facing for the analyzed cases

3.2 Reinforcements tension

The tension in the reinforcements was recorded during the analyses. As expected, it is variable and very different between geosynthetic and steel strips. The tension fluctuations are faster with the steel strips, and the peak tension is almost the double (Fig. 4). Moreover, in the steel strips case there appear flat parts, which are due to yielding. Some of the steel strips fail after 10 seconds, which leads to the failure in the model. This does not happen with geosynthetic strips. In Fig. 4 are presented half of the strips tensions for visual reasons.

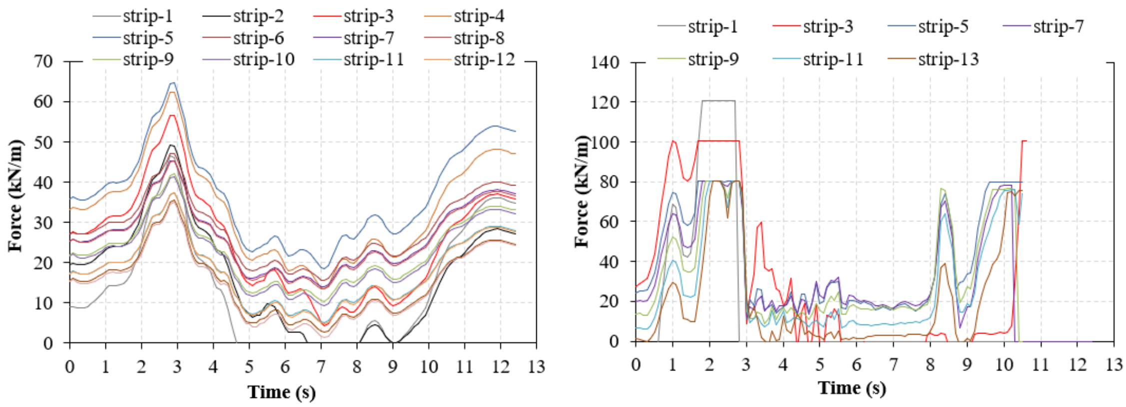

Figure 4: Peak tension in the reinforcements on geosynthetic strip (left) and steel strip (right) for the case with constant soil Young modulus

The peak tension on the strips and its position varied between the different cases. The results are summarized in Table 1. Case $k_2$max for steel is omitted due to premature failure.

Soil stiffness	Single Geostrap	Double Geostrap	Steel strips
$k_2$min	70 kN (3rd level)	92 kN (1st level)	120 kN (2nd level)
$k_2$max	72 kN (5th level)	100 kN (1st level)	-
E-constant	65 kN (5th level)	83 kN (5th level)	120 kN (2nd level)

Table 1: Maximal tension on the strips for all analyzed cases

4 CONCLUSIONS

The parametric study showed that the variation of the soil stiffness using Mohr-Coulomb model has limited effect on the deformed shape of the wall and the tension in the reinforcements. Similarly, with single and double geosynthetic strips, the results remain in a close range. On the other hand, the steel strips absorbed much more tension compared to Geostrap due to their significant stiffness.

The doubling of Geostrap lead to almost similar displacements in the facing even though the recorded tension increased. The steel strips showed higher displacements than the Geostrap probably due to less interaction surface with the soil that lead to a greater failure wedge development in the reinforced mass. The considered numerical approach is to be taken as a preliminary one. More research is needed to calibrate the model to experimental data.

REFERENCES

Bathurst, R.J., K. Hatami and M.C. Alfaro; 2002. Chapter 14 - Geosynthetic-reinforced soil walls and slopes—seismic aspects. Geosynthetics and their applications, Emerald Publishing Limited https://doi.org/10.1680/gata.31173.

Koseki, J., R. Bathurst, E. Guler, J. Kuwano and M. Maugeri; 2006. Seismic stability of reinforced soil walls. In 8th International conference of Geosynthetics, Yokohama, Japan, 18-22 September 2006, pp. 28.

Ling, H.I., Y. Mohri, D. Leshchinsky, C. Burke, K. Matsushima and H. Liu; 2005. Large-Scale Shaking Table Tests on Modular-Block Reinforced Soil Retaining Walls. Journal of Geotechnical and Geoenvironmental Engineering 131(4): 465–476.

Panah, A. and M. Ramezani; 2024. Experimentally comparison of shaking table and pseudo-static parameters of polymeric-strip reinforced-soil walls. Japanese Geotechnical Society Special Publication 10(43): 1600–1605

Safaee, A.M.; 2022. Performance of the multi-tiered GMSE walls under seismic conditions: Comparison of physical and numerical simulations. Soil Dynamics and Earthquake Engineering 159: 107316 http://dx.doi.org/10.1016/j.soildyn.2022.107316.

Seed, H.B., R.T. Wong, I.M. Idriss and K. Tokimatsu; 1986. Moduli and Damping Factors for Dynamic Analyses of Cohesionless Soils. Journal of Geotechnical Engineering 112(11): 1016–1032 http://dx.doi.org/10.1061/(ASCE)0733-9410(1986)112:11(1016).

Tatsuoka, F., J. Koseki and M. Tateyama; 1997. Performance of reinforced soil structures during the 1995 Hyogo-ken Nanbu Earthquake. Earth Reinforcement, volume 2, CRC Press.

GEOFOAM SEISMIC BUFFERS FOR UNREINFORCED RETAINING WALLS AND GEOSYNTHETIC MSE WALLS

Richard J. Bathurst[1] and Saman Zarnani[2,3]

[1] GeoEngineering Centre at Queen's-RMC, Department of Civil Engineering,
Royal Military College of Canada, Kingston, Ontario, Canada
E-mail: bathurst-r@rmc.ca, web page
[2] *formerly*, GeoEngineering Centre at Queen's-RMC, Department of Civil Engineering,
Queen's University, Kingston, Ontario, Canada
[3] *currently*, BGC Engineering, Vancouver, British Columbia, Canada
E-mail: szarnani@bgcengineering.ca

Key words: Soil reinforcement, Geofoam, Seismic buffers, Retaining walls, MSE walls

Abstract. *Geofoam is a class of geosynthetic material manufactured from expanded polystyrene (EPS). This extended abstract describes its use as a seismic buffer material placed against a rigid facing, for conventional unreinforced retaining wall structures, and in combination with layers of horizontal layers of geosynthetic reinforcement for the case of mechanically stabilized earth (MSE) walls. The vertical geofoam inclusions are used to attenuate the magnitude of the dynamic loads developed against the walls due to earthquake. The veracity of this technology is demonstrated through the results of physical reduced–scale shaking table tests of structures constructed with and without a geofoam inclusion.*

1 INTRODUCTION

This extended abstract describes physical shaking table model testing to investigate the effectiveness of geofoam seismic buffers constructed with expanded polystyrene (EPS) to reduce the dynamic (earthquake) loads on conventional rigid earth retaining walls, and the hard facing of conventional mechanically stabilized earth (MSE) walls.

2 UNREINFORCED RETAINING WALLS

The first use of geofoam seismic buffers to reduce the magnitude of the horizontal component of dynamic seismic loads against rigid earth retaining walls was reported by Inglis et al. (1996). They used a FLAC model to demonstrate that the dynamic component of horizontal earthquake loads against rigid basement walls at a building project in Vancouver, British Columbia, Canada, could be reduced by 50% by placing a 1-m thick geofoam inclusion against the concrete walls. Bathurst et al. (2007) demonstrated quantitative proof of the seismic buffer concept by carrying out a series of 1-m high reduced-scale model shaking table tests (Figure 1). A control model with no seismic buffer and six other walls with seismic buffers having different EPS bulk densities were tested. Each model was subjected to an increasing stepped sinusoidal base acceleration record.

The measured horizontal wall forces recorded at the rigid wall versus peak base acceleration are shown in Figure 2. The plots show that as the peak acceleration increased, the total force on the rigid wall and the walls with a seismic buffer increased. However, the total force is greatest for the control wall (no seismic buffer) at the end of construction, and at the same base acceleration for the three walls. At the same base acceleration, the total force is less with decreasing total buffer density. Note that the lowest bulk buffer density was achieved by

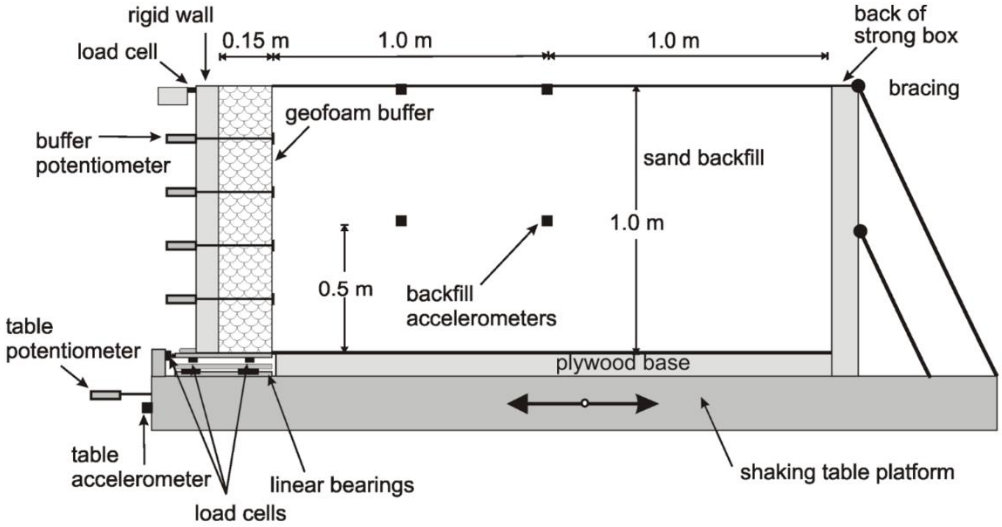

Figure 1: Cross-section view of shaking table model with geofoam seismic buffer.

removing EPS material within the buffer column prior to construction. The experimental test results were used to test the veracity of a numerical FLAC model with the same geometry, materials and base excitation. The FLAC model was then scaled up to generate synthetic response data that was used in turn to create design charts for geofoam seismic buffers (Zarnani and Bathurst 2009). The example charts in Figure 3 are for different height (H) of walls. The horizontal axis is the buffer stiffness K expressed as the ratio of the bulk elastic modulus (E) of the geofoam and thickness (t). The vertical axis is the isolation efficiency (at the same base acceleration) computed as the difference between peak dynamic force increment against the control wall minus the peak dynamic force increment with the seismic buffer divided by the peak dynamic force increment against the control wall. The larger this value, the more effective the seismic buffer to reduce the horizontal force due to shaking. EPS19 refers to the ASTM material designation for the EPS material, and f_{11} is the fundamental frequency of the system. The designations $0.3\times f_{11}$ and $1.4\times f_{11}$ mean that the numerical model was excited at a frequency of 0.3 and 1.4 times the fundamental frequency of the model, respectively.

Experimental shaking table test results and numerical simulations demonstrated proof of concept for using EPS geofoam material as a seismic buffer to attenuate dynamic earth loads against rigid retaining walls. For the range of parameters investigated by Zarnani and Bathurst

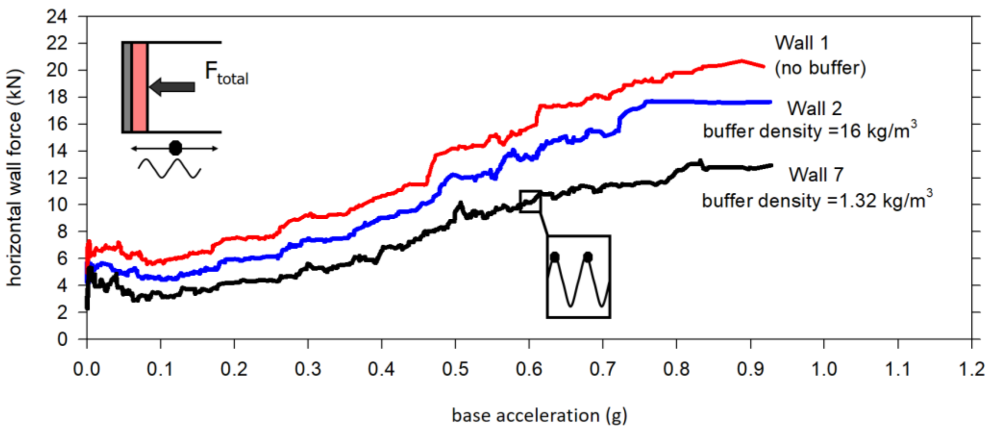

Figure 2: Total horizontal force against rigid wall at peak base acceleration.

(2009), K < 50 MN/m^3 was observed to be the practical range for the design of these systems to attenuate earthquake loads.

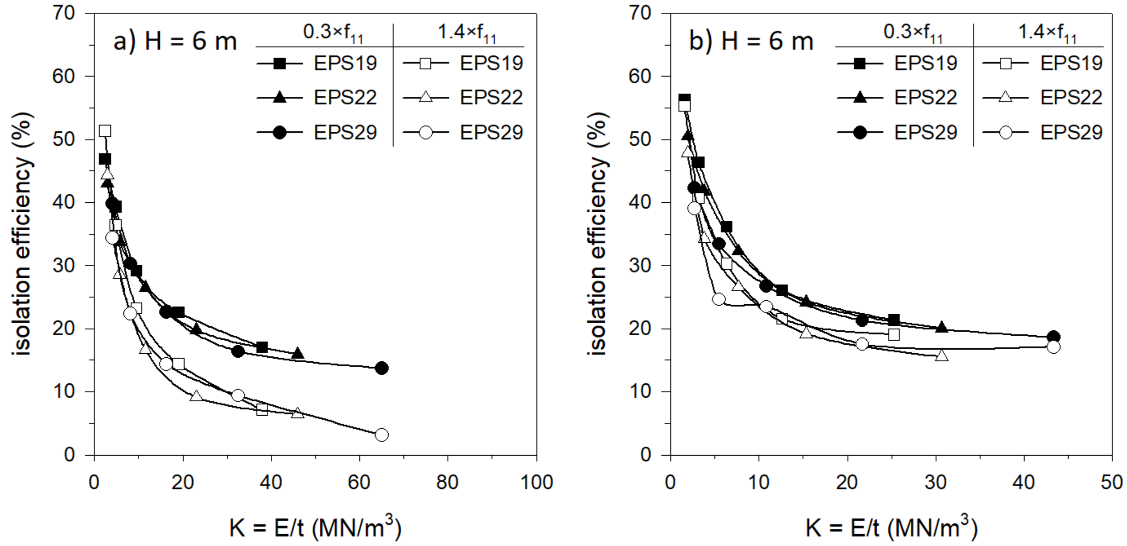

Figure 3: Example isolation efficiency design charts from Zarnani and Bathurst (2009).

3 GEOSYNTHETIC MSE WALLS

The authors extended the experimental investigation of geofoam seismic buffers to the case of incorporating the column of geofoam against the hard face of 1.42-m high reduced-scale model shaking table tests of MSE walls (Bathurst and Zarnani 2026). An example wall model (Wall 3) is shown in Figure 4. Three other models were constructed and tested with no seismic buffer and geogrid reinforcement lengths of 835 mm (Wall 1 – control) and 1035 mm (Wall 4), and another wall with combined seismic buffer and reinforcement lengths of 835 mm (Wall 2). Each wall was instrumented with displacement devices at the wall face, strain gauges and extensometers attached to each reinforcement layer, accelerometers placed at the wall face and in the sand backfill, reinforcement-facing connection load rings, and horizontal and vertical toe load cells. Each wall had a rigid face constructed from a stack of hollow steel sections bolted together, and a hinged toe. A variable-amplitude sinusoidal harmonic excitation with increasing and decaying peak acceleration portions was applied in stages to shake the models.

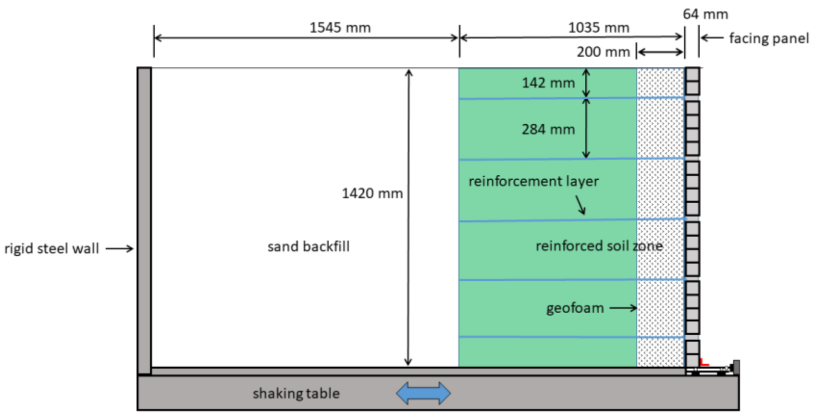

Figure 4: Example MSE model wall configuration (Wall 3) (from Bathurst and Zarnani 2026).

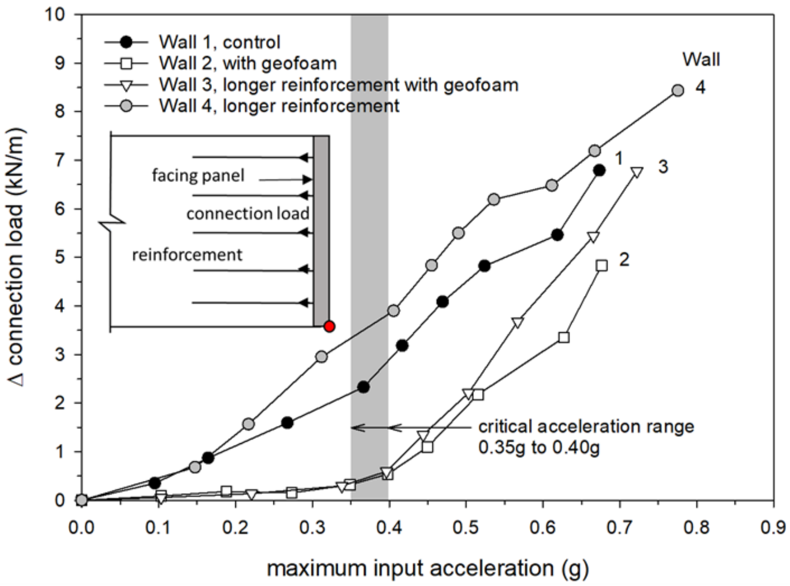

Figure 5: Post-construction sum of additional connection loads during staged shaking. Note: datum is end of construction following removal of external facing support (from Bathurst and Zarnani 2026).

Figure 5 shows the development of the sum of connection loads with increasing peak base acceleration. For the control wall (Wall 1) constructed without geofoam, there is a small but detectable increase in the rate of increase of incremental dynamic connection load and toe load in the vicinity of the critical acceleration level. However, from a practical point of view the connection loads for Wall 1 and Wall 4 increase more-or-less continuously with increasing base excitation. Over most of the plots for these two walls without geofoam, there are generally larger loads for the wall with the longer reinforcement lengths. Comparing pairs of walls with and without the geofoam inclusion shows that the seismic buffer reduces the load at the reinforcement connections. A practical benefit of geofoam inclusions at field scale is that the facing panel structural loading is less and thus cost savings may be realized. Importantly, the seismic buffers deferred the increase in connection loads observed for the control walls until a peak base acceleration of 0.4g was applied.

In conclusion, this experimental investigation demonstrated that the performance of MSE walls during earthquake was improved (i.e., reduced wall toe and connection loads) by placing a vertical geofoam seismic buffer inclusion against the MSE wall facing and between the geosynthetic reinforcement layers.

REFERENCES

Bathurst, R.J., and Zarnani, S.; 2026. Shaking table tests on combined EPS geofoam and geogrid reinforcement model GRS walls. Geosynthetics International (to appear).

Bathurst, R.J., Zarnani, S. and Gaskin, A.; 2007. Shaking table testing of geofoam seismic buffers. Soil Dynamics and Earthquake Engineering 27(4): 324-332.

Inglis, D., Macleod, G., Naesgaard, E., and Zergoun, M.; 1996. Basement wall with seismic earth pressures and novel expanded polystyrene foam buffer layer. Proceedings of the 10th Annual Symposium of the Vancouver Geotechnical Society, Canada.

Zarnani, S. and Bathurst, R.J.; 2009. Numerical parametric study of EPS geofoam seismic buffers. Canadian Geotechnical Journal 46(3): 318-338.

GEOSYNTHETIC REINFORCEMENT CONCEPTS FOR TEMPORARY CONSTRUCTION ROADS IN LINEAR INFRASTRUCTURE PROJECTS

Oliver Detert

HUESKER Synthetic GmbH, 48712 Gescher, Germany
E-mail: detert@huesker.de

Key words: Geosynthetics, Basetrac HR, Temporary construction roads, Reuse, Base reinforcement, Sustainability

Abstract. *Temporary construction roads in linear infrastructure projects require rapid installation, reliable trafficability under heavy construction traffic and efficient removal after a limited service period. Conventional granular solutions can lead to high aggregate demand, significant transport effort and considerable disposal quantities. This extended abstract presents a reuse-oriented concept for Basetrac HR geosynthetic base reinforcement in temporary construction roads. The concept is based on repeated installation, loading, removal and re-rolling of robust woven reinforcement products. The central requirements are residual tensile strength after installation and removal damage, sufficient tear resistance during recovery and a cascading use strategy after several cycles. Field trial data from repeated installation and removal indicate that selected woven products can retain a relevant proportion of their tensile strength after up to four cycles. The approach therefore offers economic and environmental potential for long temporary access roads in power transmission and cable corridor projects, where recovered reinforcement can be reinstalled in subsequent road sections or reassigned to lower-demand temporary functions.*

1 INTRODUCTION

Temporary construction roads are indispensable in linear infrastructure projects such as power line construction, underground cable routes, pipeline corridors and other long construction sites. They provide access for trucks, excavators, cable drums, cranes and tracked machinery, often over several kilometres and across highly variable subgrade conditions. These roads must be constructed rapidly, remain trafficable under repeated heavy loading and are usually removed after a comparatively short service period.

For such temporary applications, the amount of imported granular material can become a dominant cost and sustainability factor. Aggregates must be produced, transported, placed, maintained and finally removed or disposed of. In long corridor projects, even small reductions in base course thickness or material losses can therefore create significant economic and environmental benefits. Geosynthetic base reinforcement is an established method to improve load distribution, reduce rutting and increase serviceability. However, temporary construction roads require an additional performance objective: the reinforcement should ideally be recovered and reused rather than treated as a single-use component.

The present contribution introduces a reuse-oriented reinforcement concept for woven geosynthetics in temporary construction roads. The focus is not only the initial reinforcing function, but the retention of performance after installation, traffic loading, removal and reinstallation. This creates a transition from a linear use model to a circular and cascading use model for geosynthetic reinforcement in temporary infrastructure.

2 REUSE REQUIREMENTS FOR BASE REINFORCEMENT

The reuse of geosynthetics in base reinforcement imposes requirements that go beyond conventional design. In a standard application, the reinforcement must withstand installation damage, provide tensile resistance during traffic loading and interact with the surrounding aggregate. In a reuse concept, additional requirements are decisive because the product must also survive recovery and handling after the service phase.

First, the residual tensile strength after each installation and removal cycle must remain sufficient for the intended application. Mechanical damage may occur during aggregate placement, compaction, traffic loading, excavation and re-rolling. The relevant design value is therefore not the initial tensile strength alone, but the residual tensile strength after one or several practical reuse cycles.

Second, the reinforcement must be recoverable without uncontrolled rupture. Local defects such as small cuts, abrasions or broken yarns should not propagate into a complete full-width tear during pulling, lifting or winding. Tear resistance and damage tolerance are therefore central product characteristics for reusable reinforcement. Third, the product must be compatible with efficient site logistics. Recovery only becomes economical when removal, inspection, re-rolling and transport to the next installation location can be carried out with manageable time and equipment effort.

Finally, reuse should be understood as a cascading strategy. A product that no longer provides sufficient residual strength for heavily loaded base reinforcement after several cycles may still be useful as a separation or reinforcement layer in less demanding temporary applications, for example beneath soil stockpiles, in storage areas or in access routes with reduced traffic intensity.

3 FIELD TRIAL BASIS AND PERFORMANCE INDICATORS

The reuse concept was evaluated using field trial observations and laboratory testing after repeated installation and removal cycles. The practical sequence included installation of the geosynthetic, placement of a granular cover layer, loading during use, decommissioning, removal and re-rolling. Such a procedure is important because the most critical damage mechanisms are not necessarily generated in the first installation, but during the combination of traffic loading and later recovery.

For a reuse-oriented qualification, four performance indicators are proposed. The first is residual tensile strength, expressed as percentage of the reference strength after each cycle. The second is tear resistance, because local damage must not lead to sudden rupture during recovery. The third is road performance during use, assessed by deformation and trafficability indicators such as rut depth and dynamic plate load measurements. The fourth is recoverability, including removal time, contamination, roll quality and visible damage patterns.

Field trial data for a woven reinforcement product show that relevant residual strength can remain available after several cycles. For the tested product residual tensile strength in machine direction remained approximately 76.0 %, 76.1 %, 71.7 % and 69.8 % after the first to fourth removal cycle, respectively. The values are product- and site-specific, but they demonstrate the technical feasibility of repeated use when a sufficiently robust reinforcement is selected.

4 ECONOMIC AND SUSTAINABILITY POTENTIAL

The greatest benefit of reusable geosynthetic reinforcement is expected in long linear construction projects. In these projects, temporary roads are often built section by section. If a reinforcement product can be recovered from a completed section and reused in the next section, the same reinforcement area can contribute to several construction phases. This directly reduces the amount of new geosynthetic material required and can also reduce disposal quantities at the end of the work.

The economic effect is linked to several mechanisms. Reuse reduces material purchasing costs per effective use cycle. A robust reinforced base may reduce aggregate demand or maintenance effort, particularly on weak subgrades or under repeated heavy traffic. Furthermore, controlled recovery and re-rolling can reduce waste handling compared with damaged single-use textiles that are mixed with soil and aggregate residues. These effects become more relevant as project length, aggregate transport distance and disposal costs increase.

From a sustainability perspective, the concept supports resource efficiency in two ways. First, it extends the service life of the geosynthetic by using the same product several times in the same or in subsequent projects. Second, it enables cascading use: when the residual strength after three or four cycles is no longer sufficient for the original base reinforcement design, the material can still be used for lower-demand functions such as separation layers, soil storage areas or temporary working surfaces. This hierarchy of repeated use before recycling or disposal is consistent with circular construction principles.

5 PRACTICAL IMPLEMENTATION CONCEPT

A practical implementation should include a defined reuse loop. After the first installation and service period, the granular layer is removed carefully, the geosynthetic is exposed, lifted and re-rolled. Each recovered roll is then inspected and assigned to a reuse class. The classification should combine visual inspection, documentation of the number of cycles, project conditions and, where necessary, representative laboratory tensile tests.

Three reuse classes are proposed. Class A material retains sufficient quality for heavily loaded temporary construction roads. Class B material is suitable for moderate loads or reduced base reinforcement requirements. Class C material is no longer assigned to primary base reinforcement, but remains available for separation, soil stockpile reinforcement or other secondary temporary functions. This simple classification supports decision-making on site and prevents the uncontrolled reuse of damaged material in critical applications.

For design practice, reuse should be included explicitly in the project specification. Required residual strength, permissible damage, inspection intervals, re-rolling procedures and documentation requirements should be defined before construction starts. This is essential because the economic value of the concept depends on planned recovery, not on opportunistic salvage at the end of the project.

6 CONCLUSIONS

The reuse of geosynthetic reinforcement in temporary construction roads offers a promising route to reduce costs, aggregate demand and waste in linear infrastructure projects. The concept is particularly relevant for power transmission and cable corridor construction, where long temporary access roads are required and where material can potentially be moved forward from completed sections to new construction sections.

The available field trial data indicate that selected robust woven Basetrac HR products can retain a relevant proportion of their tensile strength after repeated installation and removal cycles. Residual tensile strength, tear resistance and recoverability are the decisive parameters for such applications. Small local damage must not lead to uncontrolled rupture during removal, and the product must be capable of re-rolling and handling under realistic site conditions.

A cascading reuse strategy is recommended. Reinforcement with high residual strength can be reused in primary base reinforcement. Material with reduced strength can be reassigned to less demanding functions before recycling or disposal is considered. Further work should focus on systematic field trials under different aggregates, subgrade conditions, traffic loads and removal techniques, with the objective of defining robust reuse classes and conservative design rules for temporary construction roads.

THE USE OF GEOSYNTHETICS IN THE CONSTRUCTION OF THE ECO-PARK OF DURRES: A SYMBOL OF SUSTAINABILITY, RESILIENCE AND RECYCLING STRATEGY

Lidia S. Calvarano[1] and Piergiorgio Recalcati[1]

[1] Tenax SpA, via dell'Industria 17, 23897 Viganò - LC, Italy

E-mail: lidia.calvarano@tenax.net , piergiorgio.recalcati@tenax.net

web page: https://www.tenax.net

Key words: Soil reinforcement, Reinforced fill structures, Sustainability

Abstract. *Eco Park of Durrës is a large public park with recreational and sports facilities, built on an open-air landfill where solid waste has been stored without any protection for over half a century, making the area an environmental emergency, a source of pollution and a danger for the territory and the health of the population. The remediation project focused on sustainable development and ecological innovation, aiming at promoting engineering solutions and construction technologies compatible with environmental protection. The main material used to build the park were wastes present in the landfill, which after being pre-treated were confined, remodelled, compacted to form an artificial landscape, with hills and winding paths that can be walked on, transforming the area into a public park. The highest hill, symbol of the Durrës Eco Park and made of compacted waste, hosts on one side the highest climbing wall in the Balkans which reaches a maximum height of about 30m in the centre. The front consists of a thin concrete wall that serves only as support of the steel structure that holds the climbing panels. The thrust of the waste is absorbed by an embankment made of geogrid reinforced soil, with sub-vertical front walls. The greatest challenge was to the design of a structure of considerable size in a highly seismic area; the construction method chosen (wrap-around with soil-filled bags on the front and back face of the structure) ensures the structure, while supports the waste pile, doesn't interfere with the capping system and doesn't cause damage to the waterproofing system. The design proposal represents a sustainable and resilient solution, according to a green economy strategy, in a geotechnical and environmental engineering context.*

1 INTRODUCTION

Eco Park in Durrës, in Albania, is a large public park built on a former open-air landfill that once posed a significant environmental threat to the city's outskirts. The redevelopment project was inspired by a famous local Roman mosaic "The Beauty of Durrës" (Figure 5), which serves as a metaphor for the transformation of a polluted site with negative connotations into a public space for recreation and environmental education. The site, in the Porto Romano area, about 6,0 km away from the city of Durrës, the second largest municipality in Albania, was used for over half a century as an open-air landfill where solid waste was stored without any protection, environmental permit and in violation of waste management standards, making the area a source of pollution and dangerous for the territory and the health of the population.

The primary objective of the project was to address an environmental crisis. However, this issue is not solely perceived as a technical challenge. The proposed solution had to have a dual purpose. On one hand, the remediation project focused on sustainable development and ecological innovation, aiming to promote engineering solutions and construction technologies compatible with environmental protection.

On the other hand, it was considered as a social problem that required a more complex strategy that, by focusing on the redevelopment of a deteriorated area, with the creation of green, healthy and recreational spaces for the city, intrinsically promoted ecological awareness among citizens.

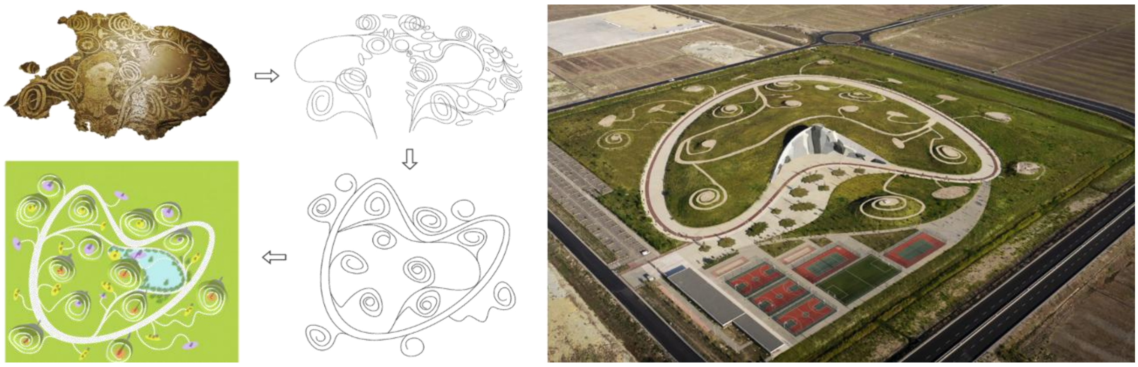

Figure 5: the Roman mosaic "The Beauty of Durrës", which inspired the architects and the evolution of the architectural project up to the final layout of the Eco Park in Durrës.

The design and construction of the Durrës Eco Park are part of a green economy strategy, where Albanian politics and economics, while focusing on protecting the territory and natural resources, are developing and supporting the waste recycling industry, in line with European environmental policies, considering waste a precious resource for the economic, social, and employment rebirth of the country. For this reason, the ecological park has a key and symbolic importance for the Albanian population. According to green economy strategy, the main materials used to build the park were wastes present in the landfill, which after being pre-treated were confined, remodelled, compacted to form an artificial landscape, with hills and winding paths that can be walked on, transforming the area into a public park.

2 ECO PARK PROJECT: DESIGNED AND BUILT USING THE SOIL REINFORCEMENT TECHNIQUE

The Durrës Eco-Park transformed a contaminated landfill into a sanitary landfill consisting of hills covered with vegetation and sculpted creating a land art intervention. The central hill, that is the focus of this memory and a symbol of the Eco Park, is the highest hill. It is constructed by using pre-treated and compacted waste. On one side is located the highest multifunctional climbing wall in the Balkans which, specifically designed to hold international competitions, reaches, in the centre, a maximum height of approximately 30 m. This wall was designed and built using the soil reinforcement technique.

At the front, it consists of a thin concrete wall, supported by piles, that serves only as support of the steel structure that holds the climbing panels (Figure 6a). The thrust of the waste pile is entirely absorbed by a reinforced soil embankment, by using mono-oriented geogrids. The embankment has a vertical front face and a rear face with an inclination of 75°.

Figure 6b shows some of the typological cross-sections and the longitudinal profile of the reinforced soil structure. A cavity was created between the concrete wall and the reinforced earth embankment. This cavity was then filled with non-compacted granular material to allow any deformations of the earth reinforced embankment face without placing any strain on the external concrete wall.

(a)

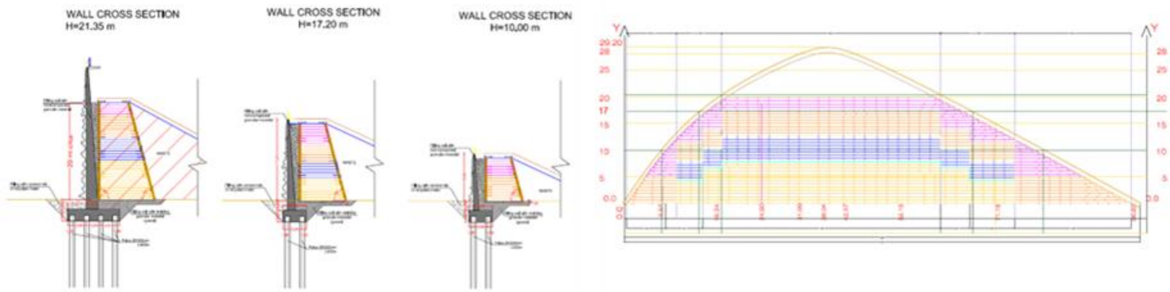

(b)

Figure 6: a) the central and largest hill of the Eco Park of Durrës, where the highest climbing wall in the Balkans is located, is composed of compacted and pre-treated waste; b) typological cross-sections and the longitudinal profile of the steep earth reinforced embankment to contain the landfill waste.

In our proposal, the wrap-around method was the construction method chosen for the soil reinforcement system. In particular, in this context, on the faces embankment, the construction method proposed has required the use of bags filled with soil (sandbags) placed on both the front and rear faces of the reinforced soil structure, over which the geogrid sheets were wrapped around. These sand-bags replace the traditional welded wire steel mesh formwork because, since the reinforced earth structure is a perimeter embankment of the landfill, it was necessary to find an engineering solution and a construction technology that ensures the structure, while supports the waste pile, doesn't interfere with the landfill capping system and doesn't cause damage to the waterproofing system (Figure 6).

The geognostic investigations and mechanical characterization of the site's soil were essential both for conducting geotechnical stability assessments and, as in this case, for defining the mechanical design parameters of the reinforced soil itself, for which the crushed rubble from some buildings that collapsed following the 2019 earthquake was reused and mixed with backfill soil.

Eurocodes 7 and Eurocode 8, for both for static and seismic conditions, were used for all the stability checks, taking into account:

- The design geometry.
- The geotechnical model.
- The seismicity of the site (PGA= 0.134 g),
- The loads acting during the construction phases (for the short-term analysis before landfill exploitation).
- The loads acting during the service life (for long term analysis after landfill

exploitation).

Under both static and seismic conditions, all the internal stability checks (allowable tensile strength and sliding of each geogrid layer) and all external stability checks (global stability, sliding, bearing capacity and overturning), performed using a calculation program specifically created for the design of reinforced soil structures, had fully satisfied the required safety factors.

Design and construction have been particularly complex due to the high seismicity of the area with a Peak Ground Acceleration (PGA) equal to= 0.134 g; the height of the geogrid reinforced structures (average height 17.0 m, maximum height up to 25.0 m) and to the inclination of the reinforced slope face (90° external face and 75° internal face).

3 CONCLUSIONS

In summary, many were the advantages of using the reinforced earth structure compared to the original traditional engineering solutions:

- Speed of time of construction (reduced by 20%) and easiness of execution (approximately 40 m^2/day of face of wrap-around geogrid reinforced earth structures required a team of three men). Finally, the use of reinforced soil technique allowed to deliver the works in time respecting the time schedule.
- Cost-effectiveness and sustainability thanks to the on-site procurement of fill material and reused of building rubble, thus eliminating the costs of quarrying and transport. In particular, the rubble was crushed with special crushers, selected and mixed with the soil until reaching a size suggested by the designers based on the calculation of the internal and external stability of the reinforced soil structures, allowing a considerable reduction in construction costs.
- Better behavior in seismic conditions. The reinforced earth constructions are able, deforming themself, to absorb the seismic stresses, even of considerable entity, without however compromising their functionality, contrary to the common rigid structures in reinforced concrete which in the same seismic conditions would risk collapsing.
- Less environmental pollution. The trucks used for the construction of reinforced earth works produce lower emissions of CO2 into the atmosphere than those associated with the construction of traditional works.

The project and the construction of the geogrid reinforced embankment have been a big challenge and definitely a great success for Tenax, thanks to the great work done by the contractor De Mare who was capable to finish the job in a very precise and accurate way despite all the logistic difficulties given by the location and by the time scheduled imposed by the construction of Durrës Eco Park.

4 ACKNOWLEDGEMENTS

Thanks to De Mare S.r.l for the photographic contribution.

REFERENCES

EN 1997-1 (2004) (English): Eurocode 7: Geotechnical design - Part 1: General rules.

EN 1998-1 (2004) (English): Eurocode 8: Design of structures for earthquake resistance - Part 1: General.

USE OF PRECAST RC ARCH (REPLACEMENT OF CONVENTIONAL RC CULVERT) IN COMBINATION WITH MSE WALLS: STRUCTURAL BASIS OF DESIGN AND SUSTAINABILITY ASSESSMENT — NAIA ISLAND, DUBAI, UAE

Karim Mohsen

VSL Middle East LLC, a member of Bouygues Construction — Dubai, United Arab Emirates
E-mail: karim.mohsen@vsl.com , web page: www.vsl.com

Key words: Precast RC arch culverts; mechanically stabilized earth (MSE) walls; soil-structure interaction (SSI); marine durability; AASHTO LRFD; lifecycle assessment.

Abstract. *This paper presents the structural basis of design and a sustainability assessment for precast reinforced concrete BEBO arch culverts used as a direct replacement for conventional reinforced concrete (RC) box culverts, in combination with Mechanically Stabilized Earth (MSE) retaining walls, at Naia Island (Umm Suqeim Island), Dubai, UAE. Two arch configurations are deployed in a severe marine tidal environment: a twin-cell E78T/6 (span 23.77 m, rise 8.48 m) marina access channel, and a triple-cell E54T/6 (span 16.46 m, rise 6.10 m) tidal flushing culvert. MSE walls using the VSoL polymeric strip system form the island's perimeter. Both systems are designed to AASHTO LRFD 10th Edition (2024) for a 75-year design life. Compared to an equivalent conventional RC box culvert, the Precast Arch + MSE approach achieves approximately 85% reduction in Global Warming Potential (GWP) and 47–50% reduction in construction cost. A multi-layered marine durability strategy delivers a predicted service life exceeding 81 years, surpassing the 75-year design target. Six tidal hydrostatic load cases and buoyancy are explicitly addressed in staged 2D finite element analysis.*

1 INTRODUCTION

Naia Island (formerly Umm Suqeim Island), Jumeirah, Dubai, UAE, required two large-span tidal-flushing culverts together with Mechanically Stabilized Earth (MSE) perimeter walls. Conventional RC box culverts rely on mass concrete and heavy rebar and carry significant material, environmental, and programme penalties for large spans. Precast RC arch systems exploit soil-structure interaction (SSI), in which the surrounding engineered fill becomes a structural component.

This paper documents the engineering case for replacing conventional RC culverts with precast BEBO arch systems combined with MSE walls at Naia Island, covering structural design, tidal hydrostatics, a quantified sustainability comparison, and a durability study referenced to CIA Z7/01 (2014) and the ECSMGE 2024 LCA findings (Malekmohammadi and Damians, I.P., 2024).

2 PROJECT OVERVIEW AND ARCH GEOMETRY

Key parties: Owner — Shamal Development LLC; Engineer — AECOM Middle East; Main Contractor — Van Oord Middle East LLC; Arch Designer — BEBO Arch International AG; MSE Designer — VSL Middle East LLC. The BEBO System (Dr Werner Heierli, 1961–62) was first validated near Zurich in 1965/66 (14.3 m span at 16 cm wall thickness) and subsequently at Recklinghausen, Australia and the USA, underpinning NCHRP Reports 473 and 647.

Parameter	BEBO E78T/6 (Marina Channel)	BEBO E54T/6 (Flushing Culvert)
Configuration / span / rise	Twin-cell, 23.77 m / 8.48 m	Triple-cell, 16.46 m / 6.10 m
Design life / code	75 yrs — AASHTO LRFD 10th Ed.	75 yrs — AASHTO LRFD 10th Ed.
Max settlement / spreading	≤ 50 mm / ≤ 25 mm	≤ 50 mm / ≤ 17 mm

Table 1: Geometric and design parameters for the two BEBO arch culverts at Naia Island.

3 DESIGN PHILOSOPHY: ARCH VS CONVENTIONAL RC CULVERT

In the BEBO arch the surrounding engineered fill is an integral structural component, converting bending and shear into axial compression in the concrete, the material's strongest mode. Arch wall thicknesses of 160–250 mm span 15–25 m, where a comparable RC box would need slabs 400–700 mm thick. The Ferguson Laboratory monitoring study confirmed SSI reduces design moments by up to 60% versus independent-structure assumptions (FHWA, 1992).

Key assumptions for Naia Island: SSI captured via 2D plane-strain FEA (LUSAS v22.0); partially cracked stiffness per AASHTO 4.5.2.2; arch-fill interface friction $\delta = 20°$; two-hinged geometry tolerating ≤ 50 mm differential settlement; seismic/temperature effects not governing for buried Dubai structures (AASHTO 3.10.1, 12.6.1).

4 MATERIALS AND MARINE DURABILITY

The marine tidal exposure (XS2/XS3/XC3-4 per BS EN 206 / ACI 318) is addressed with a C50/20 mix (65% GGBS, 5% microsilica, w/c = 0.34), 75 mm cover, SBS bitumen membrane, silane impregnation, and GFRP Mateen bar in MSE panels (eliminating corrosion risk entirely). Independent modelling (ACI Life-365 v2.2 / fib Bulletin 34; $D_{28} = 1.75\times10^{-12}$ m²/s) predicts a service life exceeding 81 years, consistent with the CIA Z7/01 framework (reliability index $\beta \geq 3.1$ for buried elements).

Property	Value
Concrete grade / Ec	C50/20 (f'c 40 MPa) / 30.8 GPa
GGBS / microsilica / w/c	65% / 5% / 0.34
Cl^- penetrability (RCPT)	Very Low — avg. 305 C/6hr
Cover (arch / MSE panel)	75 mm / 35 mm (GFRP bar)
Predicted service life	> 81 years (ACI Life-365 / fib B34)

Table 2: Key material and durability properties — arch concrete and MSE panels, Naia Island.

5 MARINE ACTIONS AND TIDAL LOAD CASES

Hydrostatic pressure ($\gamma_w = 10$ kN/m³) is derived from MHHW +1.70 m DMD, storm surge 1.15 m and 75-year sea level rise 0.93 m, giving a Design Water Level of +3.78 m DMD against a 2.2 m tidal range. Six load cases (dry baseline, HAT/LAT combinations, rapid draw-down and design water level) govern maximum earth pressure, seepage gradient and buoyancy uplift, and are applied in the staged 2D FEA together with HL-93 traffic loading.

6 MSE WALL DESIGN — VSOL POLYMERIC STRIP SYSTEM

The island's perimeter MSE walls use the VSoL polymeric strip system to AASHTO LRFD 10th Edition (2024), with precast RC facing panels (180 mm, 35 mm GFRP cover, $\varphi = 35°$ fill, $q = 18$ kPa trafficable live load). Polymeric reinforcement removes chloride-corrosion risk in the tidal/splash zone, and MSE walls typically cost 30–50% less than cast-in-place concrete walls of equivalent height (FHWA-NHI-00-043, 2001).

7 SUSTAINABILITY: PRECAST ARCH + MSE VS CONVENTIONAL RC

The ECSMGE 2024 LCA (Malekmohammadi and Damians, I.P.) compared an Arch+RSW solution against a conventional cantilever/RC deck bridge using ISO 14040 and ReCiPe 2016. The Arch+MSE solution achieves ~85% lower Global Warming Potential, ~82% lower Cumulative Energy Demand, and ~47–50% lower construction cost, driven by near-elimination of rebar and substitution of bulk concrete with compacted soil and polymeric reinforcement. At Naia Island, arch concrete volume is approximately 65–68% less than an equivalent RC box per linear metre.

Criterion	Precast RC Arch + MSE	Conventional RC Box Culvert
Concrete / rebar	55–70% / 30–45% less	Baseline (100%)
GWP / CED	~85% / ~82% lower	Baseline
Construction cost	~47–50% lower	Baseline
Settlement tolerance	≤ 50 mm (two-hinged arch)	Low — rigid structure
Span capability	Up to 30+ m	Typically ≤ 6 m per cell

Table 3: Comparative assessment — precast arch+MSE vs conventional RC box culvert (Malekmohammadi et al. 2024; FHWA-NHI-00-043).

8 ANALYSIS METHODOLOGY

Staged 2D plane-strain FEA (LUSAS v22.0) models arch installation, Zone B/A fill placement, road structure, the six hydrostatic cases and HL-93 traffic loading, with partially cracked arch stiffness (AASHTO 4.5.2.2) and arch-fill interface friction $\delta = 20°$. Load combinations follow Strength I and Service I per AASHTO LRFD 10th Edition; CANDE-2025 provides independent culvert verification.

9 CONCLUSIONS

- The precast BEBO arch + VSoL MSE wall combination is a technically and environmentally superior replacement for conventional RC box culverts above ~8–10 m span, reducing concrete volume by 65–68% and rebar by 30–45%.
- The LCA (Malekmohammadi and Damians, I.P. ECSMGE 2024) quantifies ~85% lower GWP, ~82% lower CED and ~47% lower construction cost for Arch+MSE versus conventional RC.
- MSE walls cost 30–50% less than cast-in-place RC walls (FHWA-NHI-00-043), tolerate differential settlement, and permit rapid, formwork-free construction.

- Six tidal hydrostatic load cases and buoyancy are addressed in staged 2D FEA, yielding a Design Water Level of +3.78 m DMD against a 2.2 m tidal range.
- The multi-layered durability strategy delivers a predicted service life exceeding 81 years (ACI Life-365 / fib Bulletin 34), surpassing the 75-year target and fully consistent with CIA Z7/01 and AASHTO LRFD 10th Edition (2024).

REFERENCES

AASHTO; 2024. AASHTO LRFD Bridge Design Specifications, 10th Edition. Washington D.C.

AECOM Middle East; 2025. Geotechnical Investigation Report USI-AEC-GT-INF-RPT-XX-00001.

CIA (Concrete Institute of Australia); 2014. Z7/01 Recommended Practice: Durability Planning. Engineers Media, North Sydney.

fib; 2006. Model Code for Service Life Design (Bulletin 34). Lausanne, Switzerland.

FHWA; 1992. Observed Behavior of a Concrete Arch Culvert. Univ. of Texas Ferguson Structural Eng. Laboratory.

FHWA-NHI-00-043; 2001. Mechanically Stabilized Earth Walls and Reinforced Soil Slopes — Design and Construction Guidelines.

ISO; 2006. ISO 14040: Environmental Management — Life Cycle Assessment. Geneva, Switzerland.

Malekmohammadi, K., Moncada, A., and Damians, I.P.; 2024. Concrete arches and reinforced soil: a sustainable alternative structure for road bridges. ECSMGE 2024, Lisbon, Portugal.

McGrath, T.J. et al.; 2002. NCHRP Report 473: Recommended Specifications for Large-Span Culverts. TRB, Washington D.C.

VSL Middle East LLC; 2026. MSE Wall Design Report — Naia Island, Dubai. VSoL Polymeric Strip System.

Young Engineering Consultancy Services (YECS); 2026. Engineering Durability Study — Naia Island Arch Culverts.

REINFORCEMENT OF A HUGE LANDSLIDE IN NORTHERN ITALY THROUGH A GEOGRID REINFORCED STEEP SLOPE 60.0 M HIGH

Daniele Cazzuffi[1], Piergiorgio Recalcati[2]

[1] CESI SpA, Milano (MI) - Italy
E-mail: daniele.cazzuffi@cesi.it , web page : https://www.geosyntheticssociety.org/

[2] Tenax SpA, Viganò (LC), Italy
E-mail: piergiorgio.recalcati@tenax.net, web page: www.tenax.net

Key words: Soil reinforcement, Reinforced fill structures

Abstract: *In July 1987, a major landslide occurred in Northern Italy that required significant remediation work. This paper presents the event details as well as the mitigation solutions that took place. More than 45 million cubic meters of rock avalanche collapsed, falling from the right-hand side of the valley into the river bed, 1200 m below, and running up about 300 m on the opposite side. The landslide destroyed some villages directly underneath, while a catastrophic water and debris wave hit the villages located up to 1.0 km upstream along the valley. The landslide body created a natural homogeneous dam 80 m high and 2.0 km long, completely closing the valley and thus creating an artificial lake behind it. The left-hand side of the valley, not hit directly by the landslide, was covered by debris. The main goal that guided the design choices was restoration of the valley's original shape before the landslide. It was necessary to reach the bottom of the river and excavate the deposited debris as much as possible and to the depth that was safely achievable, and to remove the debris on the left side of the valley. In order to avoid geotechnical instabilities, the left-hand side was reconstructed using temporary anchored sheet pile walls and soil reinforced slopes. The whole slope was reconstructed with 6 geogrid-reinforced slopes, each is 10 m high, separated by berms, totaling a height of 60 m. The slope inclination was 60° with a roadway over the base slope.*

The type of geosynthetics used for slope reinforcement were uni-axial extruded HDPE geogrids, the peak tensile strength ranged from 45 to 90 kN/m; the spacing was kept constant and equal to 700 mm. Wrap around technique with sacrificial welded wire steel mesh formworks at the face were used. The excavated material, consisting of gravel in a sandy-gravel matrix with negligible fines content, was used as a fill material after proper sieving using a site screen to limit the maximum grain size to 150 mm.

This is one of the tallest structures ever designed and constructed in Europe and one of the tallest in the world. The whole project (excavation and reconstruction) started in 2010 and finished in 2012. During 2013, the slopes were attacked by fire; an inspection of the site confirmed the slope stability was not compromised and additional testing on exhumed geogrids confirmed that also the geosynthetics didn't exhibit any substantial damage. In addition to the description of the event and site geology, the presentation addresses the design and construction aspects, as well as the inspection and testing operations that were adopted following the fire, together with the continuous monitoring of the huge structure.

(a)

b)

c)

d)

e)

Figures: – a) aerial view before and after the landslide; b-c) construction phase; d) fire damage to the slope; e) overall conditions after assessing the fire impact.

DISPLACEMENT MODEL FOR THE HORIZONTAL DEFORMATION OF REINFORCED SOIL WALLS FROM LEM CALCULATIONS

Pietro Rimoldi

Civil Engineering Consultant
Via Perini 18, 20157 Milano, Italy
E-mail: pietro.rimoldi@gmail.com

Key words: Reinforced soil wall, Horizontal deformations, Limit Equilibrium Calculations

Abstract. *A model for obtaining the horizontal displacements of reinforced soil walls directly from the results of LEM calculations in SLS conditions is presented; the isochronous curves of the reinforcement are used to evaluate the strains associated with the tensile force values, at different elapsed time; the integral of the strains along each layer provides the horizontal displacement for that layer; corrections are used to reduce the displacements taking into account the stiffness of the facing system and the presence of total or partial restrain at toe.*

1 INTRODUCTION

An analytical model is presented for obtaining the horizontal displacements of reinforced soil walls directly from the results of Limit Equilibrium Method (LEM) calculations in Serviceability Limit State (SLS) conditions (Rimoldi, 2018).

2 DISPLACEMENT MODEL

The proposed Displacement Model (DM) is applicable to reinforced soil walls, with either simple or complex geometry; reinforcements are primarily geogrids, or woven / knitted geotextiles, using the proper soil interaction factor for pullout. The DM is derived from LEM stability calculations, and it is aimed to calculate the wall face deformations at the end of construction and at the end of the design life. The DM has been developed based on the following assumptions (see Fig. 1):

- Geogrids will not pull out of soil, since the wall is designed such that the anchorage length L_a is large and the Factor of Safety for pullot FS_{po} is always > 1.0 for each geogrid layer;
- Therefore, each geogrid can elongate but it cannot pull out of the soil behind the potential failure line; hence strains in geogrids can occur only towards the wall face;
- Each geogrid will strain at any point at distance X_j from the face proportionally to the tensile force in that point $T(X_j)$, that is:

$$\varepsilon(X_j) = f(T(X_j)) \tag{1}$$

where: $\varepsilon(X_j)$ = strain in the geogrids at distance X_j from the wall face.

- The function $f(T(Xj)$ is derived from the isochronous curve of the geogrids at the selected time t. The DM uses the isochronous curves of the geogrids at 1 - 3 months and 120 years, which are obtained from tensile creep test results at different temperatures, elaborated on the basis of the principle of time – temperature superposition, valid for polymeric products; these curves are usually expressed in the form $T = f(\varepsilon)$; but for using Eq. (1) the isochronous curves need to be converted into the form $\varepsilon = f(T)$. Usually these curves can be expressed, with very good approximation, by a third order polynomial function (for extruded geogrids) or by a fifth order polynomial function (for woven / knitted and bonded geogrids), hence in general:

$$\varepsilon = a\, T_{\%}^{5} + b\, T_{\%}^{4} + c\, T_{\%}^{3} + d\, T_{\%}^{2} + e\, T_{\%} \qquad (2)$$

where: $T_{\%} = T / T_{ult}$, T = tensile strength under consideration (kN/m); T_{ult} = ultimate tensile strength of the geogrids (kN/m); a, b, c, d, e = parameters of the polynomial function;

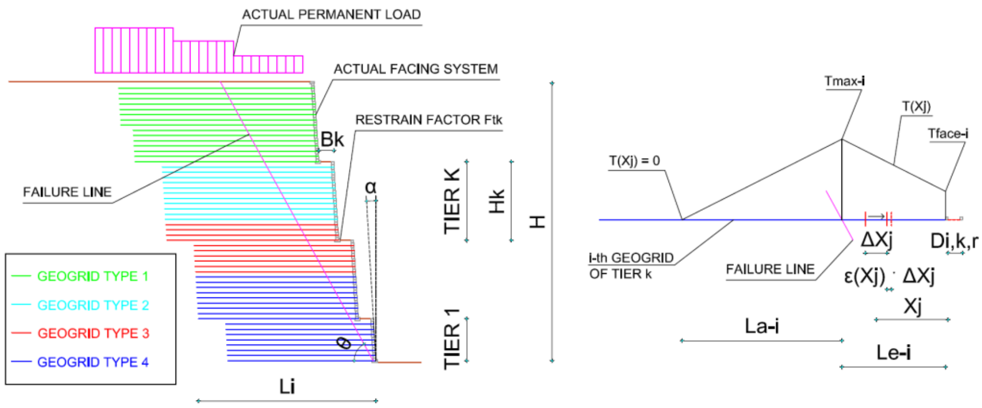

Figure 1. Scheme of the Displacement Model

- Perfect congruency is assumed between the strains and displacements of the geogrids and of the soil interlocked in the geogrids, hence: since the geogrid cannot strain towards the back, it can only strains forwards, towards the wall face; the displacement at point X_j is contrasted by the soil between X_j and the face, which will compress and react as a spring with dashpot;
- Along the potential failure line, in the point where the maximum tensile strength T_{max} occurs, at distance L_e from the face, the geogrid will elongate and the soil will move congruently with the geogrid; but the soil between the face and the potential failure line will resist the movement and will produce a counter thrust, which in turn will reduce the tensile force and the strain in the geogrid from the failure line towards the face;
- In the tie-back method used for designing reinforced soil walls with extensible reinforcement, the potential failure line is assumed to coincide with the Rankine failure line, that is a straight line with inclination θ equal to:

$$\theta = (45 + \varphi / 2) \qquad (3)$$

where: θ = inclination of the potential failure line on horizontal; φ = friction angle of fill soil.
- The distance $L_{e\text{-}i}$ between the wall face and the failure line for the i-th geogrid at elevation h_i on the base (part of tier k of the wall) considering the face batter α (constant for all tiers), is:

$$L_{e\text{-}i} = (h_i / \tan\theta) - (k - 1) \cdot B_k - h_i \tan\alpha \qquad (4)$$

where: h_i = elevation of i-th geogrids on the wall toe (m); k = consecutive tier from bottom; B_k = width of berm on top of tier k (m); α = batter of wall face from vertical (deg).
- The tensile force at face T_{face} depends on the distance between the face and the potential failure line; assuming that the variation of T between T_{max} and T_{face} is approximately linear, it is possible to evaluate $T_{face\text{-}i}$ for the i-th geogrid layer, as:

$$T_{face\text{-}i} = T_{max\text{-}i} \cdot (H - h_i) / H \qquad (5)$$

where: H = wall height (m). In favor of safety, the following limitation can be set:

$$T_{face} \geq 0.4\, T_{max} \qquad (6)$$

- At the other side of the potential failure line the tensile strength of the geogrids will decrease according to the pull out resistance provided by the soil interlocked in the geogrids. The anchorage length L_a is the length beyond the failure line required to fully anchor the tensile strength T_{max}. At distance L_a from the failure line the tensile strength of the geogrids is assumed to become equal to zero. The anchorage length L_{a-i} for the i-th geogrid can be calculated with the pullout equation:

$$L_{a-i} = T_{max-i} / (2 \, f_{po} \cdot \sigma_{vi} \cdot \tan \varphi) \tag{7}$$

where: f_{po} = pullout factor; σ_{vi} = vertical stress on the i-th geogrid (kPa); φ = friction angle of fill soil (deg). Considering that the displacements calculation is performed in serviceability conditions, the vertical stress σ_{vi} in Eq. (7) shall be calculated as the geostatic pressure due to the self-weight of the soil above and the permanent surcharge, without any accidental surcharge.

- At distance L_{a-i} from the failure line the tensile strength of the geogrids is assumed to become equal to zero, hence:

$$T(X_j) = 0 \quad \text{for } X_j \geq (L_{e-i} + L_{a-i}) \tag{8}$$

- Assuming that the variation of $T(X_j)$ between T_{max} and T_{face}, in the active wedge, and between T_{max} and zero beyond the failure line, is linear, the tensile strength in the i-th geogrid at any point X_j is:

$$T_i(X_j) = T_{face-i} + (T_{max-i} - T_{face-i}) \cdot X_j / L_{e-i} \qquad \text{for } X_j \leq L_{e-i} \tag{9}$$

$$T_i(X_j) = T_{max-i} - T_{max-i} \cdot (X_j - L_{e-i}) / L_{a-i} \qquad \text{for } X_j > L_{e-i} \tag{10}$$

- If the face cannot resist the movement of the soil, then each segment of geogrids will strain and the soil will move forwards without any contrast; therefore, in the situation where the wall has no facing or very flexible facing, the residual tensile strength of the geogrids at the face T_{face} will be equal to zero (or according to Eq. 6), and the displacement D_{ik} of the wall face at the i-th geogrid level of tier k will be equal to the integral of the elongations of the i-th geogrid:

$$D_{ik} = \Sigma \, \varepsilon(X_j) \cdot \Delta X_j \tag{11}$$

where: X_j = distance of j-th point along the geogrid from the face (m); ΔX_j = calculation segment over which ε can be considered as constant (m);

- If the wall face resists to horizontal displacements, then the residual tensile strength of the geogrids at the face T_{face} will be higher than zero, yet lower than T_{max}; such tensile strength T_{face} will stress the face elements; if these elements resist the stress (by friction, interlocking, mechanical connection, etc.) then they will produce a force that is equal and opposite to the tensile force T_{face}. The displacement of the face D_{ik} will still be given by Eq (11) but the distribution of $T(X_j)$ will be different than in the previous case.
- If there is a restrain at the toe of the wall and at the toe of each tier, like a foundation slab which limits or totally prevents the horizontal movement of the toe itself, the displacement D calculated with Eq. (11) has to be reduced accordingly; such reduction will be maximum at toe and lower and lower while the height over the toe or the berm increases. We can reasonably assume that the decrease in horizontal displacement is inversely proportional to the height over the toe or berm. Moreover, we have to consider the consistency of restrain, through a Restrain Factor F_t, which will assume the value of 1.0 for perfect restrain, and a value of zero for no restrain. Hence for the i-th geogrid layer of tier k, considering perfect restrain at toe, the reduced horizontal displacement for the i-th geogrids becomes:

$$D_{i,k,r} = D_{i,k} \cdot (1 - (H_k - h_{i,k}) / H_k) \tag{12}$$

where: $D_{i,k,r}$ = reduced horizontal displacement of the i-th geogrid layer tier k due to restrain at toe (m); $D_{i,k}$ = horizontal displacement of the i-th geogrid layer of tier k without restrain at toe (m); H_k = height of tier k (m); $h_{i,k}$ = height of the i-th geogrids on the toe of tier k (m)

- When specifically dealing with the general situation of tiered walls (where a simple wall can be considered just a tiered wall with 1 tier only), the following considerations are introduced:
- If we take a picture of a tiered wall at 1 - 3 months or 120 years after construction has started, for sure the second tier, third tier, etc., will have travelled sitting on first tier, second tier, etc., hence the final position of the face has to take into account all the successive movements of what is below; but the movement of the second tier as a consequence of the movement of the first tier is like shifting forward the seat of the car, yet the passenger of the second tier doesn't get an internal deformation of itself as a consequence of the seat movement; moreover, if we stack some shoe boxes and we move slowly the bottom box, all other boxes will move as well, but these other boxes will not deform.
- About the movement of the tier on top as a consequence of the movement of the tier at bottom: the present DM is derived from LEM calculations, hence displacements are calculated for each layer based on the tensile strength generated in geogrids when the wall is fully built; therefore the successive displacements of each layer and hence of each tier are already synthetically included; hence the displacements calculated by the DM are already the final ones after all construction steps and related movements have occurred.
- The displacement produced by the tier below on the tier above has the equivalent effect of a non-perfect restrain at toe of the tier above. Hence this effect can be introduced in the DM in a simple and rational way by limiting the restrain at each tier toe, through the now introduced Restrain Factor at toe F_t; only if F_t is set equal to 1.0 the restrain is perfect and the toe of each tier will not move at all; while for $F_t < 1.0$ the toe is allowed to get a portion of the horizontal movement of the tier below. - Hence with partial restrain at toe Eq. (11) becomes:

$$D_{i,k,r} = F_{tk} \cdot D_{i,k} \cdot (1 - (H_k - h_{i,k}) / H_k) \quad (13)$$

where: F_{tk} = Restrain Factor at toe of tier k (F_{tk} = 1 for perfect restrain, that is no horizontal movement at toe; F_{tk} = 0 for no restrain, that is free horizontal movement at toe.

- The serviceability limit shall refer to post construction displacements, which are equal to the difference between the displacements at 120 years (or at set post construction time) and the displacements at 1 - 3 months; such differential displacement is due to the tensile creep of the geogrids; hence for the serviceability limit we shall consider:

$$\Delta D_{i,r} = D_{i,k,r}\,(t = 120 \text{ years or set time}) - D_{i,k,r}\,(t = 1 - 3 \text{ months}) \quad (14)$$

- The post construction creep strain of the structure can be calculated as:

$$\Delta\varepsilon_{ij\text{-structure}} = \Delta D_{i,r} / L_i \quad (15)$$

where: L_i = total length of the i-th geogrid (m).

REFERENCES

Rimoldi, P.; 2018. Horizontal displacements of reinforced soil walls from Limit Equilibrium calculations. Proc. of the 11th Int. Conf. on Geosynthetics, Seoul, Korea, September 2018, 14 p.

DESIGN AND DURABILITY OF POLYMERIC-COATED STEEL WOVEN WIRE MESH REINFORCEMENTS UNDER THE NEW EUROCODE 7-3 (2025) FRAMEWORK

Francesco Masola[1], Marianna Lucia Ferrara[2], Paolo Gualandi[3] and Pietro Rimoldi[4]

[1] Maccaferri Central Europe s.r.o., Senica, Slovakia
E-mail f.masola@maccaferri.com , web page: https://www.maccaferri.com/

[2] Officine Maccaferri S.p.A., Bologna, Italy
E-mail: m.ferrara@maccaferri.com , web page: https://www.maccaferri.com/

[3] Maccaferri Central Europe s.r.o., Senica, Slovakia
E-mail p.gualandi@maccaferri.com , web page: https://www.maccaferri.com/

[4] Civil Engineering Consultant, Milano, Italy
E-mail pietro.rimoldi@gmail.com

Key words: double-twisted wire mesh, PWM reinforcement, Eurocode 7

Abstract. *The new Eurocode 7 – Part 3 (EN 1997-3:2025) introduces a dedicated framework for the design of reinforced fill structures employing polymeric-coated steel woven wire mesh (PWM) reinforcement. This contribution presents an integrated overview of the Eurocode-based procedure, the underlying durability mechanisms, and the implications for design practice by aligning material characterization, damage evaluation, and corrosion modeling within a unified reduction-factor framework.*

1 INTRODUCTION

Reinforced soil structures are currently built using three main families of reinforcement products: fully polymeric geosynthetics (GSY, including geogrids, geotextiles, geostrips), polymeric-coated steel woven wire meshes (PWM) and purely metallic reinforcements such as steel strips, bars or welded wire meshes. In PWM, the tensile resistant elements are low-carbon steel wires, generally protected by a zinc–aluminum metallic coating and an external polymeric coating (e.g. PVC, PE, PA, polyolefin), whereas geosynthetics rely entirely on polymeric tensile members and purely metallic systems rely only on steel with metallic coatings. The differing composition leads to markedly different mechanical and durability behavior under installation damage and long-term environmental exposure.

The new Eurocode 7 Part 3 “Geotechnical structures” introduces explicit rules for reinforced fill structures, including slopes, walls, abutments and basal reinforcement. Within Chapter “9.3 Materials” of EN 1997-3 (2025), PWM are defined as a separate category of reinforcing element, with specific provisions for characteristic tensile strength, reduction factors for durability and partial factors for ultimate limit state verification. In parallel, recent research has proposed test-based procedures to determine reduction factors for PWM that are compatible with EN 10223-3, EN 17738, ISO and ISO/TS 20432.

The design and durability assessment of PWM under the new Eurocode 7-3 framework can be consistently implemented using a set of laboratory and full-scale tests that quantify mechanical damage, coating degradation and corrosion of the steel core.

2 REDUCTION FACTORS AND DURABILITY ACCORDING TO EUROCODE 7-3 DESIGN FRAMEWORK

Chapter 9.3.5 of EN 1997-3 (2025) states that the representative tensile resistance is obtained from the characteristic tensile strength multiplied by the specific factor η_{pwm}. The reduction factor for PWM shall be determined as $\eta_{pwm} = \eta_{dmg} \cdot \eta_{cor}$, where η_{dmg} accounts for the adverse effects of mechanical damage during transportation, installation and execution, and η_{cor} accounts for degradation by corrosion over the design service life. The same clause notes that η_{dmg} may be assessed by EN 17738 testing and that η_{cor} is based on the residual strength of the product when wires exposed to corrosion, due to the loss of integrity of the coating, are assumed ineffective.

The installation damage to PWM typically produces negligible immediate loss of steel tensile resistance, but local nicks in the coating can expose the steel wire and trigger long-term corrosion. As a conservative design assumption, the durability evaluation of polymeric-coated steel wire mesh geosynthetics requires assessing the number of wires that can be considered instantly corroded at the points where the polymeric coating is damaged and the steel wire is exposed. Hence, in this case, the effect of installation damage can be evaluated by the following procedure, which is consistent with ISO/TS 13434:2007 “Geosynthetics – Guidelines for the assessment of durability” (Fig. 1): perform the installation-damage procedure; retrieve the damaged specimens; carry out a visual and microscopic inspection to identify the points where the steel wire became exposed; cut the steel wires at the points where they were exposed (taking into account that multiple instances of damage on the same steel wire are counted as one exposed wire); perform tensile tests according to ISO 10319:2015 on the reference and the damaged specimens; the ratio of the tensile strength of the specimens with the cut damaged wires to that of the specimens with no cuts provides the minimum retained strength.

Figure 1. Schematic procedure for installation-damage assessment and identification of exposed wires

For practical purposes, the steel wire can be considered totally corroded in a very short time at the point of coating damage; that is, the steel wire can be considered instantly corroded or, equivalently, totally cut and no longer contributing to the tensile strength of the steel mesh. This conservative assumption allows the effect of mechanical damage to be included in the η_{cor} partial factor.

Table 1 shows typical values of η_{cor} and η_{dmg} factors for PWM with different types of fill.

Material	Maximum particle size (mm)	η_{cor}	η_{dmg}
Crushed stones	200	0.82	1.00
Coarse gravel	38	0.87	1.00
Sandy gravel	9.5	0.95	1.00
Sands	2	1.00	1.00
Silts and clays	0.06	1.00	1.00

Table 1. Typical values of η_{cor} and η_{dmg} factors for PWM with different types of fill

3 CONNECTIONS AND INTERFACE FRICTION

EN 1997-3 requires verification not only of tensile rupture, pull-out, and direct shear of reinforcing elements, but also of the structural resistance of facings and of the connections between reinforcing elements and facing units. The standard further states that where the connection relies purely on friction, the shear resistance between facing elements and reinforcing elements shall be verified.

The two connection concepts relevant for reinforced fill practice are mechanical connections and friction-based connections between the front element and the reinforcement. For integrated systems fabricated from one continuous double-twisted mesh element, the facing and reinforcement are manufactured as a continuous piece, avoiding discrete mechanical connectors and therefore limiting local connection weak points; however, local facing stability still requires verification.

It has to be noted that for tall structures the PWM reinforcement is considered as secondary reinforcement, while the primary reinforcement is usually a high strength geogrid, connected to the PWM by friction on the overlapped length.

An extensive laboratory test campaign (Kiwa, 2024) measured the interface friction between PWM and two types of geogrid reinforcement. The tests, shown in Fig. 2, provided the interface friction coefficients for pull-out (k_{pg}) and direct shear (μ_{pg}) for a front element made of polymeric-coated steel woven wire mesh combined with a geogrid reinforcement, as shown in Tab. 2. These values are directly relevant because EN 1997-3 requires direct-shear resistance along the interface between fill and reinforcing element to be verified using representative interface parameters determined from tests or comparable experience.

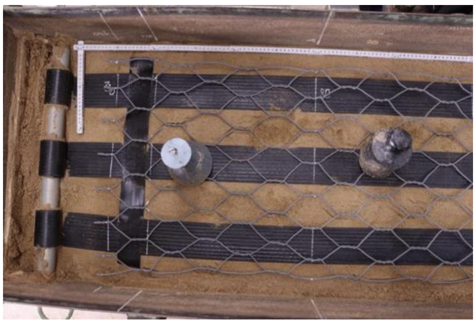

Figure 2. Tests on interface friction between PWM and geogrid reinforcement

Material	Average k_{pg}	Average μ_{pg}
Extruded geogrid + PWM	0,58	0,37
Woven geogrid + PWM	0,60	0,39

Table 2. Pull-out test results in soil: coefficient of interaction between geogrids and PWM

4 MATERIAL DURABILITY AND DESIGN IMPLICATIONS

The durability of PWM reinforcement depends primarily on the ability of the coating system to keep the steel wire isolated from aggressive soil conditions over the intended service life.

Interpretation of thermal-aging tests on the polymeric coating by Arrhenius regression yields a service-life estimate greater than 250 years at 30°C (TRI, 2026), while additional oxidation-induction data suggest even longer protective potential under moderate temperatures.

Tests using the ASTM A975-21 procedure on Maccaferri Polimac-coated PWM (Rimoldi et al, 2023) have shown that the maximum corrosion length (mm), even at very low pH (acid environment with pH lower than 0.2), is always less than one mesh repetition and tends to reach a plateau after approximately 1500 h, as shown in Fig. 3. Since the length of corrosion penetration is less than half the twisted length, corrosion occurring in one wire will not affect any other wire of the hexagonal mesh; hence the effect of corrosion is limited to the single wire where the damage occurred, which is considered instantly corroded for the evaluation of η_{cor}.

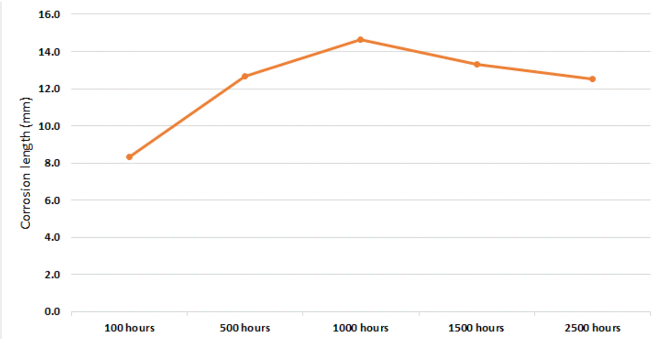

Fig. 3. Length of the corrosion penetration along the Polimac coated steel wire vs immersion time at pH=0.137

The new code framework therefore improves consistency in durability verification, clarifies the role of connection and facing checks, and provides a rational basis for long-service reinforced fill structures based on PWM reinforcement.

5 CONCLUSIONS

EN 1997-3:2025 provides an explicit and technically consistent basis for the design of reinforced fill structures using PWM reinforcements. The standard recognizes that these reinforcements require a dedicated resistance model because their steel core carries the tensile load, whereas their long-term performance is controlled by the protective coating system and by the localized onset of corrosion at damaged points.

REFERENCES

EN 1997-3:2025. Eurocode 7: Geotechnical design – Part 3: Geotechnical structures.

KIWA, 2024. Determination of pull-out resistance according to DIN EN 13738. KIWA GmbH, Germany.

Rimoldi, P, Vicari, M., Trovato, F., 2023. Determination of the Reduction Factors applied to polymeric coated steel woven wire mesh reinforcement in new Eurocodes. Proc. 12th Int. Conf. Geosynth., Roma, Italy.

TRI, 2026. Accelerated aging of PoliMac coating: Equivalent to 250 years at 30 °C. TRI Europe, Mazowieckie, Poland.

CONSTRUCTION TOLERANCES AND SERVICE-LIFE ASSESSMENT OF GEOSYNTHETIC REINFORCED SOIL STRUCTURES WITH VERTICAL FACINGS

J. E. Jaramillo Castro[1], H. Hangen[2]

[1] HUESKER Synthetic GmbH,
48712 Gescher, Germany
E-mail: Jaramillo@HUESKER.de, web page: https://www.HUESKER.com/

[2] HUESKER Synthetic GmbH,
48712 Gescher, Germany
E-mail: Hangen@HUESKER.de, web page: https://www.HUESKER.com/

Key words: Reinforced Soil Retaining Wall, Tolerances, Deformation

Abstract. *Construction tolerances are frequently used as an acceptance criteria to demonstrate that a structure, such as a retaining wall, has been constructed in accordance with the design specificationsFor permanent structures, geometric deviations also form the basis for structural assessment throughout the service life of the asset. Consequently, construction tolerances should not be considered as isolated numerical limits but as part of an integrated engineering process extending from design through construction to long-term inspection.*

In the case of geosynthetic reinforced structures (GRS), EN 14475 already recognises their character as flexible systems that should be designed to accommodate realistic construction tolerances and anticipated deformations. It also contains reference values for construction tolerances depending on the facing system. Nevertheless, practical implementation frequently raises questions regarding measurement procedures, documentation of the completed geometry and the interpretation of measured deviations during subsequent inspections. Shortcomings in the definition of measurement procedures are especially critical for vertical or near-vertical structures, where construction tolerances and subsequent deformations under service loads may result in an unintended outward or negative batter, potentially leading to questions regarding the long-term safety assessment of the structure.

This paper reviews the current approach adopted in EN 14475 and compares it with guidance from specialist foundation engineering, where tolerance management is addressed more systematically throughout the project life cycle. Based on these observations, the paper aims to motivate the discussion on the future evolution of execution standards for GRS as EN 14475, particularly in view of the ongoing implementation of the second generation of Eurocode.

1 INTRODUCTION

Geosynthetic reinforced soil (GRS) retaining structures are now widely used for highways, railways and other transport infrastructure. Advances in reinforcement materials, facing systems and design methods have enabled increasingly slender structures, greater wall heights and the widespread application of near-vertical and vertical reinforced soil retaining walls with a wide variety of architectural facing solutions. At the same time, the role of these structures has evolved. Rather than being regarded solely as earthworks, permanent reinforced soil retaining structures are increasingly considered engineered infrastructure, including bridge abutments, with a service life extending over many decades. The increasing use of vertical facings has also raised expectations regarding geometric accuracy, architectural appearance and long-term structural performance.

This development has consequences beyond structural design. Besides demonstrating ultimate and serviceability limit states, designers, contractors and asset owners are increasingly concerned with construction quality, long-term deformation behaviour and periodic structural inspections.

These aspects are already reflected, for example, in EN 14475, the European execution standard for reinforced soil structures. The standard recognises that reinforced soil structures are inherently flexible and may undergo deformations both during construction and throughout their service life. It further requires that realistic construction tolerances and the expected deformation behaviour of the selected system be considered during design.. Consequently, construction tolerances are not merely workmanship criteria but should be regarded as an integral part of the overall engineering concept.

In practice, however, discussions on construction tolerances often focus primarily on the numerical values specified for individual facing systems. Considerably less attention is paid to the associated measurement procedures, the interpretation of measured deviations between the designed geometry and the as-built geometry (hereinafter referred to in this document as geometric construction deviations), and the documentation required for future structural inspection and assessment. Furthermore, aesthetic imperfections are often not clearly distinguished from geometric deviations that may indicate developing structural problems. These aspects become increasingly relevant because geometric deviations, regardless of their origin, may influence not only future structural assessments but also the contractual acceptance of the completed works and, consequently, have both technical and commercial implications.

Against this background, the treatment of construction tolerances in current execution standards such as EN 14475 deserves further discussion, particularly with regard to the specification, measurement and interpretation of geometric construction deviations. Experience gained in specialist foundation engineering, where these aspects are addressed in a more systematic manner throughout the project life cycle, may provide valuable guidance for this discussion, particularly in view of the implementation of the second generation of Eurocode 7.

2 CONSTRUCTION TOLERANCES – CURRENT GUIDANCE IN EN 14475

In general, detailed design documentation should provide all information necessary for the proper installation of the selected reinforced soil system. During the tender and contract phase, however, neutral execution standards such as EN 14475 often constitute the principal basis for specifying construction requirements.

Although EN 14475 establishes the general engineering principles for the execution of reinforced soil structures, several practical questions arise during their implementation. One example concerns the assessment of local facing geometrical construction deviations.

Annex C of EN 14475 illustrates the determination of local facing geometrical construction deviations by means of a 4 m straightedge (Figure 1 left). While this provides a practical measurement principle, the detailed measurement procedure is intentionally left open to engineering judgement, giving rise to several practical questions, including:

- Where exactly should the straightedge be positioned on the facing?
- Should this measure be repeated in several locations, at the same cross section and in that case, in which interval?
- May it bridge offsets between adjacent facing units or gabion baskets?
- How should local irregularities of natural stone facings be considered?

- Should the maximum measured deviation be reported, or should several measurements be evaluated?
- How many measurements are required to adequately characterise the geometry of the completed wall?
- Should measurements always be carried out at predefined locations to ensure repeatability and thus comparability during future inspections?
- Which surveying accuracy and measurement equipment are appropriate for the intended engineering purpose?

By comparison, standards addressing the assessment of surface flatness in building construction, such as DIN 18202, define not only permissible deviations but also the measurement arrangement, reference lengths and evaluation procedure (Figure 1 right).

This simple comparison highlights the different approaches adopted for the assessment of geometric deviations in conventional concrete structures and GRS structures. It also illustrates the importance of clearly defining the measurement procedure and acceptance criteria from the outset of a project in order to avoid differing interpretations at later stages. Establishing these principles during the planning and tender stages helps to avoid differing interpretations and potential disputes during construction, contractual acceptance, and future structural assessment.

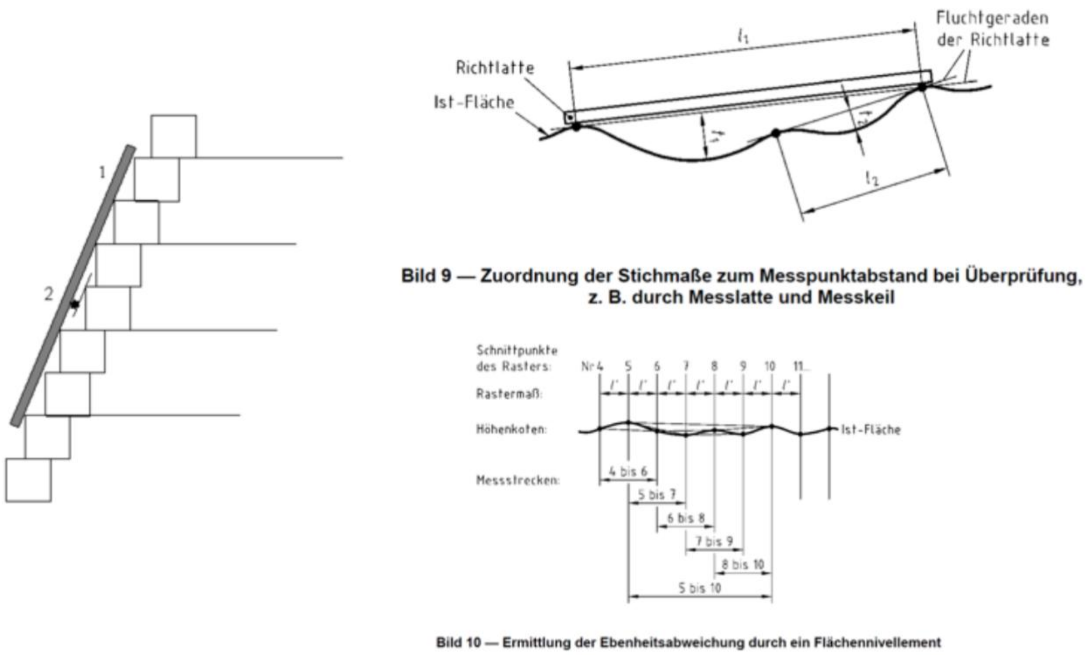

Figure 7. Left: Assessment of local facing deviations using a 4 m straightedge according to EN 14475 (Annex C, Figure C.13). Right: Standardised procedure for determining local deviations from flatness according to DIN 18202.

4 SERVICE-LIFE DEFORMATIONS – ASSESSMENT OF MONITORING RESULTS

Construction tolerances are primarily intended to verify that a reinforced soil structure has been executed in accordance with the design assumptions and the project specification. During the service life of the structure, however, the engineering focus changes. Rather than assessing construction quality, the objective is to evaluate whether the structural behaviour of the completed system remains consistent with the behaviour anticipated during design.

During design, the deformation behaviour of the reinforced soil structure is commonly predicted using appropriate geotechnical models and the available site investigation data. With the introduction of the second generation of Eurocode 7, serviceability limit state (SLS) verification and the prediction of deformations are expected to receive even greater emphasis than in current practice. The design therefore typically includes predictions of settlements, consolidation effects, reinforcement creep and other time-dependent deformations expected throughout the service life of the structure.

Like all geotechnical predictions, however, these assessments remain subject to uncertainty. This uncertainty arises not only from the limitations of numerical models and the inherent variability of soil properties, but also from the fact that the actual boundary conditions during the service life may differ from those assumed during design. Changes in traffic loading, groundwater conditions, climatic influences or adjacent construction activities may all affect the long-term deformation behaviour of the structure. Consequently, the purpose of monitoring is not merely to confirm the design predictions but also to identify changes in structural behaviour resulting from evolving boundary conditions throughout the service life.

One of the major advantages of reinforced soil structures is their inherent deformation capacity. Unlike rigid retaining structures, they are able to accommodate differential settlements and other ground deformations without an immediate loss of structural performance. Consequently, moderate deformations observed during service do not necessarily indicate structural deficiencies but may simply reflect the expected behaviour of a ductile structural system.

Following completion and contractual acceptance of the works, the interpretation of monitoring results therefore requires a different engineering reference. During construction, measured geometric construction deviations are assessed relative to the design geometry. During the service life, however, deformations should be evaluated relative to the documented geometry of the completed structure at the time of acceptance. This documented reference geometry represents the agreed baseline against which future observations should be compared. Additionally, as required, for example, by ZTV-ING (BAST, 2026) in Germany, it is strongly recommended that the design documents for the structure include a stability analysis considering both the predicted geometric construction deviations (based on the construction tolerances) and the anticipated deformations

Accordingly, a measured value alone does not constitute an engineering assessment. Before conclusions regarding the structural behaviour of the completed structure can be drawn, the following questions should be answered:

- What has been measured?
- Where has it been measured?
- When has it been measured?
- How has it been measured?
- Which reference geometry has been adopted?
- For which engineering purpose has the measurement been performed?
- What level of deviation is acceptable from both an aesthetic and a structural perspective?

Only the combination of a clearly defined measurement procedure, a documented reference geometry and a consistent interpretation of monitoring results enable geometric construction deviations to be distinguished reliably from genuine structural deformations occurring during the service life of the structure.

5 LESSONS LEARNT FROM SPECIALIST FOUNDATION ENGINEERING

The challenges discussed above are not unique to reinforced soil structures. Current guidance in specialist foundation engineering (Hauptverband der Deutschen Bauindustrie e.V., Bundesfachabteilung Spezialtiefbau, 2024) treats construction tolerances as part of an integrated quality assurance process covering design, construction, contractual acceptance and the assessment of completed works. Accordingly, the discussion extends beyond numerical tolerance values to include realistic, technically achievable requirements together with clearly defined measurement and assessment procedures.

A key element of this approach is the early dialogue between the client, the designer and the contractor. Rather than prescribing arbitrary geometric requirements, the expected construction accuracy is discussed in relation to the selected construction method, the available equipment and the intended function of the completed structure. Where demanding tolerances are specified, the associated increase in construction effort, surveying requirements and execution costs is recognised at an early stage.

The same engineering philosophy appears equally applicable to reinforced soil structures. EN 14475 already requires that construction should be compatible with the expected deformation behaviour of the selected system and achievable within realistic tolerances. Experience from specialist foundation engineering suggests that these principles can be implemented more effectively if the associated measurement and assessment procedures are discussed and agreed during the planning and tender stage rather than after construction has been completed.

Consequently, project specifications should establish not only both permissible geometric construction deviations and deformations but also the engineering purpose behind them. This includes agreement on:

- functional and aesthetic requirements of the facing;
- realistic and technically achievable construction tolerances;
- measurement procedures and the required survey accuracy;
- documentation of the reference geometry at completion; and
- assessment criteria for deviations identified during construction and deformations measured in future inspections.

Such an approach provides greater transparency for all parties involved and establishes a common engineering basis for contractual acceptance and future structural assessment

8 CONCLUSIONS

EN 14475 already establishes the fundamental engineering principles by recognising the flexibility of reinforced soil structures and the need for realistic construction tolerances of GRS (understood as the permitted geometrical construction deviations). The present paper suggests that these principles should be applied more systematically throughout the entire project life cycle by defining not only achievable limits for geometrical construction deviations but also and equally important the associated detailed measurement procedures. Additionally, it is also important to include a definition for the measurement of deformations after constructions, especially its reference geometry and assessment criteria. In this context and as already defined for other conventional civil structures, construction tolerances, should be considered not only as acceptance criteria but also as an essential element of the long-term assessment of structural behaviour. Since they will be crucial for the definition of the reference geometry to measure the deformation during operation of the structure.

Experience from specialist foundation engineering demonstrates that such an integrated approach improves transparency for all parties involved and establishes a common engineering basis for contractual acceptance and future structural assessment.

Accordingly, the future discussion should focus less on introducing new tolerance limits than on achieving a common understanding of how both geometric construction deviations and deformation are measured, documented and interpreted throughout the service life of permanent reinforced soil structures.

REFERENCES

BASt; 2026. ZTV-ING – Zusätzliche Technische Vertragsbedingungen und Richtlinien für Ingenieurbauten, Gesamtfassung, Teil 1–9, Ausgabe 2026/01. Bundesanstalt für Straßen- und Verkehrswesen (BASt), Bergisch Gladbach, Germany.

CEN; 2009. EN 14475:2006+A1:2009. Execution of Special Geotechnical Works – Reinforced Fill. European Committee for Standardization (CEN), Brussels, Belgium.

CEN; 2024. FprEN 1997-1. Eurocode 7 – Geotechnical Design – Part 1: General Rules. European Committee for Standardization (CEN), Brussels, Belgium.

CEN; 2024. FprEN 1997-3. Eurocode 7 – Geotechnical Design – Part 3: Geotechnical Structures. European Committee for Standardization (CEN), Brussels, Belgium.

DIN; 2019. DIN 18202:2019-07. Tolerances in Building Construction – Buildings. Deutsches Institut für Normung (DIN), Berlin, Germany.

Verein zur Förderung fairer Bedingungen am Bau e.V.; Hauptverband der Deutschen Bauindustrie e.V., Bundesfachabteilung Spezialtiefbau; 2024. Merkblatt Toleranzen im Spezialtiefbau. Berlin, Germany. (in German).

LRFD CALIBRATION OF MSE WALL LIMIT STATES IN THE NEW 2025 CANADIAN HIGHWAY BRIDGE DESIGN CODE

Richard J. Bathurst[1]

[1] GeoEngineering Centre at Queen's-RMC, Department of Civil Engineering,
Royal Military College of Canada, Kingston, Ontario, Canada
E-mail: bathurst-r@rmc.ca, web page

Key words: Soil reinforcement, Load and resistance factor design (LRFD), MSE walls, Canadian Highway Bridge Design Code (CHBDC), Internal stability limit states

Abstract. *Mechanically stabilized earth (MSE) walls constructed with steel and geosynthetic reinforcing elements are now well-established technologies. This extended abstract describes the basic framework of the load and resistance factor design (LRFD) approach that is used for geotechnical design using the most recent edition of Canadian Highway Bridge Design Code (CHBDC). The abstract then explains how measured data from instrumented full-scale MSE walls have been used to calibrate the design equations that appear in the CHBDC for tensile strength, pullout strength and soil failure limit states. A simple closed-form solution is used to carry out the calculation of the resistance factor for the case of a prescribed load factor. The equation is easily implemented in a spreadsheet and thus avoids the use of Monte Carlo simulation which is often unfamiliar to geotechnical engineers, or at least viewed as tedious. The main objective of this abstract is to explain how resistance and load factors that appear in the CHBDC have been computed, and thus give practicing design engineers confidence in their use.*

1 INTRODUCTION

The Canadian Highway Bridge Design Code (CHBDC) (CSA 2025) is the authoritative document in Canada for the load and resistance factor design (LRFD) of geotechnical foundations including mechanically stabilized earth (MSE) walls. The focus of this extended abstract is an explanation of the fundamentals of the internal limits states for MSE walls as found in the CHBDC and how the resistance factors were calibrated.

2 GENERAL

For the case of a limit state design equation with a single nominal load (Q_n) and a single nominal resistance (R_n), the CHBDC requires that:

$$\varphi R_n - \gamma_Q Q_n \geq 0 \qquad (1)$$

where $\varphi \leq 1$ is the resistance factor and $\gamma_Q \geq 1$ is the load factor. The concept is that if this equation is satisfied at time of design, then the designer is assured that a minimum margin of safety against this limit state not being satisfied, is achieved in a probabilistic sense. Internal limit states are shown in Figure 1.

In the CHBDC, the calculation of the nominal load (T_{max}) under operational conditions can be computed using the simplified method, the stiffness method and the coherent gravity method (for inextensible steel reinforcement only). The details of these equations are found in the

CHBDC and in the references that appear at the end of this abstract and are not repeated here. Similarly, there are different pullout equations (models) for the pullout strength of the reinforcement (P_c) depending on the reinforcement type.

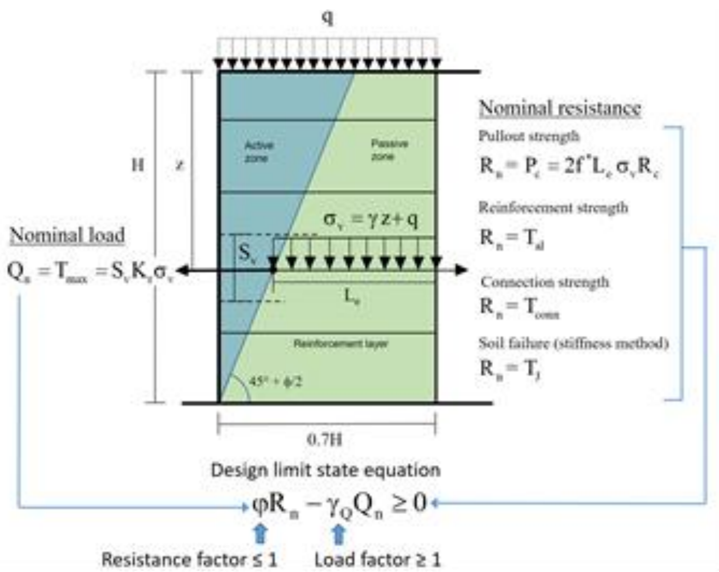

Figure 1: Internal limit states for MSE walls.

LRFD calibration involves determining the magnitude of the resistance factor for a prescribed load factor so that a target probability of failure is satisfied. In contemporary reliability-based design and analysis, this margin of safety is expressed by reliability index β. Figure 2 shows Equation 2 which can be used to calculate the resistance factor for geosynthetic MSE wall internal limit states (Bathurst et al. 2017). This equation is actually a shorter version of the larger equation that appears in the cited reference because correlation coefficients between bias values and nominal values, and between nominal load and nominal resistance terms have been excluded for simplicity. Equation 3 shows that if all statistical quantities remain unchanged, then the resistance factor will increase linearly with load factor for the same target reliability index β.

Uncertainty or variability in nominal load and resistance terms at time of design

Uncertainty due to accuracy of load and resistance models

$$\varphi = \gamma_Q \frac{\left(\dfrac{\mu_{\lambda_R}}{\mu_{\lambda_Q}}\right)\sqrt{\dfrac{(1+COV_{Q_n}^2)(1+COV_{\lambda_Q}^2)}{(1+COV_{R_n}^2)(1+COV_{\lambda_R}^2)}}}{\underbrace{\exp\left\{\beta\sqrt{\ln\left[(1+COV_{R_n}^2)(1+COV_{\lambda_R}^2)(1+COV_{Q_n}^2)(1+COV_{\lambda_Q}^2)\right]}\right\}}} \quad (2)$$

Reliability Index

$$\varphi = K \times \gamma_Q \quad (3)$$

Figure 2: Calculation of resistance factor for limit state functions with lognormal distributions of load and resistance bias values and lognormal distributions of nominal load and resistance values at time of design.

The terms highlighted in yellow are statistical quantities that capture the uncertainty in the estimate of the resistance factor due to the accuracy (bias) of the analytical models (or prescribed values) used to compute Q_n and R_n. Bias (λ) is the ratio of a measured (observed) value to a predicted value. Bias values for each load model have been compiled from measured tensile loads deduced from large databases of instrumented full-scale MSE walls. Each measured value is divided by the corresponding predicted load value using a particular load model for the same wall type. Quantities $\mu_{\lambda Q}$ and $COV_{\lambda Q}$ are the mean and coefficient of variation of the population of collected load bias values, respectively. Similarly, pullout bias statistics have been computed from collections of laboratory pullout tests from tests carried out on reinforcement materials of the same type (e,g., geogrids, geotextiles, PET straps, steel grid and steel strips) and the same soil type (typically sand). Quantities $\mu_{\lambda R}$ and $COV_{\lambda R}$ are the mean and coefficient of variation of the population of collected resistance (pullout) bias values, respectively. The accuracy of any load or resistance model can be understood to improve as $\mu_\lambda \rightarrow 1$ and $COV_\lambda \rightarrow 0$. Lognormal distributions have been shown to provide sufficiently accurate approximations to the distributions for load and resistance bias data; hence, Equation 2 is useful to compute resistance factors.

The green coloured terms in Equation 2 are statistical quantities that quantify the uncertainty in the choice of nominal load and resistance values at time of design. Quantities COV_{Qn} and COV_{Rn}, are the coefficient of variation of the nominal load and resistance values, respectively. A key feature of the CHBDC is the concept of level of understanding that is applied to each limit state calculation at time of design. The three levels of understanding are:

- High understanding: extensive project-specific investigation procedures and/or knowledge are combined with prediction models of demonstrated quality to achieve a high level of confidence with performance predictions;
- Typical understanding: typical project-specific investigation procedures and/or knowledge are combined with conventional prediction models to achieve a typical level of confidence with performance predictions;
- Low understanding: limited representative information (e.g., previous experience, extrapolation from nearby and/or similar sites, etc.) combined with conventional prediction models to achieve a lower level of confidence with performance predictions.

For LRFD calibration of internal limit states for MSE walls, values of COV_{Qn} and COV_{Rn} = 0.1, 0.2 and 0.3 were assigned to high, typical and low levels of understanding. The load factor in Equation 2 is $\gamma_Q = 1.25$ for tensile strength, pullout and connection strength limit states and $\gamma_Q = 1.1$ for the soil failure limit state using the stiffness method. The target reliability indices are $\beta = 2.33$, except for the soil failure limit state which is $\beta = 1.0$. The value of $\beta = 2.33$ corresponds to a probability of failure of the limit state design equation of 1/100 if Equation 1 is just satisfied. This may appear too large, but the MSE walls are highly strength redundant systems with respect to internal stability; when one layer of reinforcement fails, there are other layers to compensate. The combination of load factor $\gamma_Q = 1.1$ and target $\beta = 1.0$ is justified knowing that greater risk of failure can be tolerated for the soil failure service limit state as explained by Bathurst and Allen (2023).

When all other parameters remain constant in Equation 2, the magnitude of the resistance factor will increase with increasing level of understanding. Hence, by investing to improve project understanding, the designer is rewarded with a higher resistance factor leading to a more cost-effective retaining wall solution. Finally, computed resistance factors are rounded to the nearest 0.05 values before appearing in the CHBDC. In some cases, the computed resistance factor will exceed 1.00, in which case the resistance factor is capped at 1.00.

3 CONCLUSIONS

The following are the important points from the work summarized in this abstract:

- A procedure based on rigorous reliability theory was developed to compute resistance factors for internal limit states for geosynthetic MSE walls;
- The accuracy of the load and resistance models (model bias) and uncertainty in the magnitude of nominal load and resistance terms at time of design are considered explicitly;
- Model bias data are available for geogrid (Bathurst et al. 2019), steel strip (Bathurst et al. 2021), steel grid (Bathurst et al. 2025a), polymeric (PET) straps (Bathurst et al. 2025b) for different design load and resistance models;
- The calculation of resistance factors can be done using a spreadsheet and thus Monte Carlo simulation is avoided;
- In LRFD Canadian practice, the designer (and owner) are rewarded with a higher resistance factor for greater quality and quantity of project data to compute load and resistance values, more experience, simple structures, and so on;
- Computed resistance factors using the general approach described here appear in the current and next edition of the Canadian Highway Bridge Design Code (CHBDC)

REFERENCES

CSA; 2025. Canadian Highway Bridge Design Code. CAN/CSA-S6-25. Canadian Standards Association (CSA).

Bathurst, R.J. and Allen, T.M. 2023. LRFD calibration for soil failure limit state using the Stiffness Method. Canadian Geotechnical Journal 60(7): 1006-1014.

Bathurst, R.J., Allen, T.M. and Bozorgzadeh, N. 2025a. LRFD calibration for internal limit states of steel grid MSE walls. ASCE Journal of Geotechnical and Geoenvironmental Engineering 151(9): 04025095-1.

Bathurst, R.J., Allen, T.M., Lin, P. and Bozorgzadeh, N. 2019. LRFD calibration of internal limit states for geogrid MSE walls. ASCE Journal of Geotechnical and Geoenvironmental Engineering 145(11):04019087.

Bathurst, R.J., Bozorgzadeh, N. and Allen, T.M. 2021. LRFD calibration of internal limit states for MSE walls using steel strip reinforcement. ASCE Journal of Geotechnical and Geoenvironmental Engineering 147(12): 04021156.

Bathurst, R.J., Javankhoshdel, S. and Allen, T.M. 2017. LRFD calibration of simple soil-structure limit states considering method bias and design parameter variability. ASCE Journal of Geotechnical and Geoenvironmental Engineering 143(9): 04017053-1-14.

Bathurst, R.J., Miyata, Y. and Allen T.M. 2025b. LRFD calibration of internal limit states for polymer (PET) strap MSE walls. ASCE Journal of Geotechnical and Geoenvironmental Engineering 151(1): 04024140.

DESIGN METHOD OF VENEER COVER SOILS UNDER STATIC AND SEISMIC LOADING CONDITIONS

Fabrizia Trovato[1], Pietro Rimoldi[2], Marianna Ferrara[1] and Giulia Lugli[1]

[1] Officine Maccaferri Spa,
Via Del Faggiolo 1/12, 40132, Bologna, Italy
E-mail: f.trovato@maccaferri.com; m.ferrara@maccaferri.com;
g.lugli@maccaferri.com;
web page: https://www.maccaferri.com/

[2] Consultant, Milano, Italy
E-mail: pietro.rimoldi@gmail.com;

Key words: Soil reinforcement, Soil veneer stability, Landfill applications, Eurocodes 7, Geosynthetics

Abstract. *This paper presents a limit-equilibrium design framework for assessing the stability of veneer cover soils placed on landfill capping slopes. The method is based on the active/passive wedge model proposed by Koerner and Soong and is adapted to the Eurocode 7 Limit State Design framework using the Resistance Factoring Approach. The stability of the veneer is governed by the shear strength of the critical soil-geosynthetic or geosynthetic-geosynthetic interface, the tensile resistance of any intentional reinforcement, and the effects of seismic actions and seepage-induced pore pressures. Particular attention is given to the role of project-specific interface testing, long-term design strength of geosynthetic reinforcement, pseudo-static seismic verification, and drainage measures to limit pore pressure build-up. In this context, engineered multicomposites geosynthetics may provide an effective design solution by combining drainage and reinforcement functions within a single product, thereby improving veneer stability while simplifying the overall capping system.*

1 INTRODUCTION

Landfill capping systems are designed to limit infiltration, control gas emissions and protect the underlying barrier system. They typically consist of several geosynthetic components covered by a thin vegetated soil layer, known as the soil veneer. Veneer stability is a critical design issue because low shear-strength interfaces within the geosynthetic liner system may act as preferential sliding surfaces, especially when pore pressure builds up above the barrier layer. Where interface resistance is insufficient, an intentional geosynthetic reinforcement, such as a geogrid or reinforced geocomposite, can be introduced to provide tensile resistance, while the hydraulic barrier components should not be considered as reinforcement. The proposed methodology is based on the active/passive wedge model by Koerner and Soong, adapted to the Eurocode 7 Limit State Design framework using the Resistance Factoring Approach, and also considers seismic loading, interface shear stress distribution and seepage-induced pore pressures.

2 VENEER STABILITY: ACTIVE/PASSIVE WEDGE MODEL

The analytical model considers a veneer cover soil of uniform thickness h, placed on a slope at angle β above the liner system (Figure 8). Two interacting rigid wedges are separated by a vertical inter-wedge plane at mid-slope:

- Active wedge (upper slope): tends to slide downward; generates an active inter-wedge force EA acting on the passive wedge.
- Passive wedge (toe): resists sliding through friction and cohesion along the liner interface; generates a passive inter-wedge force EP.

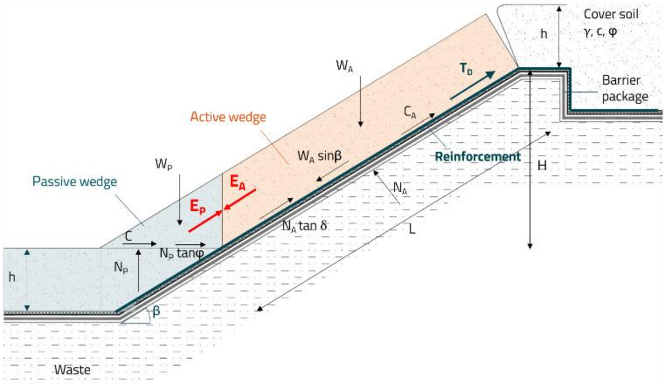

Figure 8: Veneer stability scheme under static gravitational loading with geosynthetic reinforcement (modified from Koerner and Soong, 1998)

Stability is satisfied when FS = $E_P/E_A \geq \gamma_{R,sliding}$ (EC7 sliding resistance factor). From horizontal force equilibrium on the passive wedge:

$$EP = [C + WP \cdot \tan \varphi] / [\cos \beta - \sin \beta \cdot \tan \varphi) \qquad (1)$$

From vertical force equilibrium on the active wedge:

$$EA = (1/\sin \beta) \cdot [WA \cdot (1 - \cos 2\beta - \cos \beta \cdot \sin \beta \cdot \tan \delta) - CA \cdot \sin \beta] \qquad (2)$$

Where WA and WP are the weights of the active and passive wedges; C and CA are the cohesive and adhesive contributions along the relevant shear planes; φ is the friction angle of the cover soil; δ is the interface friction angle between the veneer soil and the underlying liner; and β is the slope angle.

3 EUROCODE 7 LIMIT STATE DESIGN

The active/passive wedge model is implemented within the Eurocode 7 Limit State Design framework. In the proposed methodology, the Resistance Factoring Approach (RFA) is adopted for veneer stability, using the A1+M1+R3 combination.

In this approach, actions are amplified through the A1 factors, geotechnical parameters are used at their characteristic values according to M1, and the calculated resistance is checked against the R3 partial resistance factor. For the Italian National Annex, as adopted in NTC 2018, the relevant values are $\gamma_G = 1.30$ for unfavourable permanent actions, $\gamma_Q = 1.50$ for unfavourable variable actions, and $\gamma_{R,sliding} = 1.10$ for sliding verification. The Ultimate Limit State condition is therefore expressed as:

$$FS = EP/EA \geq \gamma_{R,sliding} = 1.10 \qquad (3)$$

Where E_A and E_P are the active and passive inter-wedge forces calculated using the factored actions and the characteristic geotechnical parameters. Under seismic conditions, the load amplification factors are taken as equal to 1.00, consistently with the seismic design combination.

4 MULTICOMPONENT LINER SYSTEM

In landfill capping applications, the veneer cover soil is placed above a multicomponent geosynthetic liner system, where each layer provides specific functions such as drainage, filtration, separation, protection or hydraulic containment. However, the presence of several geosynthetic layers introduces multiple interfaces, whose shear strength may control veneer stability. Geomembranes and GCLs may be affected by shear stress transfer within the liner package, but they should not be considered as intentional reinforcement elements, since their primary function is hydraulic containment and environmental protection.

4.1 Interface shear stress analysis

The weight of the veneer cover soil generates shear stresses along the interfaces of the geosynthetic liner package. Since veneer stability is often governed by the weakest interface, the interface friction angle should be determined through laboratory testing on project-specific materials, rather than assumed from literature values. Relevant standards include ASTM D5321 and EN ISO 12957-1 for direct shear testing, and EN ISO 12957-2 for inclined plane testing, the latter being particularly suitable for landfill capping due to the low normal stresses applied by the veneer cover.

The shear stress mobilized along the i-th interface can be expressed a:

$$\tau_i=\sigma_N \cdot tan\delta_i \tag{4}$$

where σ_N is the normal stress acting on the interface and δ_i is the interface friction angle of the i-th contact surface. The difference between shear stresses acting above and below each geosynthetic layer may generate tensile or compressive forces within the liner package. These forces should be checked against the Long-Term Design Strength of the relevant geosynthetic layer, ensuring that barrier components such as geomembranes and GCLs are not unintentionally mobilized as reinforcement elements.

7 GEOSYNTHETIC REINFORCEMENT DESIGN

When the stability criterion is not satisfied, a geosynthetic reinforcement shall be introduced below or within the veneer cover soil. This reinforcement is commonly provided by a geogrid, a high-strength geotextile or a reinforced geomat specifically designed to carry tensile loads. The reinforcement provides a design tensile force TD (Figure 8), acting parallel to the slope and opposing the downslope movement of the active wedge. In this model, the tensile contribution reduces the active inter-wedge force and improves the overall stability of the veneer system. The design tensile strength of the reinforcement is obtained from the ultimate tensile strength by applying the relevant reduction factors for installation damage, creep and chemical durability:

$$TD = Tult /(RF_{id} \cdot RF_{cr} \cdot RF_{ch} \cdot RF_b) \tag{5}$$

For short-term construction conditions, creep and durability effects may be neglected and the corresponding reduction factors can be taken as 1.0. For seismic conditions, the event duration is short and the creep reduction factor is also taken as 1.0, while installation damage and durability factors remain applicable.

8 SEISMIC

Seismic and seepage conditions may significantly affect veneer stability and should be considered in the design when relevant. Under seismic loading, the stability assessment can be performed using a pseudo-static approach, where horizontal and vertical seismic forces are applied to the active and passive wedges. The horizontal component acts in the direction of potential sliding, while the vertical component should be checked with both signs, as it modifies the normal stress acting on the critical interface. In seismic conditions, the creep reduction factor for the reinforcement may be taken as 1.0, while installation damage and durability reduction factors remain applicable. The complete formulation of the pseudo-static wedge equilibrium is reported in Rimoldi et al. (2022).

Seepage may also govern the design, as pore water pressures reduce the effective normal stress along the critical interface and therefore decrease the available shear resistance. Two main conditions should be considered: horizontal water build-up from the toe and parallel-to-slope seepage along the liner interface. Both conditions may increase the required reinforcement strength. For this reason, an adequate drainage layer should be provided below the veneer soil and above the barrier system to limit pore pressure build-up. Where both drainage and reinforcement are required, either separate functional layers or engineered Multicomposites geosynthetics combining drainage, filtration, separation and reinforcement functions may be adopted. The analytical treatment of seepage forces is detailed in Rimoldi et al. (2022).

9 CONCLUSIONS

This paper presents a limit-equilibrium framework for the analysis and design of veneer cover soils on landfill capping slopes. The active/passive wedge model proposed by Koerner and Soong is adapted to the Eurocode 7 Limit State Design framework using the Resistance Factoring Approach.

The method highlights that veneer stability is mainly governed by the shear strength of the critical interface within the geosynthetic liner package. Therefore, project-specific interface shear testing is essential for reliable design. Where the available interface resistance is insufficient, a geosynthetic reinforcement can be introduced, provided that its long-term design strength and anchorage are properly verified.

Seismic and seepage conditions may significantly affect the stability of the veneer cover and should be considered when relevant. In particular, pore pressure build-up above the barrier layer can reduce the available shear resistance; therefore, adequate drainage measures are recommended. Where both drainage and reinforcement are required, separate functional layers or engineered Multicomposites geosynthetics may provide effective solutions for improving veneer stability and simplifying the capping system.

REFERENCES

Koerner, R.M. and Soong, T.Y. (1998) Analysis and Design of Veneer Cover Soils. Proc. Sixth International Conference on Geosynthetics, IFAI, Atlanta, Ga., USA: pp. 1–23.

Rimoldi, P., et al. (2022). Application of Eurocode 7 for the analysis and design of veneer cover soils in static and seismic load conditions. Proceedings of the 7th European Geosynthetics Conference, EuroGeo7, Warsaw, Poland.

EN ISO 12957-1/-2. Geosynthetics – Determination of friction characteristics – Part 1: Direct shear test; Part 2: Inclined plane test. International Organization for Standardization, Geneva.

3D NUMERICAL MODELLING OF GEOGRIDS ISOLATED AND CONFINED IN SOIL

Lucas Paiva [1], Robertt Valente [2], António Miguel Paula [3] and Margarida Pinho-Lopes [4]

[1] CERIS, Department of Civil Engineering, University of Aveiro,
Campus Universitário de Santiago, 3810-193 Aveiro, Portugal
E-mail: lucaspaiva@ua.pt, web page: https://www.ua.pt

[2] TEMA, Department of Mechanical Engineering, University of Aveiro,
Campus Universitário de Santiago, 3810-193 Aveiro, Portugal
E-mail: robertt@ua.pt, web page: https://www.ua.pt

[3] GICoS, Instituto Politécnico de Bragança,
Campus de Santa Apolónia, 5300-253 Bragança
E-mail: mpaula@ipb.pt, web page: https://ipb.pt/pt

[4] CERIS, Department of Civil Engineering, University of Aveiro, Portugal
Campus Universitário de Santiago, 3810-193 Aveiro, Portugal
E-mail: mlopes@ua.pt , web page: https://www.ua.pt

Key words: Extruded geogrid, hyperbolic constitutive model; orthotropic response; digital image correlation

Abstract. *This work presents a 3D numerical modelling framework for the mechanical response of geogrids, progressing from in-isolation tensile characterisation to constitutive modelling and then to soil-geogrid interaction. The numerical modelling was carried out using Abaqus®. Detailed geometry and nonlinear hyperbolic constitutive models were calibrated from standard wide-width tensile tests. Building on this, a simple orthotropic formulation based on the Hill48 yield surface was calibrated from multi-directional tensile data and applied to a geogrid-reinforced strip footing. To better explore the potential of 3D numerical models to assess the effects of mechanical damage on the load-carrying capacity of geogrids, these models were combined with an experimental programme in which wide-width tensile tests were performed with full-field strain measurements via digital image correlation (DIC), for both virgin and damaged samples of a geogrid. nalys of strain fields showed load distribution changes due to damage, a pattern that can alter the load transmission pathways and, thus, reduce load-bearing efficiency. Overall, a multi-scale modelling pathway was developed for the case of extruded geogrids.*

1 BACKGROUND

Numerical modelling, particularly through the Finite Element Method (FEM), has become a well-established tool for investigating the mechanical behaviour of geosynthetics, both in isolation and when embedded in soil. FEM offers significant advantages, including the ability to represent complex geometries and boundary conditions, capture soil–geosynthetic interaction, and incorporate nonlinear constitutive models that closely reproduce the response of geosynthetic-reinforced structures. Nevertheless, the calibration of such models remains a persistent challenge, as accurately defining boundary conditions and material properties typically requires a large number of parameters, some of which can only be determined through elaborate testing procedures or iterative trial-and-error approaches. Owing to this complexity, FEM analyses commonly rely on simplifications regarding geometry, material properties, and interface or contact conditions, to maintain computational tractability while preserving the representativeness of the simulated behaviour.

This work presents a three-dimensional numerical modelling framework for analysing the mechanical response of geogrids, progressing from in-isolation tensile characterisation to constitutive modelling simplification and then to soil-geogrid interaction. The work summarised herein has been reported previously, for example by: Paiva et al. (2023, 2025, 2026) and Paiva (2026).

2 MATERIALS AND METHODS

The software Abaqus® was used for the 3D numerical modelling. First, the in-isolation response of geogrids was studied, and then their in-soil response was analysed.

To model the in-isolation response, a two-step process was followed (Paiva et al., 2023): 1) validation of the numerical models using data from the literature; 2) application of the model to represent the in-isolation tensile response of three geogrids. The numerical model was validated using data presented by Hussein and Meguid (2016) referring to a biaxial extruded geogrid. To carry out the validation exercise, the same geometry, constraints and material properties, as defined by Hussein and Meguid (2016), were adopted, varying aspects related to element shape, integration function, mesh and stabilisation. Similarly to Hussein and Meguid (2016), data from uniaxial tensile tests along machine and cross-machine directions were analysed, averaged to obtain a global response of the geogrid. For the case study, a four-step process was followed (Paiva et al., 2023): 1) data on tensile tests of three extruded geogrids was collected, corresponding to five specimens tested per geogrid; 2) an overall load-strain curve was selected to represent each material; for that purpose a data-driven procedure was developed; 3) hyperbolic constitutive models were used to represent the load-strain response of each geogrid, estimating the corresponding parameters; 4) the tensile tests were modelled numerically using 3D models based on the conclusions of the validation exercise and the constitutive models fitted to the experimental response. The case study included data for three extruded geogrids: GG1 and GG2 were polypropylene, biaxial, extruded geogrids, with tensile strength along the machine direction (MD) equal to 20 and 40 kN/m, respectively; GG3 was a high-density polyethylene, uniaxial, extruded geogrid, with tensile strength of 68 kN/m along MD. The wide-width tensile tests modelled were carried out according to EN ISO 10319:2015, using a video-extensometer to measure the deformation of specimens submitted to a strain rate of 20%/min; 5 specimens per geogrid were tested.

A model to represent the typical orthotropic behaviour of extruded geogrids, using data from tensile tests, was later presented by Paiva et al. (2025). Again, a validation exercise was carried out using data from a realistic problem for a geogrid embedded in soil, assessing the influence of orthotropy on the reinforcement and the overall soil–geogrid system.

Lastly, to better explore the potential of 3D numerical models to assess the effects of mechanical damage on the load-carrying capacity of geogrids, these models were combined with experimental programme in which wide-width tensile tests were performed with full-field strain measurements via digital image correlation (DIC), for both virgin and damaged samples of a geogrid (Paiva et al., 2026). Then, Abaqus® was used to define a 3D model of a problem for a footing on soil reinforced with a geogrid. Different scenarios were analysed, including damage conditions similar to those induced for the in-isolation tensile tests.

3 MAIN RESULTS

The three-dimensional numerical modelling of geogrids carried out in Abaqus® was performed by integrating hyperbolic constitutive laws with damage and fracture formulations and validated using wide-width tensile test data. The validation exercised, carried out using data from Hussein and Meguid (2016), allowed identifying optimal modelling parameters. Then, the methodology was validated using in-isolation uniaxial tensile tests on three extruded geogrids. Representative load–strain curves were derived from five specimens per geogrid via a Piecewise Interpolating Polynomial, yielding low coefficients of variation and root-mean-square deviation. Hyperbolic constitutive models were subsequently fitted to these curves, accounting for the variable thickness of the constituent elements. The numerical predictions reproduced the experimental initial stiffness, peak tensile force, corresponding strain, and the location of maximum plasticity with good accuracy. The proposed framework (Paiva et al., 2023) further enables flexible representation of post-peak softening and sudden fracture, offering a robust and replicable tool for simulating the tensile response of geogrids.

The orthotropic modelling framework proposed by Paiva et al. (2025) for the short-term tensile response of geogrids, based on the Hill48 yield criterion, enables direct calibration of orthotropic parameters from standard tensile test data through a data-driven approach. Numerical simulations of in-isolation tensile tests showed good agreement with experimental results, confirming the ability of the model to reproduce the directional stress–strain behaviour of geogrids. When applied to a geogrid-reinforced strip footing, the orthotropic formulation yielded a higher predicted bearing capacity than its isotropic counterpart, indicating that conventional isotropic simplifications may under- or overestimate reinforcement performance, particularly for highly orthotropic materials. These findings support the adoption of orthotropic constitutive descriptions in the numerical analysis of geosynthetic-reinforced systems whenever directional orthotropy is significant.

An experimental programme incorporating digital image correlation (DIC) was combined with the described 3D finite element modelling to calibrate an orthotropic constitutive model capable of reproducing the tensile response of both undamaged and notched geogrid specimens (Paiva et al., 2026). The integration of experimental and numerical in-isolation tensile data helped clarify how localised damage modifies the strain field and, consequently, the internal load transfer pathways within the geogrid. Extending the analysis to the reinforced soil revealed that damage primarily degrades performance by disrupting load redistribution within the foundation, as the loss of continuity narrows the stress-transmission pathways and reduces overall load-bearing efficiency. The proposed methodology therefore provides a quantitative basis for damage assessment in geogrids and illustrates the value of coupling full-field experimental measurements with numerical modelling to elucidate the complex mechanical behaviour of geosynthetic reinforcements.

5 CONCLUSIONS

The findings summarised herein reinforce the broader implication that constitutive calibration cannot be dissociated from geometric representation in geogrid modelling. Predictive analyses must therefore integrate geometry, constitutive anisotropy, and interaction-induced damage rather than address them separately. The results further indicate that a comparatively simple orthotropic constitutive description is capable of supporting both in-isolation tensile analyses and relatively soil–geogrid interaction cases, indicating a possible shift from highly detailed material formulations towards more computationally efficient, application-oriented models. In addition, the assessment of mechanical damage during interaction is substantially enhanced by combining full-field experimental measurements obtained through digital image correlation with three-dimensional numerical interpretation. Taken together, these contributions establish a coherent multi-scale modelling pathway for extruded geogrids, bridging material characterisation, structural response, and damage evaluation within a unified framework.

ACKNOWLEGMENTS

This study was funded by the PRR—Recovery and Resilience Plan and by the NextGenerationEU funds at Universidade de Aveiro, through the scope of the Agenda for Business Innovation ‘‘*Transform - Transformação digital do setor florestal para uma economia resiliente e hipocarbónica*’’ (Project no.34 with the application C644865735-00000007). The first author acknowledges the financial support by the Portuguese Foundation of Science and Technology – FCT under the MIT Portugal PhD Grant PRT/BD/153383/2021. The financial support of FCT is also gratefully acknowledged by the authors through projects UIDB/6438/2025 (https://doi.org/10.54499/UID/06438/2025) of research unit CERIS, UIDB/00481/2020 (TEMA), UIDP/04450/2020 and CENTRO-01-0145-FEDER-022083 (CENTRO 2020).

REFERENCES

Hussein, M., and Meguid, M.; 2016. A three-dimensional finite element approach for modeling biaxial geogrid with application to geogrid-reinforced soils, Geotextiles and Geomembranes 44(3): 295–307. http://dx.doi.org/10.1016/j.geotexmem.2015.12.004

Paiva, L.; 2026. Geosynthetics for sustainable cities: 3D models and mechanical damage. PhD thesis in Civil Engineering. University of Aveiro, Portugal.

Paiva, L., Pinho-Lopes, M., Valente, R., Paula, A.M. (2023). Three-dimensional modelling of in-isolation tensile response of geogrids using hyperbolic constitutive models. Finite Elements in Analysis and Design, 225, 104008. https://doi.org/10.1016/j.finel.2023.104008

Paiva, L., Pinho-Lopes, M., Valente, R. & Paula, A.M. (2025). A simple 3D orthotropic model for the tensile response of geogrids: In-isolation and soil–geogrid interaction applications. Geotextiles and Geomembranes, 53(6), pp. 1687-1698. https://doi.org/10.1016/j.geotexmem.2025.07.010

Paiva, L., Pinho-Lopes, M., Valente, R. & Paula, A.M. (2026). Digital image correlation for mechanical damage assessment in geogrids: experimental characterization and 3D numerical modeling of soil-geogrid interaction. Computers and Geotechnics. 197(September 2026), 108225. https://doi.org/10.1016/j.compgeo.2026.108225

PULL-OUT AND DIRECT SHEAR TESTS ON GEOGRID–RECYCLED AGGREGATE INTERFACES

Maximilien Van Breusegem[1], Nicolas Denies[1], Nathan Lauwers[2]

[1] Buildwise,
23 Kleine Kloosterstraat, Zaventem, 1932, BELGIUM
E-mail: maximilien.van.breusegem@buildwise.be,
E-mail: nicolas.denies@buildwise.be,
web page: https://www.buildwise.be/

[2] Stadsbader,
1 b2 Avenue A. van Osslaan, Bruxelles, 1120, BELGIUM
E-mail: nathan.lauwers@stadsbader.com,
web page: https://www.stadsbader-contractors.be/

Key words: Reinforced fill structures, recycled aggregates, geosynthetics-fill materials interaction, direct shear box tests, pull-out tests

Abstract. *This paper presents the results of laboratory tests conducted on three different geogrids and three types of recycled aggregates. The mechanical behaviour of geosynthetic-recycled aggregate interfaces is investigated using direct shear box tests and pull-out tests. In the construction of reinforced fill structures, most design guidelines traditionally require the use of natural sand and gravel. However, considering the increasing scarcity of natural aggregates and the large quantities of recycled aggregates available worldwide, recycled aggregates are increasingly being considered as a sustainable and cost-effective alternative for the construction of reinforced fill structures.*

1 INTRODUCTION

Historically, natural sand and gravel have been the most commonly used fill material for reinforced soil structures due to their favourable mechanical properties, particularly their high friction angle and excellent drainage capacity. However, the construction sector has been facing an increasing shortage of natural sand resources for several years. This shortage, combined with increasingly stringent environmental constraints, raises important questions regarding the long-term sustainability of current construction practices.

The construction industry has been identified as one of the key sectors in the transition towards a circular economy. Within this context, recycled aggregates are considered a particularly valuable resource because of their widespread availability and favourable mechanical properties. Furthermore, the procurement cost of recycled aggregates is generally significantly lower than that of natural material.

Despite these advantages, the use of recycled aggregates as a substitute for natural sand in reinforced fill structures remains relatively uncommon. Several technical questions still need to be resolved. These include:

- the compatibility of recycled aggregates with the geogrids or geostrips currently used on the market;
- their ability to provide adequate drainage performance when used as reinforced fill material.

To address the first issue, a comprehensive laboratory testing programme was conducted. Direct shear tests and pull-out tests were performed to characterise the interaction between several types of recycled aggregates and geosynthetics (geogrids and geostrips). The objective was to quantify the interface properties and assess the suitability of these materials for reinforced fill structures. Furthermore, this article present one of the first reinforced fill structures in Belgium to be constructed using recycled aggregates.

2 FILL MATERIALS SELECTION

The first phase of the study focused on identifying materials representative of the recycled aggregate market. Particular attention was paid to the particle size distribution of the selected materials, as gradation directly influences the hydraulic conductivity of the fill, its compaction characteristics, and the interaction mechanisms developed at the interface with geogrid reinforcements. The grain-size distribution curves were compared with the recommended application domains defined in LASR guidelines (FHWA, 2021), as well as with the requirements specified in EN 14475 for reinforced fill structures.

Based on these analyses, three recycled materials were selected for further investigation: a mixed recycled aggregate, a recycled sand, and a lime-treated recycled material named Teracalco. The performance of these alternative materials was subsequently evaluated and compared with that of natural sand, which was used as a reference fill material as typically used for the construction of reinforced fill structures in Belgium.

3 LABORATORY TESTS

The friction angles of the selected materials (see Table 2) were determined prior to the direct shear and pull-out testing programme. The results indicate that all recycled materials exhibited higher shear strength than the natural sand. Similar trend has been reported during investigations on the use of recycled aggregates in stone columns (Verstraelen, 2026).

Material	Friction angles φ [°]	
	Peak values	Residual values
Reference - Natural sand	37	33.4
Teracalco	41	39.7
Mixed aggregates	51.5	52.1
Recycled sand	37	35.9

Table 2: Friction angles of the selected fil materials

The direct shear tests were performed by a partner laboratory (laboratory #1) using a large-scale shear box measuring 500 mm × 500 mm x 200 mm (2 × 100 mm in height). Normal stresses of 90, 180 and 270 kPa were applied, corresponding approximately to reinforced fill heights of 5, 10 and 15 m above the geogrid reinforcement, respectively. The maximum horizontal displacement allowed by the testing apparatus was 50 mm. Prior to testing, the fill material was compacted in several layers to reproduce field conditions as closely as possible.

The pull-out tests were conducted by two partner laboratories. The pull-out box has a length of 900 mm. Different normal stresses were applied depending on the laboratory: 10, 20, 50, 70 and 100 kPa in Laboratory #2, and 10, 20 and 30 kPa in Laboratory #3. As for the direct shear tests, the fill material was compacted in successive layers before testing.

The test results are summarized in Table 3 and expressed as interaction coefficients. The interaction coefficient is defined here as the ratio of tan φ_{int} and tan φ. Where φ is the friction angle of the fill material only, tan φ is the ratio of the shear stresses and the normal stresses applied on the surface of the tested material, φ_{int} is the friction angle of the interface *'fill material-geosynthetic'* and tan φ_{int} is the ratio of the shear stresses applied on the interface and the normal stresses applied on the surface of the tested material.

Interaction coefficient *'fill material-geosynthetic'* (based on the maximal value from the test – peak value)					
Type of tests	Type of geosynthetic	Natural sand	Teracalco	Mixed aggregates	Recycled sand
Direct shear box (LAB #1)	Geogrid #1	0.94	0.91	0.68	1
	Geogrid #2	0.92	0.9	0.9	1.01
	Geogrid #3		0.94	0.96	
Pull-out (LAB #2)	Geogrid #1		0.93	0.7	soon expected
	Geogrid #4		0.8	0.64	soon expected
Pull-out (LAB #3)	Geostrip #5		0.51	0.27	0.57

Table 3 : Interaction coefficient *'fill material-geosynthetic'*

A higher interaction coefficient indicates a more efficient transfer of tensile loads from the reinforcement to the surrounding fill. The results highlighted in the green cells of Table 2 allow a direct comparison between the two testing methods, as they were obtained using the same reinforcement and the same fill material. The results highlighted in orange indicate that, for the materials investigated in this study, recycled sand exhibited a higher interaction coefficient than natural sand.

4 APPLICATION ON SITE

In 2025, as part of the redevelopment works on the R4 ring road in Ghent (Belgium), a reinforced fill structure was constructed using recycled aggregates as fill material (see Fig. 1). The design of the structure was based on a conservative design friction angle f' of 27° for the fill material. Although relatively low, this value was deliberately selected to maximise the range of recycled materials that could potentially be used within the project.

The project specifications required the fill material to be compacted to an average dry density corresponding to at least 98% of the Modified Proctor optimum. Field compaction quality was verified using dynamic plate load tests performed on each layer during the construction.

According to the job specifications, a deformation modulus of 11 MPa was sufficient to guarantee the design friction angle f' of 27°. For this project, however, a more stringent acceptance criterion was adopted, requiring a minimum modulus of 17 MPa for every compacted layer. This additional requirement was introduced to ensure a consistently high level of compaction and mechanical performance throughout the whole reinforced fill structure.

The reinforcement system consisted of Huesker FortracT geogrids with nominal tensile strengths ranging from 55 to 150 kN/m, selected according to the local design requirements and loading conditions.

Figure 1: Reinforced fill structure build with recycled aggregates as fill material in the scope of the works on the R4 ring road in Ghent (Belgium)

5 CONCLUSIONS

Based on these preliminary results, the interaction properties of recycled aggregates with geosynthetics commonly used in the Belgian market with a reinforcement function appear to be satisfactory. More specifically, the interaction coefficients presented in Table 3 are generally considered by design engineers to be compatible with safe and economically viable design of reinforced fill structures.

In addition to interface performance, the hydraulic behaviour of recycled aggregates should also be verified on a project-specific basis. Adequate permeability must be ensured in order to provide sufficient drainage within the reinforced fill and prevent the development of excess pore water pressures. This aspect falls outside the scope of the present paper.

REFERENCES

CEN. (2006). EN 14475:2006 - Execution of special geotechnical works – Reinforced fill. European Committee for Standardization (CEN), 2006, Annex A.

FHWA (2021). Mechanically Stabilized Earth (MSE) Wall Fills: A Framework for Use of Local Available Sustainable Resources (LASR) (FHWA-HIN-21-002). Federal Highway Administration, U.S. Department of Transportation.

Verstraelen, J.; 2026. Construire dans l'argile : regard croisé franco-belge – Colonnes ballastées à base de granulats recycles. Journée d'étude franco-belge CFMS-GBMS, 17 March 2026.

EVALUATION OF THE ACCURACY OF ANALYTICAL MODELS FOR PULLOUT STRENGTH USING POLYMERIC STRAPS REINFORCEMENTS

Anibal Moncada[1,2], Ivan P. Damians[1,2,3], and Richard J. Bathurst[4]

[1] Department of Civil and Environmental Engineering (DECA), Universitat Poliècnica de Catalunya (UPC), Campus Nord UPC, 08034 Barcelona, Spain.

[2] International Centre for Numerical Methods in Engineering (CIMNE), Campus Nord UPC, 08034 Barcelona, Spain. (http://www.cimne.com)

[3] VSL International Ltd, Barcelona, Spain

[4] Geoengineering Centre at Queen's-RMC, Civil Engineering Department, Royal Military College of Canada, Canada.

Key words: Pullout tests, polyester strap reinforcements, reinforced soil walls, bias statistics.

Abstract. *This work presents the results of pullout tests carried out to evaluate the performance of PET strap reinforcement at different vertical stresses (or simulated depths). Tests were carried out using a well-graded, granular soil with negligible fines content. Pullout strength behaved non-linearly with respect to vertical pressure. The accuracy of three analytical models (linear and non-linear) used to calculate the friction interaction factor was quantified using bias statistics. Data showed higher spread between measured and calculated values at shallow depths. Model accuracy dependency with calculated pullout strength and vertical pressure was explored. Non-linear pullout models were found to be more accurate, on average, than the linear pullout model.*

1 BACKGROUND

Pullout strength of polymeric straps (P_r in AASHTO (2024) or R_{po} in EN 1997-3 (2025)) will depend on reinforcement geometry (width w, effective length L_e, and the two contact interfaces, i.e., $C = 2$), applied vertical pressure (σ_v), and friction interaction factor (e.g., f'). AASHTO guidelines specify a simple linear equation (Eq. 1). EN 1997-3 uses a differential formulation, which, for a given geometry and vertical stress, is equivalent to the AASHTO formulation. In the case of NF P 94-270 (2020), f' is related to the apparent soil-reinforcement interaction coefficient, $F^*_{(z)}$, which varies with soil gradation and friction angle. The value of $F^*_{(z)}$ decreases linearly with depth up to 6 m, after which it remains constant, similar to the value of F^* for all steel reinforcement types in AASHTO (2024). For the AASHTO formulation, the friction interaction factor is a function of scale factor α to account for reinforcement extensibility ($\alpha = 1$ for inextensible reinforcement, and $\alpha < 1$ for extensible reinforcement), pullout friction factor F^*, which is a function of the soil friction angle (ϕ), and interaction coefficient $R_i = \tan\delta / \tan\phi$ (Eq. 2). R_i has a default value of 0.67 for all polymeric materials (AASHTO, 2024). Pullout strength can be calculated as follows:

$$P_r = f'(C\ w\ L_e\ \sigma_v) \quad (1)$$

In which,

$$f' = \alpha F^* = \alpha R_i \tan(\phi) = \alpha \tan(\delta) \quad (2)$$

Miyata et al. (2019) proposed an exponential pullout model with the interaction factor f' computed as:

$$f' = f_1 + (f_0 - f_1) / \exp(c_0\, \sigma_v / p_a) \quad (3)$$

Here, f_0, f_1, and c_0 are dimensionless coefficients and p_a is the atmospheric pressure (101 kPa) used to normalize the vertical stress term. Other examples of use of an exponential model can be found in the literature (e.g., Pierozan et al., 2022).

The present work evaluates the accuracy of AASHTO, NF and nonlinear pullout friction models using bias statistics with pullout tests data with polymeric strap reinforcements and two types of granular soils.

2 TESTING METHODOLGY

Tests were carried out using a rigid steel box measuring 1250 mm long, 500 mm wide, and 750 mm high. These dimensions are in conformity with ASTM D6706-1 (2021) recommendations. Figure 1 shows the pullout equipment components. This equipment has been previously used to assess the pullout response of steel ladder reinforcements (Damians et al., 2024), and for some limited preliminary PET strap pullout tests with different installation procedures (Moncada et al., 2025). Properties of fill materials, including a well graded gravely sand and recycled asphalt pavement (RAP) are detailed in Table 1.

Vertical pressures were applied using a steel plate and hydraulic actuator and measured using a pressure cell located between the loading plate and the hydraulic piston. A high-density expanded polystyrene foam block layer was placed between the soil and loading plate covering the entire contact area to provide a uniformly distributed surcharge. Horizontal displacements were applied to the specimen at a constant rate of 1 mm/min using the hydraulic actuator at the front of the test box. The steel clamp system was designed to apply a uniform displacement across the pullout specimen while avoiding relative slipping. Displacements were measured at the front and back of the reinforcement specimen using transducer devices (extensometers) with ±0.01 mm accuracy. Measurements were taken as close to the box opening as possible to avoid measuring in-air reinforcement axial elongation rather than in-soil displacements. Tests were continued until a peak pullout strength was observed and the rate of displacement at the tail-

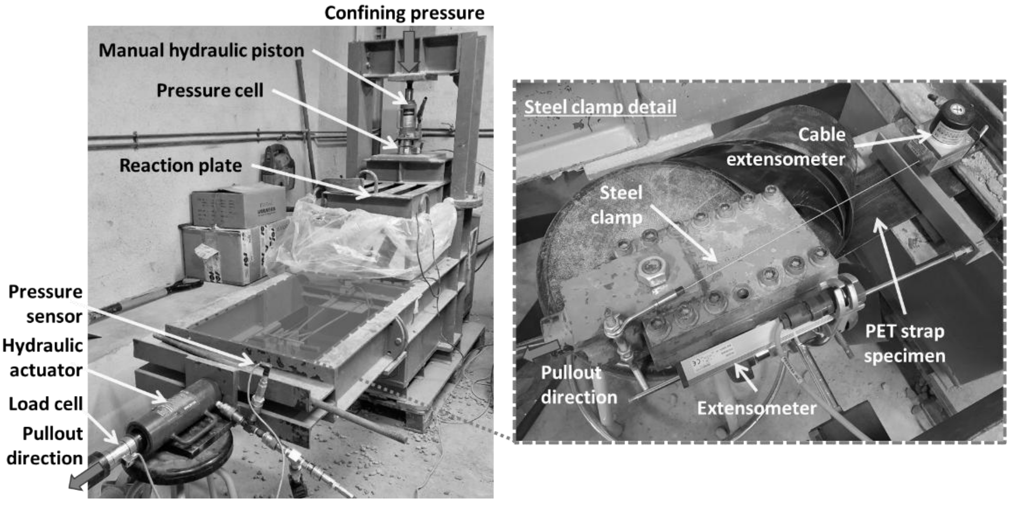

Figure 1. Pullout test equipment with details of the steel clamp.

end and the head-end were the same as specified in the ASTM D6706 (2021) test protocol. Tested specimens are polymeric straps made from high-tenacity PET fibres enclosed in a HDPE sheath (UTS = 34.4 kN/strap at 11.2% strain with a secant stiffness modulus at 2% strain of $J_{1\%}$ = 497 kN/strap).

Soil type	Unit weight (kN/m3)	Peak friction angle (º)	Cohesion (kPa)	Coefficient of curvature (-)	Coefficient of uniformity (-)	Fines content (%)
SW with gravel	21.5	44	0	1.98	33.6	6.7
SW (RAP)	20.4	32	0	1.30	11.7	2.8

Table 1. Fill materials characteristics.

3 BIAS ANALYSIS

Measured pullout strength was compared to calculated values. The relative accuracy of each model was evaluated using the mean (μ) and coefficient of variation (COV) of the bias values (ratio between measured and predicted values), and Pearson's correlation coefficient (ρ) (Miyata et al., 2019). Bias statistics have been used to calibrate pullout models that have empirical factors (e.g., Huang and Bathurst 2009). Bias statistics are also necessary to carry out reliability theory-based internal stability pullout analysis (e.g., Bathurst et al., 2020) and for load and resistance factor design calibration (e.g., Bathurst et al., 2025). A model is considered appropriate as mean bias value approach one ($\mu \rightarrow 1$), COV is small, and correlation between bias and calculated pullout strength and vertical pressure is negligible (i.e., $\rho \rightarrow 0$).

The AASHTO model (Eq. 2) is, on average, conservative, (μ = 1.74) with a large spread in bias values (COV = 0.60) (Fig. 8a). At a 5% level of significance, predicted pullout strength and vertical pressure show a strong dependency with calculated bias values, with Pearson's correlation coefficient values of ρ = -0.63 and ρ = -0.67, respectively. A strong correlation can be understood as a strong dependency of predicted pullout strength and vertical pressure on model accuracy. In the case of the NF model, results show an overestimation of pullout strength (μ = 0.72), with a lower spread than the AASHTO model (COV = 0.52). At a 5% level of significance, predicted pullout strength and vertical pressure show a strong dependency with calculated bias values, with Pearson's correlation coefficient values of ρ = -0.58 and ρ = -0.40, respectively. The exponential model (Eq. 3) calculated using coefficient values from Miyata et al. (2019) has higher average accuracy (μ = 0.84) and reduced spread (COV = 0.37) than the linear model. At a 5% level of significance, correlations were computed between bias and

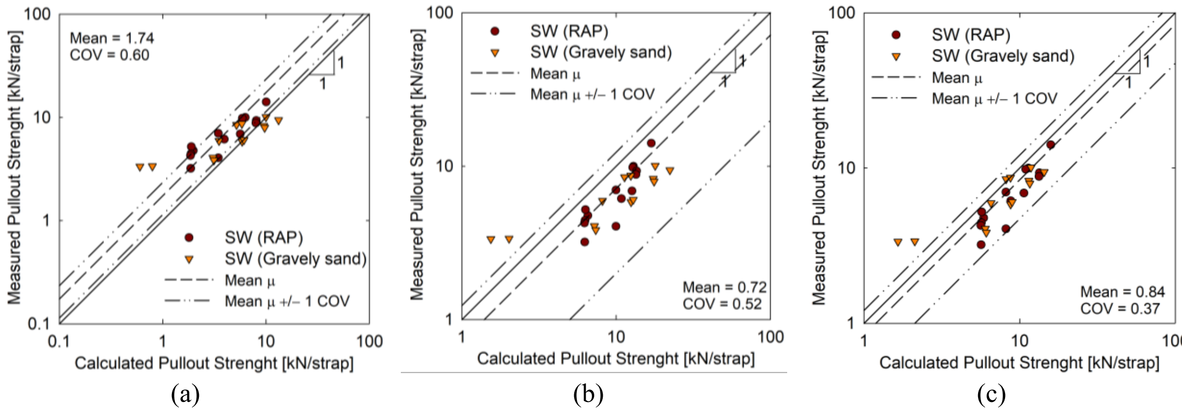

Figure 2. Measured and calculated pullout strength using (a) AASHTO, (b) NF, and (c) exponential models.

predicted pullout strength and vertical pressure (i.e., Pearson's correlation coefficient values of $\rho = -0.50$ and $\rho = -0.38$, respectively). The large majority of the bias data corresponds to vertical pressures of $\sigma_v > 20$ kPa.

4 CLOSING REMARKS

- Pullout data of polymeric straps was observed to have a non-linear behaviour with respect to vertical pressure.
- Accuracy of friction interaction factor models was studied using bias analyses. Linear (AAHSTO) and non-linear (NF and exponential) models were considered.
- On average, non-linear models showed less variation, were the exponential model showed to be the most accurate and lowest spread

REFERENCES

AASHTO; 2024. LRFD Bridge Design Specifications, 10th Ed. American Association of State Highway and Transportation Officials (AASHTO), Washington, DC, USA.

ASTM D6706-01; 2021. Standard test method for measuring geosynthetic pullout strength in soil American Society for Testing Materials (ASTM International), West Conshohocken, PA, USA.

Bathurst, R.J., Miyata, Y., Allen, T.M.; 2020. Deterministic and probabilistic assessment of margins of safety for internal stability of as-built PET strap reinforced soil walls. Geotextiles and Geomembranes, 48: 780-792

Bathurst, R.J., Miyata, Y., Allen, T.; 2025. LRFD calibration of internal limit states for polymer strap MSE Walls. Journal of Geotechnical and Geoenvironmental Engineering, 151(1), 04024140.

Damians, I.P., Moncada, A., Olivella, S., Lloret, A., Josa, A.; 2024. Physical and 3D numerical modelling of reinforcements pullout test. Scientific Reports, 14(1), 7355.

EN 1997-3; 2025. Eurocode 7 — Geotechnical Design — Part 3: Geotechnical Structures. EUROPEAN STANDARD, Ref. No. EN 1997-3, March, 2025. European Committee for Standardization, Technical Committee CEN/TC 250 "Structural Eurocodes", Brussels, Belgium.

Huang, B., Bathurst, R.J.; 2009. Evaluation of soil-geogrid pullout models using a statistical approach. ASTM Geotechnical Testing Journal, 32(6): 489-504.

Miyata, Y., Bathurst, R.J., Allen, T.M.; 2019. Calibration of PET strap pullout models using a statistical approach. Geosynthetics International, 26(4), 413-427.

Moncada, A., Girbau, N., Damians, I.P.; 2025. Analysis of physical PET strap reinforcement pullout tests data. IGS - 4th Technical Workshop on Soil Reinforcement (TCR): Reinforcement and Drainage in Soil Structures 2024, E3S Web of Conferences 662, 01004.

NF P 94-270; 2020. Calcul géotechnique: Ouvrages de soutènement. Remblais renforcés et massifs en soil cloué. Norme française, Association Française de Normalisation (AFNOR), La Plaine Saint-Denis, France.

Pierozan, R.C., Araujo, G.L.S., Palmeira, E.M., Romanel, C., Zornberg, J.G.; 2022. Interface pullout strength of polymeric strips embedded in marginal tropical soils. Geotextiles and Geomembranes, 50(1), 20-39.

GSY/GSY INTERFACE CHARACTERIZATION BY MEANS OF INCLINED PLANE AND DIRECT SHEAR TESTS

Paolo Carrubba[1], Marilene Pisano[2], Giuseppe Cardile[2]and Nicola Moraci[2]

[1] University of Padova, Department ICEA, School of Engineering
35129 Padova, Italy
E-mail: paolo.carrubba@unipd.it

[2] Mediterranean University of Reggio Calabria, DICEAM Department
89122 Reggio Calabria, Italy
E-mail: marilene.pisano@unirc.it, giuseppe.cardile@unirc.it, nicola.moraci@unirc.it

Key words: interface shear strength, landfill cover systems, testing methods

Abstract. *The paper addresses the characterization of the interface between different geosynthetics used in landfill cover systems under both static and seismic loading conditions. In this context, it is shown that the correct characterization of the GSY/GSY interface shear strength in landfill covers can be achieved using laboratory equipment suitable for low contact stresses, such as the inclined plane and the direct shear apparatus, with tests performed at a constant loading rate. These testing methods allow the observation of interface failure mechanisms and enable the identification of the most appropriate interface friction angle to ensure an adequate level of safety against slipping on the inclined cover system.*

1 INTRODUCTION

Geosynthetics perform multiple and complementary geotechnical functions in landfill cover systems, including rainwater drainage, biogas collection, waterproofing, reinforcement, and erosion control. Rainwater drainage is commonly provided by drainage geocomposites consisting of a geotextile acting as a filter and a geospacer ensuring adequate in-plane flow capacity. Proper filter opening and discharge capacity are essential to prevent clogging and water accumulation within the cover soil. Waterproofing is generally achieved using a geomembrane, often combined with a geosynthetic clay liner (GCL) where a compacted clay barrier cannot be installed. Protective geonets may also be placed above the geomembrane to reduce the risk of damage during construction. Beneath the impermeable barrier, an additional drainage geocomposite is frequently installed to collect and vent landfill biogas. Where steep slopes or differential settlements are expected, geogrids can improve cover stability by increasing the interface strength and reducing tensile stress in the weaker geosynthetic. Finally, geomats or geocells are used to limit surface erosion and promote vegetation establishment. The resulting multilayer system shows several GSY/GSY and GSY/soil interfaces, working at both low normal stresses and shear strength. Accurate characterization of their interface strength is therefore essential for the design of reinforcement systems and anchorage trenches.

This paper summarizes laboratory investigations performed using two recently developed testing devices: a direct shear apparatus operating at constant loading rate and an inclined plane apparatus (Pavanello et al., 2018a, 2022a,b). Both devices are specifically designed to characterize interface friction under low contact stresses and provide consistent, comparable results. The experimental findings confirm that interface friction is a key parameter governing landfill cover stability. In particular, interface behaviour depends on the kinematic failure mode, the type of geosynthetics in contact, surface wear, the presence of interstitial fluids, and, where applicable, the relative density of the adjacent granular soil.

2 LABORATORY EVALUATION OF GEOSYNTHETIC INTERFACE STRENGTH

Geosynthetic interface strength can be evaluated under static, cyclic, seismic, and different normal stress conditions. For low contact stresses, the main laboratory methods are direct shear tests (constant displacement or loading rate) and inclined plane tests.

The standard direct shear test, performed at constant displacement rate, is the most widely adopted method for evaluating geosynthetic interface shear strength. The test is conducted on specimens measuring at least 0.30×0.30 m, with one interface element fixed and the other sliding under constant normal stress. The shear strength envelope is obtained by repeating the test under different normal stresses, typically 50, 100, and 150 kPa. Although the interface strength is commonly expressed in terms of adhesion (α) and friction angle (φ_{tan}), the real failure envelope is often nonlinear, particularly at low normal stresses. Consequently, the secant friction angle (φ_{sec}) provides a more representative parameter for cover systems, where normal stresses are generally below 50 kPa.

To overcome some limitations of the conventional procedure, a direct shear device operating at constant loading rate has recently been developed (Pavanello et al., 2022a, b). In this apparatus, the horizontal load increases progressively while the normal load remains constant, allowing the mobilized friction angle to be determined from the ratio between the applied horizontal force and the box weight (see Fig. 1). Unlike the standard test, where displacement is imposed at a constant rate, the gradual increase in shear load enables a more accurate evaluation of the interface strength at the onset of sliding. Furthermore, the device can operate under very low normal stresses (down to approximately 5 kPa), making it suitable for reproducing the stress conditions typical of landfill cover systems. Depending on the interface characteristics, both gradual and sudden sliding modes have been observed, although peak interface strength is generally mobilized at very small displacements. An additional advantage of direct shear testing is the possibility of performing tests under submerged conditions.

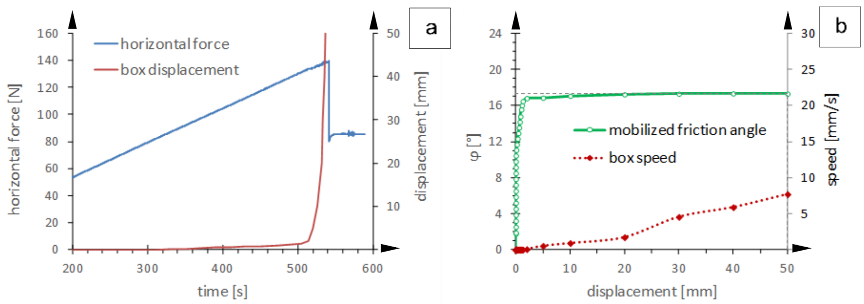

Figure 9: Direct shear test at constant loading rate for a GMB_{smooth}-GCD interface: (a) horizontal force and box displacement versus time; (b) mobilized strength angle and box velocity versus displacement (Pavanello et al., 2022a)

The inclined plane test provides an alternative method for evaluating geosynthetic interface friction. The test consists of a box resting on a tilting plane, with the two geosynthetics fixed to the plane and to the base of the box. The plane inclination increases until the box reaches a displacement of 50 mm, thus conventionally defining a standard interface strength angle (φ_{stand}). A more representative parameter can be obtained by considering the inclination corresponding to the first measurable displacement (typically 1 mm), which defines the first detachment friction angle (φ_0). Since the conventional 50 mm displacement may occur while the box is already moving, φ_{stand} should be regarded as an index parameter rather than a purely static strength angle (Gourc and Reyes-Ramirez, 2004).

Two distinct failure mechanisms may occur during inclined plane testing (see Fig. 2). In sudden sliding, the box accelerates immediately after detachment and the interface strength becomes dynamic. In gradual sliding, motion develops progressively and the measured strength includes a viscous component associated with sliding velocity, leading to a kinematic friction angle greater than φ_0. A further procedure, known as the force method (Briançon et al., 2011; Carbone et al., 2015), measures the restraining force required to keep the box in static equilibrium after sliding, allowing the limiting friction angle (φ_{lim}) to be determined. Because φ_{lim} excludes viscous effects while representing fully mobilized interface strength, it provides the most conservative parameter for design. Large-displacement inclined plane tests further demonstrate that wet conditions significantly reduce interface friction and that φ_{lim} remains consistently lower than both φ_0 and φ_{stand}.

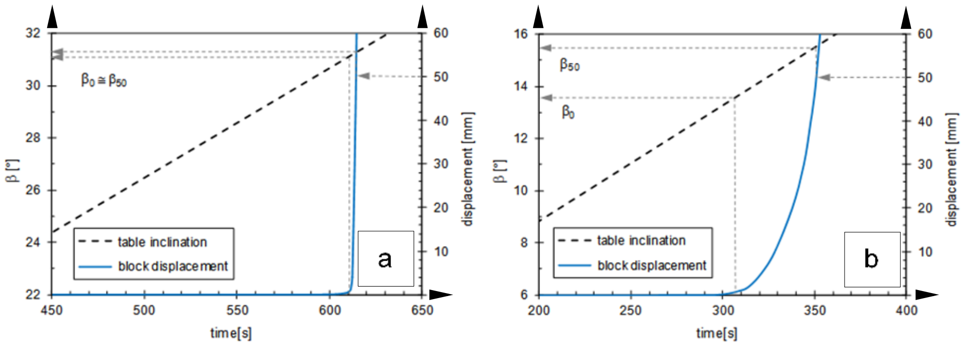

Figure 2: Two different sliding behaviours: (a) dry $GMB_{textured}$-GCD showing a sudden sliding mode; (b) dry GMB_{smooth}-GCD showing a gradual sliding mode (Pavanello et al., 2021)

In addition to static interface characterization, geosynthetic interfaces must also be evaluated under dynamic loading conditions, such as those induced by earthquakes. Dynamic behaviour has been investigated using shaking table devices, dynamic direct shear tests, and inclined plane tests (Pavanello et al., 2018b; Ross and Fox, 2015; Wartman and Bray, 2003).

The shaking table test is the most widely adopted technique. One geosynthetic specimen is fixed to the vibrating table, while the other is attached to a freely sliding block. Tests have been performed under both harmonic loading and recorded seismic motions, while complementary investigations have employed dynamic direct shear devices. Dynamic inclined plane tests have also been developed by combining a shaking table with an inclined surface supporting the sliding block. The interpretation of these tests is based on Newmark's sliding block model (Newmark, 1965). During shaking, the block moves together with the table until the horizontal acceleration exceeds the critical acceleration, a_{crit}. Beyond this threshold, sliding occurs and the dynamic interface friction angle, φ_{dyn}, can be evaluated, accounting for both the plane inclination and the excess acceleration.

Experimental results (see Fig. 3) highlight the influence of the interface failure mechanism. For interfaces exhibiting sudden sliding, the dynamic friction angle is generally equal to or lower than the first detachment friction angle. Conversely, gradual sliding interfaces show increasing dynamic friction with sliding velocity due to the contribution of a viscous component of strength becoming more significant as relative displacement speed increases.

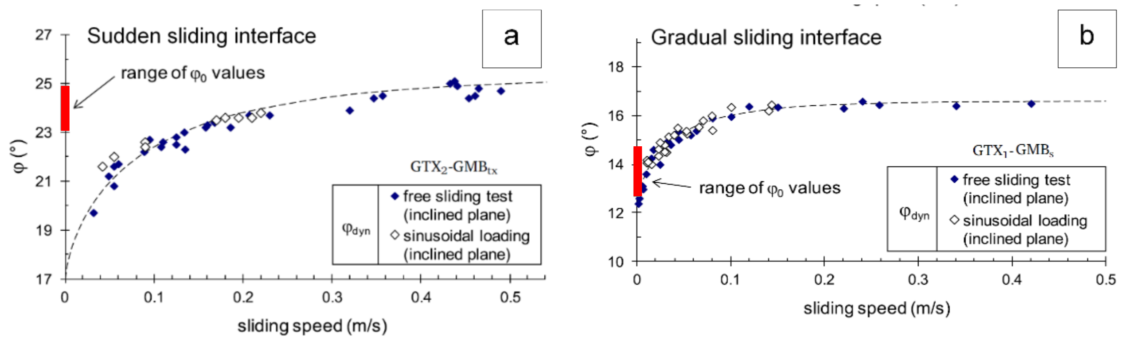

Figure 3: Dynamic friction versus relative sliding velocity for two different interfaces: (a) textured geomembrane/non woven geotextyle, showing a sudden sliding mode; (b) smoot geomembrane/non woven geotextyle, showing a gradual sliding mode (Pavanello et al., 2018a)

REFERENCES

Briançon, L., Girard, H. and Gourc, J.P.; 2011. A new procedure for measuring geosynthetic friction with an inclined plane. Geotextiles and Geomembranes 29(5): 472–482.

Carbone, L., Gourc, J.P., Carrubba, P., Pavanello, P. and Moraci, N.; 2015. Dry friction behaviour of a geosynthetic interface using inclined plane and shaking table tests. Geotextiles and Geomembranes 43(4): 293–306.

Gourc, J.P. and Reyes-Ramirez, R.; 2004. Dynamics-based interpretation of the interface friction test at the inclined plane. Geosynthetics International 1(6): 439–454.

Newmark, N.; 1965. Effects of earthquakes on dams and embankments. Géotechnique 15(2): 139–160.

Pavanello, P., Carrubba, P. and Moraci, N.; 2018a. Dynamic friction and the seismic performance of geosynthetic interfaces. Geotextiles and Geomembranes 46: 715–725.

Pavanello, P., Carrubba, P. and Moraci, N.; 2018b. The determination of interface friction by means of vibrating table tests. Geotextiles and Geomembranes 46: 830–835.

Pavanello, P., Carrubba, P. and Moraci, N.; 2021. The characterisation of geosynthetic interface friction by means of the inclined plane test. Geotextiles and Geomembranes 49(1): 257–275.

Pavanello, P., Carrubba, P. and Moraci, N.; 2022a. Evaluation of geosynthetic interface friction at low normal stress: Comparison between two different test procedures. Acta Scientiarum Polonorum Architectura 21(4): 3–10.

Pavanello, P., Carrubba, P. and Moraci, N.; 2022b. Geosynthetic interface friction at low normal stress: Two approaches with increasing shear loading. Applied Sciences 12(3): 1065.

Ross, J.D. and Fox, P.J.; 2015. Dynamic shear strength of GMX/GCL composite liner for monotonic loading. Journal of Geotechnical and Geoenvironmental Engineering 141(7): 11.

Wartman, J., Bray, J.D. and Seed, R.B.; 2003. Inclined plane studies of the Newmark sliding block procedure. Journal of Geotechnical and Geoenvironmental Engineering 129(8): 673–684.

TENSILE BEHAVIOUR OF GEOSYNTHETICS MADE FROM RECYCLED POLYMERS AFTER MECHANICAL DAMAGE UNDER REPEATED LOADING

Fernanda B. Ferreira[1,2], Pedro B. Ribeiro[3], Patrícia C. Lopes[3,2] and Maria de Lurdes Lopes[2]

[1]GeoBioTec, Department of Geosciences, University of Aveiro,
Santiago Campus, 3810-193 Aveiro, Portugal
E-mail: fbf@ua.pt, web page: https://www.ua.pt/pt/geobiotec

[2]CONSTRUCT, Faculty of Engineering, University of Porto,
R. Dr. Roberto Frias, 4200-465 Porto, Portugal
E-mail: lcosta@fe.up.pt, web page: https://www.fe.up.pt/construct/

[3]School of Engineering, Technical University of Porto,
R. Dr. António Bernardino de Almeida, 4249-015 Porto, Portugal
E-mail: 1161567@isep.ipp.pt, cpl@isep.ipp.pt, web page: https://isep.ipp.pt/

Key words: Soil reinforcement, Mechanical Damage, Recycled geosynthetics, Recycled construction and demolition (C&D) wastes, Sustainability

Abstract. *Promoting sustainable consumption and production practices, together with the responsible use of non-renewable natural resources, is crucial for tackling the sustainable development challenges currently faced by humanity. The construction sector significantly impacts the environment through high raw material demand and waste generation, highlighting the need for eco-friendly practices to reduce carbon emissions. Using recycled aggregates as alternative fill materials in geosynthetic-reinforced systems can play a vital role towards achieving more sustainable development. Moreover, incorporating geosynthetics manufactured from recycled polymers in such applications can further contribute to promoting circular economy principles in the construction sector. In this study, the mechanical damage of recycled-polymer geosynthetics under repeated loading was assessed through a series of laboratory tests. Different types of aggregates were considered, including a synthetic standard aggregate and different recycled construction and demolition (C&D) materials. Mechanical damage simulation tests were initially performed to simulate the degradation that geosynthetics may experience during field installation. The damaged geosynthetic specimens were then subjected to in-isolation wide-width tensile tests to determine the variations in tensile strength and secant stiffness at low strains with respect to those of fresh specimens. A comparison was established between the behaviour of conventional geosynthetics and that of geosynthetics manufactured from recycled polymers. Overall, the results show that using recycled C&D wastes combined with geosynthetics manufactured from recycled polymers may be regarded as a promising approach to address global sustainability requirements.*

SUSTAINABILITY EVALUATION OF DIFFERENT BACKFILL MATERIALS USED IN GEOSYNTHETIC REINFORCED SOIL WALLS

Anibal Moncada[1,2], Ivan P. Damians[1,2,3], and Richard J. Bathurst[4]

[1] Department of Civil and Environmental Engineering (DECA), Universitat Poliècnica de Catalunya (UPC), Campus Nord UPC, 08034 Barcelona, Spain.

[2] International Centre for Numerical Methods in Engineering (CIMNE), Campus Nord UPC, 08034 Barcelona, Spain. (http://www.cimne.com)

[3] VSL International Ltd, Barcelona, Spain

[4] Geoengineering Centre at Queen's-RMC, Civil Engineering Department, Royal Military College of Canada, Canada.

Key words: Sustainability assessment, life cycle analysis, reinforced soil walls, MIVES

Abstract. *The paper details the sustainability evaluation of idealized geosynthetic reinforced soil walls constructed with different backfill materials (high-quality granular material, recycled concrete aggregate, and locally available soils with medium to low fines content) using a multicriteria decision-making methodology (MIVES). Sustainability assessments cover environmental, economic, and social components. Environmental and economic requirements were evaluated using a life cycle assessment approach. The social requirement was evaluated with survey results related to reinforcement applications of geosynthetics. The use of locally available soil proved to be the most economic, with lower environmental impact, and overall, the most sustainable alternative amongst the backfill soil options investigated, even when these soils have less mechanical strength.*

1 INTRODUCTION

Local and global design requirements are being quickly modified to include the evaluation of global warming potential (GWP), or rather CO_2 eq. emissions, in early decision-making processes. A common method used to quantify the carbon footprint of a project are life cycle assessments (LCAs). LCAs allow to quantify the environmental impact of a solution or project through several environmental indicators (including GWP among them) based on a life cycle inventory (LCI). An LCI includes all material and processes involved in the raw material production, transportation and construction processes, use and maintenance, demolish, and disposal of the project. While global warming potential is a relevant and impactful indicator, other environmental indicators, such as land and water use, or human toxicity, should also be taken in consideration with (arguably) equal weight. Having said this, environmental assessments (often called environmental sustainability) cover only a portion of an integral sustainability assessment. According to the latest European standards (e.g. EN 17472) environmental, economic, and social aspects must be thoroughly evaluated when assessing the sustainability of different alternatives. The evaluation of each requirement (i.e., environmental, economic, and social) is based on environmental, economic, and social indicators. Environmental indicators involve the use of resources and generation of emissions. Economic indicators involve the costs and effect on the economy of the project. Social indicators can cover a wide range of settings, including resilience, public opinion, and workers/local health and safety effects, among others. The selection of indicators is often related to project specific characteristics, legal requirements, geographic location, and/or stakeholders' interest/requirements. Standards such as EN 17472 (2022) include an extended list of possible indicators for each requirement. Sustainability assessments are aimed to compare different solutions, rather than define a definitive solution. Each individual indicator will have a specific measuring technique and/or measuring units. Consequently, when comparing alternatives, each indicator will only be comparable with its own category. The evaluation of requirements quantified by several indicators requires the use of multi-criteria tools which allow the aggregation of measurements with a wide range of units. The Integrated Value Model for Sustainability Assessment (MIVES, due to its acronym in Spanish) (Josa et al., 2008) and the Quantitative Assessment of Life Cycle Sustainability (QUALICS) (Reddy et al., 2024) are key examples of multi-criteria evaluation tools. These models allow to prioritize (or rather, make a decision) based on value theory using well-defined decision trees, which incorporate different indicators (with different measuring units and/or scales) as an aggregated value.

There are several examples of sustainability assessments related to civil engineering using MIVES, including the evaluation of prefabricated structures (wood, steel, and concrete elements) (Pons, 2014) and, more relevant to geotechnical engineering, the evaluation of different earth retaining solutions (Damians et al., 2018). The present document is based on the work Moncada et al. (2026), in which idealized geosynthetic reinforced soil walls constructed with polyester reinforcement layers and different backfill materials are compared using MIVES.

2 METHODOLOGY

Sustainability assessments were carried out using MIVES (Josa et al., 2008). Figure 1 shows a schematic representation of the structure of MIVES. The use of different fill materials in reinforced soil walls with rigid facing elements and polymeric reinforcement layers is explored. Backfill material alternatives include quarried granular material (GR), construction and demolition wastes (i.e., recycled concrete aggregates), and two different locally available soils (LAS 1 and LAS 2), where differences are for mechanical properties only, being LAS 2 the

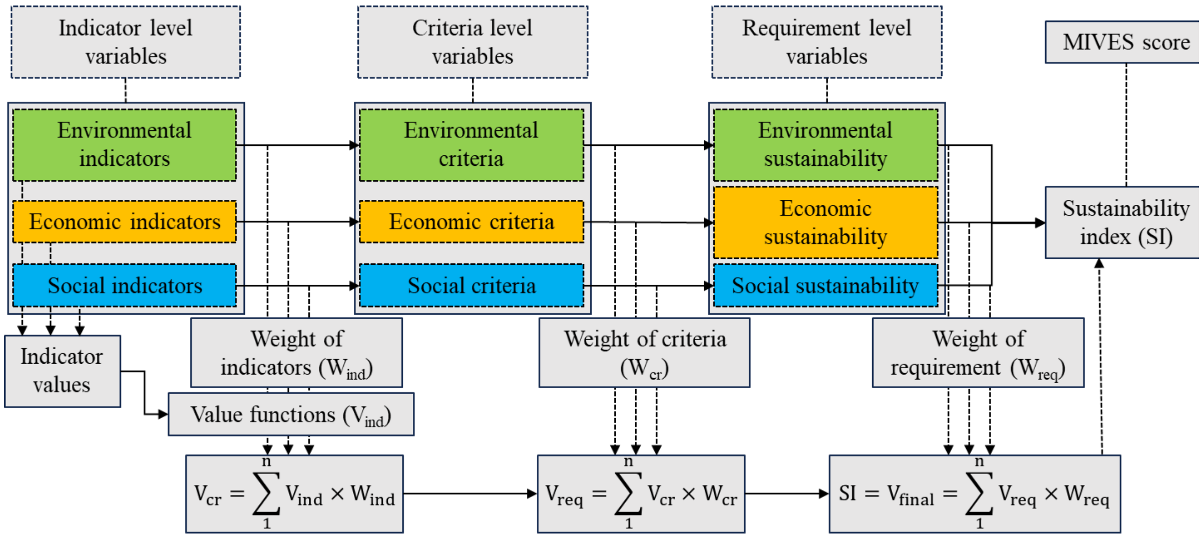

Figure. 1. Schematic representation of the MIVES methodology for a sustainability assessment (adapted from Josa et al. 2008)

alternative with the lowest strength parameters). All materials are assumed to comply with chemical and mechanical requirements. Wall heights of 3 to 9 m were analyzed. Further details of the LCI can be found in the work of Moncada et al. (2026).

The environmental requirement was quantified using the ReCiPe method (Huijbregts et al., 2017) and the ecoinvent v3.8 (Allocation, cut-off classification) environmental database (Wernet et al., 2016). End-point environmental indicators (i.e., aggregated score of 17 different mid-point environmental indicators) were used as input values. The economic requirement involved the costing of the life cycle inventory. The social requirement was quantified using design and construction indicators together with resilience indicators, evaluated using an online survey handed out to students and professionals involved in the geotechnical industry.

Sustainability indexes (SI) were calculated with a probabilistic approach. For this, life cycle inventory quantities and prices were defined using a minimum, maximum, and modal value, used in triangular distributions. Using Monte Carlo simulations, probability distribution functions of SI scores were calculated using beta-PERT (Program Evaluation and Review Technique) distributions, defined by minimum, maximum, and mode for each wall solution. A beta-PERT distribution is an asymmetrical continuous probability distribution, similar to a smoothed triangular distribution, but assigns lower probabilities to the extreme (minimum and maximum) values.

3 RESULTS

Figure 2 shows the probability distribution function (Fig. 2a) and cumulative distribution function (Fig. 2b) foe the calculated SI scores for a wall height of 6 m for the four backfill materials being compared. A probabilistic approach allows to quantify and visualize different probable scenarios included in the LCI. Results show that, for a wall height of 6 m and the described boundary conditions, the use of competent locally available soil (often called marginal fill) is the most sustainable solution. The local soil with poorer mechanical properties (LAS 2) shows a reduced score compared to LAS 1, mainly attributed to the variations in design required to satisfy limit equilibrium conditions due to lower mechanical properties. It is important to distinguish as the most probable alternative as results show an overlapping of the probability distribution function, meaning that, given project uncertainties, the ranking of alternatives can vary. From a practical point of view, the calculated SI allows engineers to

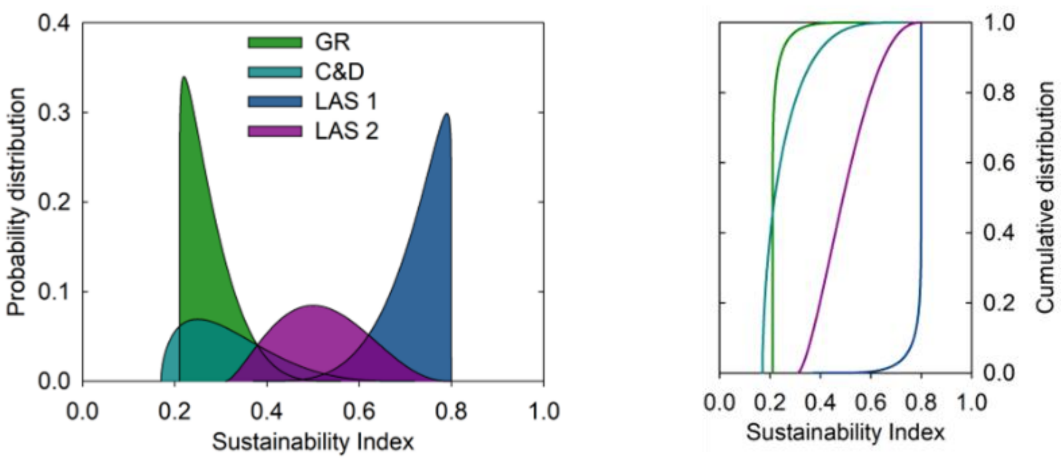

(a) (b)

Figure. 2. (a) probability distribution and (b) cumulative distribution functions of the sustainability index for 6-m-high reinforced soil walls with different backfill materials (adapted from Moncada et al. 2026).

clearly prioritize different solutions for a common problem. As the process by which the SI is obtained involves the definition of requirement priorities (i.e., weighting scenarios), stakeholders' preferences are included within the calculated hierarchy, thus, serve as direct justification for the selection of a particular alternative.

4 CONCLUSIONS

- Sustainability assessments were carried out using the Integrated Value Model for Sustainability Evaluation (MIVES). Environmental, economic, and social/functional requirements were considered when assessing different backfill alternatives for reinforced soil structures.
- Sustainability index (SI) scores are used to rank alternatives. The use of localy available soil (LAS) shows to be the mos sustainable alternative across all wall heights.

REFERENCES

Alarcón B., Aguado A., Manga R., Josa A.; 2011. A value function for assessing sustainability: application to industrial buildings. Sustainability 3(1): 35–50.

Damians, I.P., Bathurst, R.J., Adroguer, E.G., Josa, A., Lloret A.; 2018. Sustainability assessment of earth retaining wall structures. Environmental Geotechnics 5(4): 187-203.

EN 17472:2022; 2022. Sustainability of construction works. Sustainability assessment of civil engineering works. Calculation methods. European Committee for Standardization Technical Committee CEN/TC 350 "Sustainability of construction works"., Brussels, Belgium.

Huijbregts, M.A.J., Steinmann, Z.J.N., Elshout, P.M.F, Stam, G., Verones, F., Vieira, M., Zijp, M., Hollander, A., van Zelm, R.; 2017. ReCiPe2016: a harmonized life cycle impact assessment method at midpoint and endpoint level. International Journal of Life Cycle Assessment 22: 138–147.

Josa A., San José T., Cuadrado J.; 2008. El caso de la EHE. In Jornada sobre sostenibilidad en la tecnología del hormigón: MIVES, una herramienta de apoyo a la toma de decisiones. Barcelona, Spain, pp. 84–95 (in Spanish).

Moncada, A., Damians, I.P., Olivella, S., Bathurst, R.J.; 2026. Sustainability assessments of geosynthetic reinforced soil walls with polyester reinforcement layers. Geosynthetics International. (AoP).

Pons, O.; 2014. Assessing the sustainability of prefabricated buildings. In Eco-efficient Construction and Building Materials (pp. 434-456). Woodhead Publishing.

Reddy, K.R., Janga, J.K., Kumar, G.; 2024. Sustainability and resilience: a new paradigm in geotechnical and geoenvironmental engineering. Indian Geotechnical Journal.

Wernet, G., Bauer, C., Steubing, B., Reinhard, J., Moreno-Ruiz, E., Weidema B.; 2016. The ecoinvent database version 3 (part I): overview and methodology. International Journal of Life Cycle Assessment 21(9): 1218–1230.

WALLS AND CONVENTIONAL EARTH RETAINING STRUCTURES

Edoardo A. Forte[1], Fabrizia Trovato[1] and Giulia Lugli[1]

[1] Officine Maccaferri S.p.A.,
Via del Faggiolo, 1/12 (40132 Bologna).
E-mail: e.forte@maccaferri.com, web page: https://www.maccaferri.com/

Key words: Life Cycle Assessment, Sustainability, Mechanically Stabilized Earth, Earth Retaining Structures, Cantilever Wall, Global Warming Potential

Abstract: *This paper presents a Life Cycle Assessment (LCA) study comparing the environmental performance of mechanically stabilized earth (MSE) systems with conventional cantilever retaining walls. An LCA-based tool was developed in accordance with ISO 14040/14044 and EN 15804 to evaluate Global Warming Potential (GWP) across all life cycle stages, from material production to end-of-life. The comparison is based on equivalent retaining structures providing the same function under comparable boundary conditions. Results are calculated for the full wall length defined by the user. Typical examples for 100 m long walls with different heights show that MSE solutions can reduce total GWP by approximately 70-85% compared with conventional cantilever walls, mainly due to the reduced use of reinforced concrete. The study highlights the importance of sustainable design in geotechnical engineering and demonstrates the effectiveness of LCA tools in supporting low-carbon infrastructure decisions.*

1 INTRODUCTION

Sustainable development, as defined by the Brundtland Report (1987), is development that meets the needs of the present without compromising the ability of future generations to meet their own needs. In engineering, sustainable design aims to maximise social benefits while reducing environmental impacts, considering the broader effects of design on society and the environment.

Sustainable engineering is commonly described through three interconnected pillars: environment, economy, and society performance. A key tool for assessing the environmental pillar is Life Cycle Assessment (LCA), defined by ISO 14040 as the compilation and evaluation of the inputs, outputs, and potential environmental impacts of a product system throughout its life cycle. LCA therefore provides a consistent framework to quantify the environmental consequences of engineering decisions across the entire life cycle. For construction works, the EN 15804 framework provides a structured approach by separating production, transport, construction, use and end-of-life stages.

Environmental impacts are typically evaluated through indicators such as global warming potential (GWP), abiotic depletion, acidification, eutrophication, photochemical oxidation, and ozone layer depletion. Comparative LCA studies have shown that geosynthetic-based solutions can reduce environmental impacts by limiting the use of cement, steel, natural aggregates, earthworks and transport. However, meaningful comparisons require equivalent technical functions, clearly defined system boundaries, a consistent functional unit and a transparent life cycle inventory.

2 LCA-BASED TOOL FOR MSE AND CONVENTIONAL RETAINING STRUCTURES

2.1 Compared systems and functional unit

The tool compares two alternative retaining systems designed to provide the same earth-retaining function: a conventional reinforced concrete cantilever wall and an MSE wall. The cantilever wall resists earth pressures mainly through a reinforced concrete stem and base slab. The MSE wall combines precast concrete facing panels, high-strength polymeric reinforcing strips and compacted backfill, which provides high structural stability and long-term performance to be achieved with a lower quantity of reinforced concrete. Maccaferri has a strong experience with MSE structures, designed for the construction of vertical retaining walls. Figure 10 shows a typical MSE system front facing view and reinforcement installation.

Figure 10: Typical MSE front facing view and reinforcement installation.

A key aspect of the methodology is the definition of a consistent functional unit. In this study, the functional unit is an earth retaining structure of defined height and length, designed for the same service life and comparable geotechnical boundary conditions. The examples presented consider a wall length of 100 m, while results may also be expressed per metre of wall length to facilitate comparison with other studies.

The comparison is therefore made between equivalent structural solutions rather than individual products. This is important because the environmental benefit of the MSE system is not related only to the geosynthetic reinforcement itself, but to the more efficient structural configuration that reduces the demand for concrete, steel and associated construction activities.

2.2 Development of a new LCA tool

To quantify the environmental benefits provided by the MSE system, a comprehensive LCA-based tool has been developed to compare MSE walls with conventional reinforced concrete cantilever walls. The tool provides a project-level assessment of the Global Warming Potential (GWP) of the two solutions. GWP is expressed in CO_2-equivalents and is used to quantify the contribution of greenhouse gas emissions to climate change. It was selected as the primary indicator because it is widely used in LCA studies, easily understood in engineering comparisons, and increasingly relevant in the regulatory framework for construction products, where climate-change-related environmental performance is progressively becoming part of product declarations.

The tool is designed to be simple and user-friendly, requiring only a limited number of input parameters. The user needs to define the main project data, including wall height, wall length, transport distances and transport modes for the principal construction materials. Based on these inputs, the tool automatically performs the necessary calculations. It first determines the required quantities of all materials involved in the solution, including structural components, excavation volumes, and any backfilling materials. In addition, it estimates the main site operations associated with construction activities. Each of these elements is then associated with corresponding emission factors, coming from EPDs or from recognized LCA databases, allowing the tool to convert material quantities, construction processes, and transportation activities into Global Warming Potential (GWP) values. These contributions are finally aggregated to provide a complete assessment of the total environmental impact of the retaining structure over its life cycle, enabling a consistent comparison between different design alternatives.

The assessment follows the main life cycle modules defined in the EN 15804 framework. For the production stage (A1–A3), emissions are calculated by associating the mass or volume of each component with the corresponding emission factors for construction materials. The transport stage to site (A4) is evaluated by defining transport distances and modes and then estimating emissions for each transport mode. For the construction and installation phase (A5), emissions are estimated from site activities typical of retaining earth structures, such as excavation, soil compaction, and concrete pouring, using appropriate activity-based emission factors. Finally, the end-of-life stage (C1–C4) is assessed by accounting for emissions related to demolition, transport of waste, waste processing, and final disposal of all materials used in the construction.

Although other environmental indicators may be included in future developments, the present version of the tool focuses on GWP as the primary and most immediately applicable indicator for comparing alternative retaining wall solutions

3 RESULTS AND DISCUSSION

The tool was applied to typical MSE and cantilever retaining walls with heights of 4 m, 6 m, 8 m and 10 m and a wall length of 100 m. Overall, across all four configurations, the MSE solution achieved a total GWP reduction of approximately 70% to 85% compared with conventional cantilever wall. The reduction increased with wall height, as the material demand of the reinforced concrete cantilever wall grows more rapidly than that of the MSE alternative. The largest savings were observed in the materials production stage, A1–A3, where reductions reached up to 85% relative to the cantilever alternative. This result is mainly due to the lower volume of reinforced concrete required by the MSE wall. In the cantilever system, the concrete stem and base slab are the dominant contributors to embodied carbon, with emission factors exceeding 290 kgCO_2e per cubic metre. In contrast, in the MSE solution, concrete is mainly limited to the thinner precast facing panels. As a result, increasing wall height leads to a progressively larger difference in material demand and, consequently, in environmental impact.

Transport and construction stages also contribute to the total impact, but their relative importance depends on project-specific assumptions such as transport distances, material sources and site operations. For this reason, the tool is intended not only to produce a single comparison value, but also to support sensitivity analyses on key parameters, including concrete emission factors, backfill type, transport distance and end-of-life scenario. The results are consistent with previous comparative LCA studies showing that geosynthetic-based systems can reduce environmental impacts when they replace material-intensive conventional solutions.

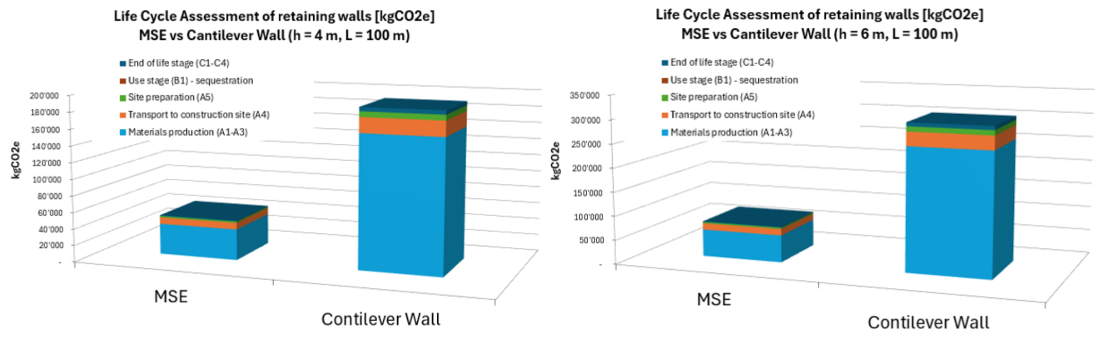

Figure 11: LCA comparison between MSE and Cantilever Wall for two sections (left: 4 m heigh, 100 m long wall; right: 6 m heigh, 100 m long wall).

4 CONCLUSIONS

This study presents an LCA-based tool for comparing MSE walls with conventional cantilever retaining walls under equivalent functional and geotechnical assumptions. The tool calculates total GWP for the wall length defined by the user and can also provide normalised results per metre of wall length. The analysed examples show that MSE solutions can reduce total GWP by approximately 70-85%, mainly due to the reduced use of reinforced concrete. The methodology also highlights the importance of transparent system boundaries, reliable emission factors and sensitivity analyses. Future developments will include further scenarios related to low-carbon concrete, alternative backfills, transport assumptions and end-of-life options.

REFERENCES

Brundtland, G.H.; 1987. *Report of the World Commission on Environment and Development: Our Common Future*. United Nations / Oxford University Press, 1987.

ISO 14040:2006 / ISO 14044:2006. Environmental management – Life cycle assessment – Principles and framework / Requirements and guidelines. International Organization for Standardization.

EN 15804:2012+A2:2019. Sustainability of construction works – Environmental product declarations – Core rules for the product category of construction products. European Committee for Standardization (CEN).

USE OF CLSM (CONTROLLED LOW STRENGTH MATERIAL) AS REINFORCED BACKFILL MATERIAL IN MSE WALL

Raynoos R. Ahmed

VSL Middle East LLC, a member of Bouygues Construction — Dubai, United Arab Emirates
E-mail: raynoos.ahmed@vsl.com, web page: www.vsl.com

Key words: Mechanically Stabilized Earth (MSE), Controlled Low Strength Material (CLSM), Polymeric strip, Reinforced backfill, Sustainable construction.

Abstract. *Mechanically Stabilized Earth (MSE) walls conventionally employ well-graded granular backfill reinforced with steel or polymeric strips to ensure adequate internal and external stability. However, increasing scarcity of high-quality granular materials, stringent compaction requirements, construction constraints in confined urban environments, and the growing emphasis on sustainable infrastructure have prompted the search for alternative reinforced backfill materials. This study investigates the feasibility of using Controlled Low Strength Material (CLSM) as a reinforced backfill material in polymeric strip reinforced MSE wall systems. CLSM is a self-compacting, cementitious flowable fill that eliminates the need for mechanical compaction while providing uniform placement and controlled strength development. A comprehensive review of current design practices, material characteristics, construction methodology, and practical implementation is presented. Laboratory investigations were conducted on a CLSM mixture specifically developed for reinforced backfill applications, achieving a 28-day compressive strength of approximately 2.5–3.0 MPa with a unit weight of 20–21 kN/m³ and a water-to-cement ratio of 2.7. The proposed construction methodology incorporates controlled lift heights of 450 mm to limit temporary hydrostatic pressure on facing panels while allowing progressive hardening between successive placements. Compared with conventional granular backfill, CLSM offers significant advantages including elimination of compaction-induced reinforcement damage, improved panel alignment, complete encapsulation of reinforcement, negligible post-construction settlement, enhanced quality control through plant batching, and reduced construction duration. Although the initial material cost of CLSM is higher, reductions in labour, equipment, inspection, and construction time may result in lower overall project costs. The study demonstrates that CLSM has considerable potential as an alternative reinforced backfill material for MSE walls, particularly in projects with restricted construction access or demanding quality and sustainability requirements. Further experimental and numerical studies are recommended to evaluate long-term soil–reinforcement interaction, lateral earth pressure behaviour, and design provisions for widespread implementation.*

REFERENCES

Controlled Low Strength Materials, Reported by ACI Committee 229 (ACI 229R-99).

33 YEARS OF INSTRUMENTATION EXPERIENCE WITH GEOTEXTILE BASAL REINFORCEMENT

Oliver Detert

HUESKER Synthetic GmbH, 48712 Gescher, Germany
E-mail: detert@huesker.de

Keywords: Basal reinforcement, Geotextile reinforcement, Soft soil, Long-term monitoring, Strain measurement, Embankment stability

Abstract. *This contribution summarizes 33 years of instrumentation experience from the B211 Großenmeer bypass, a road embankment constructed on peat and highly organic silts using a high-strength geotextile basal reinforcement. The project represents an early German application of the surcharge and preloading method in combination with geotextile basal reinforcement for a federal road on very soft organic subsoil. The instrumentation programme was established at a particularly unfavourable section in order to obtain high reinforcement utilization and included strain measurements in the geotextile, settlements, pore water pressures, and groundwater levels. The long-term strain measurements show that the system reached a stable state after approximately four years, with strains near the embankment centre remaining largely constant over the following decades. However, the interpretation of these measurements also demonstrates an important limitation: strain alone does not directly define the actual tensile force or residual load-bearing contribution of the reinforcement. Creep, relaxation, installation damage, chemical influences and changing soil-reinforcement interaction must be considered. The case history therefore provides both evidence of long-term system stability and a critical basis for improved interpretation of instrumented reinforced embankments.*

1 INTRODUCTION

Basal reinforcement with high-strength geotextiles is an established measure for embankments on soft soils. Its main function is to improve short-term stability during construction by mobilizing tensile resistance at the base of the embankment and by reducing shear stresses and lateral spreading in the weak subsoil. In projects on peat, organic silts or other very soft soils, this function is particularly important because the increase in effective stress and undrained shear strength may be delayed by excess pore water pressures during rapid embankment construction.

The B211 Großenmeer bypass provides a rare long-term case history for this application. The road was constructed on a 3 to 5 m thick layer of peat and highly organic silts underlain by Pleistocene sands. The construction method consisted of preloading and surcharge, with a preload height of 4.5 m plus an additional surcharge of 0.9 to 2.3 m. Construction started in 1986 and the road was opened to traffic in autumn 1990. The embankment base reinforcement was a high-strength geotextile product, Stabilenka 400.

Because the project was one of the first German federal road applications of this type on peat, an extensive monitoring programme was implemented. The objective was not only to verify serviceability and stability, but also to improve the understanding of the load transfer mechanism, the consolidation and deformation behaviour of the subsoil and the short- and long-term behaviour of the geotextile reinforcement. After more than three decades, the measurement data provides valuable insight into the reliability and interpretation of instrumented geotextile basal reinforcement systems.

2 PROJECT BACKGROUND AND REINFORCEMENT MECHANISM

The mechanical function of basal reinforcement becomes relevant when the embankment load generates horizontal spreading forces and shear stresses in the soft foundation soil. Without reinforcement, the imbalance of horizontal stresses and the limited undrained shear strength of the subsoil can lead to progressive deformation, local shear failure or global base and slope failure. The reinforcement provides tensile resistance at the embankment base, takes up part of the spreading forces in the slope region. As a result, shear demand in the subsoil is reduced and the stability of the construction stage is improved.

3 INSTRUMENTATION CONCEPT

The instrumentation was installed at a section with particularly unfavourable ground conditions in order to obtain a high utilization of the geotextile and to generate meaningful measurement data. Special displacement transducers were developed for strain measurements on high-strength geotextile fabrics under extreme construction-stage loading. The system used inductive displacement transducers with a measuring range of 20 mm over a base length of 20 cm, corresponding to a maximum measurable strain of 10%. Nine transducers were arranged at 2 m spacing, beginning at the embankment centreline.

The reinforcement measurements were complemented by geotechnical monitoring of the foundation soil. Settlements and pore water pressures were recorded to relate reinforcement strain to the evolving deformation and consolidation process. This combined monitoring concept is essential because the measured strain in the reinforcement is not an isolated material response. It is the result of construction sequence, embankment geometry, subsoil stiffness, consolidation state, reinforcement-soil interaction and the time-dependent behaviour of the polymeric reinforcement.

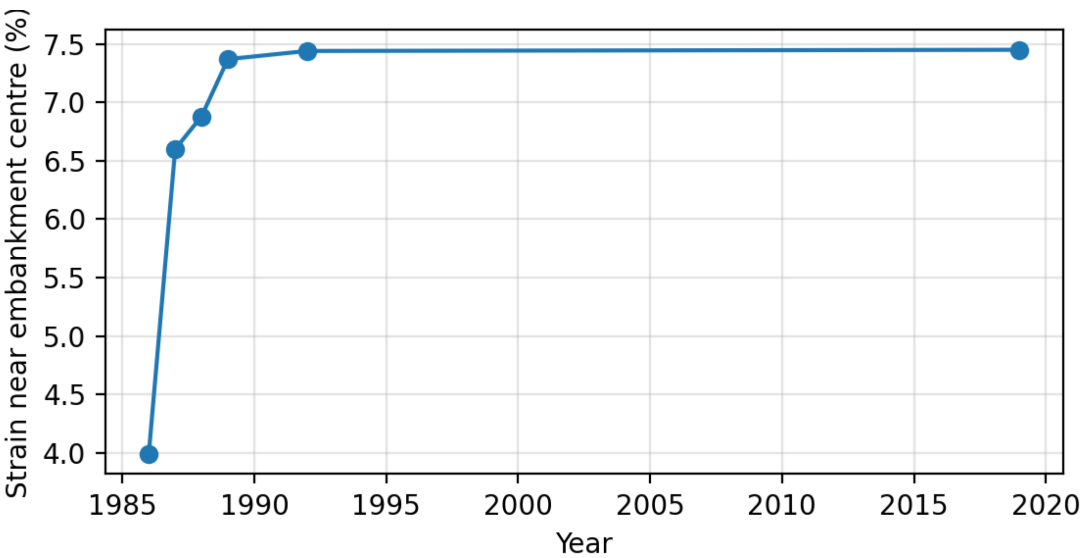

Figure 1: Long-term strain history near the embankment centreline based on selected monitoring values from 1986 to 2019.

4 LONG-TERM MEASUREMENT RESULTS

The strain measurements show the characteristic development of a reinforced embankment constructed with preloading and surcharge on soft organic subsoil. During the early construction and consolidation period, strains increased significantly as the embankment load was applied and the reinforcement mobilized tensile resistance. Near the embankment centreline, the selected strain values increased from approximately 4.0% in 1986 to about 6.6% in 1987 and approximately 7.4% by 1989 to 1992. The measurements from 2019 indicate a value of approximately 7.45%, demonstrating that the deformation state was practically maintained over several decades.

This behaviour supports the conclusion that the reinforced foundation system reached a stable state after approximately four years. Thereafter, no significant additional deformation was observed in the reinforcement. The measured strain state was effectively preserved within the soil-reinforcement system. From an engineering perspective, this is an important positive finding: the system did not show progressive long-term deformation, and the basal reinforcement contributed to a stable embankment structure throughout the monitoring period.

5 INTERPRETATION OF STRAIN, CREEP AND RELAXATION

The case history also illustrates a critical limitation of conventional strain monitoring. A measured geotextile strain cannot be converted directly into a single tensile force without considering the time-dependent behaviour of the polymer and the interaction with the surrounding soil. Geosynthetics are polymeric materials and therefore exhibit viscoelastic and viscoplastic behaviour. Under sustained load, creep may increase strain with time; under constant strain, relaxation may reduce tensile force. The activated tensile force inferred from a short-term load-strain relationship can therefore differ from the force that remains after years or decades at the same measured strain.

The presentation data illustrates this effect by comparing short-term interpretation with creep and relaxation considerations. For a measured strain level of approximately 7.3%, a short-term interpretation indicated an activated tensile force of about 360 kN/m. Consideration of creep over three years reduced the interpreted force to approximately 252 kN/m. After 29 years and with relaxation effects, the interpreted force was approximately 240 kN/m, corresponding to about 60% utilization. Additional interpretation using long-term isochrones indicated that part of the restoring force is lost due to plastic deformation components.

Consequently, strain monitoring is highly valuable for assessing deformation history and system stabilization, but it is not sufficient on its own to quantify the current load-bearing contribution or residual capacity of the reinforcement. Installation damage, chemical reactions such as hydrolysis, creep, relaxation, the changing stiffness and strength of the subsoil and the degree of soil-geotextile interaction all influence the interpretation. For future instrumented projects, direct force measurement in geosynthetic reinforcement would provide an important additional basis for quantitative assessment.

6 CONCLUSIONS

The B211 Großenmeer bypass represents an exceptional long-term case history of geotextile basal reinforcement on soft organic soil. The 33-year monitoring record demonstrates that the reinforced embankment system reached a stable deformation state after approximately four years and that the measured reinforcement strains remained largely constant over the following decades. This confirms the long-term stability of the system and supports the use of high-strength geotextile basal reinforcement for embankments constructed on very soft subgrades.

At the same time, the case history provides an important methodological lesson. Strain measurements alone do not allow a direct conclusion regarding the actual tensile force, the residual load-bearing contribution or the remaining safety margin of the reinforcement. The measured strain is preserved by the soil-reinforcement system, while the corresponding force may change due to creep, relaxation and other time-dependent processes. A scientifically sound interpretation therefore requires consideration of polymer behaviour, installation damage, chemical durability, subsoil consolidation and soil-reinforcement interaction.

The experience from Großenmeer underlines the value of long-term instrumentation for validating design assumptions and improving the understanding of reinforced embankments. Future monitoring concepts should combine deformation measurements with direct or indirect force measurements wherever possible. This would allow a more reliable quantification of the reinforcement contribution and support more robust design approaches for geotextile basal reinforcement on soft soils.

BASAL REINFORCEMENT DESIGN FOR PILED EMBANKMENTS: A PARAMETRIC COMPARISON BETWEEN ANALYTICAL APPROACHES AND NUMERICAL MODELLING.

Oltion Korini [1] **Mara St. Clair** [1]

[1]Geoquest Company, 280 avenue Napoleon Bonaparte, 92500 Rueil-Malmaison, France

Abstract. *Geosynthetics are commonly used to stabilize soil structures such as piled embankments. Several analytical design methods, based on differing assumptions, often yield contrasting results. A parametric study is carried out on hypothetical piled embankment configurations and the results from three analytical design guidelines (BS8006-1, CUR226 and LDC) are compared with three-dimensional (3D) numerical models using FLAC3D. Pile spacing and embankment height are varied while the soil, geosynthetic reinforcement and pile properties remain constant. The results show that CUR226 closely agrees with the numerical results, whereas BS8006-1 and LDC are notably more conservative.*

1 OBJECTIVES

This study compared three analytical approaches for basal reinforcement design:

- BS8006-1
- CUR226
- Load Displacement compatibility (LDC)

The analytical predictions of each model were compared with three-dimensional numerical modelling performed with FLAC3D. The numerical models clarified the load transfer mechanisms and basal reinforcement activation in both transverse and longitudinal directions.

2 METHODOLOGY

A series of hypothetical piled embankment configurations were evaluated parametrically. The study focused on the influence of two geometric parameters that control the behavior of the system:

- embankment height and
- pile spacing

Other characteristics, such as foundation and embankment soil properties, pile properties and geosynthetic reinforcement properties, were kept constant.

3 ANALYTICAL COMPARISON

- Each analytical method produced substantially different predictions for maximum geosynthetic tension, strain and settlement.
- Of the three methods assessed, CUR 226 gave the closest agreement with mobilized tension in the FLAC3D model in the cases studied.
- Pile spacing strongly influenced the required reinforcement tensile strength due to changes in the span to be supported by the geosynthetic.
- Embankment height influenced load transfer by changing the applied vertical load and arching behavior within the fill.

4 NUMERICAL MODELLING

The FLAC3D results showed that soil arching was more clearly observed in the transverse direction than in the longitudinal direction and therefore, the geogrid mobilization was not uniform in both reinforcement directions. These observations suggest that the assumptions of the analytical models may not fully capture longitudinal load-transfer effects or that construction sequences and boundary conditions of the model limit the deformation that may be experienced in the field.

5 CONCLUSIONS

This study confirms that the selection of an analytical design method strongly influences the estimated geosynthetic reinforcement requirements.

CUR 226 provided the closest agreement with FLAC3D for the analyzed hypothetical cases and therefore offers a valuable preliminary prediction of the reinforcement required for similar case conditions.

Further validation using field monitoring data is necessary to strengthen the basis for applying the most representative analytical method for design in practice.

ENHANCING RAILWAY BALLAST PERFORMANCE THROUGH RECLAIMED MATERIALS AND INNOVATIVE GEOSYNTHETIC CONFINEMENT

Stanislav Lenart[1], Siva R. Karumanchi [1]

[1] I Slovenian National Building and Civil Engineering Institute (ZAG), Dimičeva 12, SI-1000 Ljubljana, Slovenia

E-mail: stanislav.lenart@zag.si, web page: https://www.zag.si/en

Key words: ballast, railway track, geosynthetics, confining pressure, small-scale test

Abstract. *Insufficient effective confining pressure within the ballast layer can lead to the permanent rotation of grains, causing increased wear and abrasion. Augmenting confinement may not only mitigate ballast degradation but also enhances overall performance of the track. The increased confining pressure causes the increase of ballasted track stiffness and reduction of resilient as well as permanent deformation. This paper outlines the development of a cost-effective solution aimed at boosting ballast layer confinement without disrupting maintenance procedures. It involves incorporating specific secondary raw material elements along the track shoulder, combined with a horizontal geosynthetic reinforcing layer at the base of the ballast layer. These shoulder elements not only impact the track's geometry but also facilitate a reduction in required ballast volume. The efficacy of the ballast confinement mechanism has undergone small-scale testing as well as large scale testing to prove the concept of reinforcement. Numerical modelling has played a crucial role in supporting the optimal design of this solution.*

1 INTRODUCTION

Ballasted railway tracks are widely used because of their simple construction and favorable damping & drainage characteristics. However, ballast degradation, settlement, and lateral spreading caused by insufficient confinement remain major challenges affecting track performance and maintenance requirements (Prasad and Hussaini, 2022; Guo et al., 2022). Since ballast behavior is strongly influenced by lateral confinement, numerous reinforcement techniques, including geosynthetics, geocells, geosynthetic bags, and shoulder reinforcement systems, have been developed to improve track stability and reduce permanent deformation (Leshchinsky and Ling, 2013; Biabani et al., 2016; Kachi et al., 2010). Enhanced confinement becomes particularly important when reclaimed ballast or rubber-modified ballast materials are used, as these materials may exhibit reduced shear strength despite their environmental benefits (Indraratna et al., 2017; Gong et al., 2019; Guo et al., 2022; Lenart and Karumanchi, 2025). This paper presents a sustainable ballast confinement concept combining prefabricated shoulder elements mechanically coupled by a horizontal geosynthetic layer to increase effective confinement, improve track stability, and facilitate the use of reclaimed ballast materials (Lenart et al., 2026).

2 CONCEPT OF THE BALLAST CONFINEMENT SYSTEM

In conventional ballasted railway tracks, resistance to lateral deformation is provided primarily by the ballast shoulders. Under repeated train loading, ballast particles tend to spread laterally, resulting in a gradual loss of confinement and the accumulation of permanent deformation.

The proposed confinement concept addresses this challenge by introducing light structural shoulder elements on either side of the ballast layer. These elements are mechanically interconnected at the top and bottom through a planar geosynthetic layer placed at the ballast–subgrade interface, to prevent sliding and overturning respectively (Fig. 1). The geosynthetic layer acts as a tensile tie between the shoulder elements, enabling lateral forces generated within the ballast to be transferred and resisted by the structural shoulders (Lenart et al., 2026).

The proposed mechanism is particularly beneficial for railway tracks incorporating secondary, recycled, or otherwise modified ballast materials, whose mechanical performance may be inferior to that of conventional fresh ballast. By providing additional confinement, the system can mitigate excessive lateral deformation and contribute to maintaining long-term track geometry and performance.

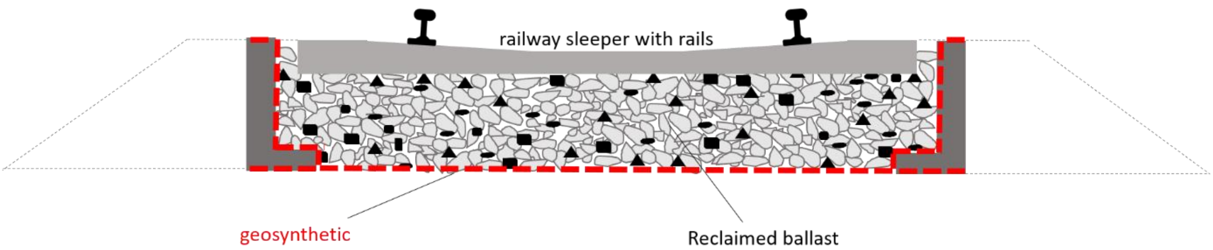

Figure 1: Conceptual illustration of the proposed ballasted track system with shoulder confinement elements and horizontal geosynthetic coupling.

3 EXPERIMENTAL PROGRAM

A small-scale physical model was initially developed to verify the proposed confinement concept, in which the ballast shoulder elements were mechanically coupled by a geosynthetic layer fixed to both the top and bottom of the shoulders. The tests demonstrated that the geosynthetic connection effectively restricted lateral movement and rotation of the shoulder elements. Based on these findings, finite element modelling was subsequently performed to optimize the geometry of the shoulder elements and the mechanical properties of the geosynthetic and other system components (Lenart et al., 2026). The optimized design was then validated through large-scale laboratory testing under cyclic railway loading. The response of proposed ballasted track system with shoulder confinement elements was compared with conventional ballasted track. Reduced settlements, improved stability, and enhanced lateral confinement were confirmed in case of proposed solution compared with a conventional ballasted track. Finally, the new proposed system was named as CIRTRACK and it was demonstrated under field conditions, providing practical evidence of its feasibility and effectiveness for railway applications (Lenart et al., 2026).

4 RESULTS AND DISCUSSION

4.1 Mechanical improvements

The results demonstrate that the proposed ballast confinement system can significantly improve the mechanical performance of ballasted railway track. The key mechanism is the mechanical coupling of both ballast shoulders through the geosynthetic layer. This coupling limits lateral spreading of the ballast and mobilizes additional confining pressure within the ballast layer. Fig. 2 presents the horizontal pressure in ballast in the longitudinal and transverse directions. It is of similar range for proposed CIRTRACK ballasted track system with shoulder confinement elements, where for conventional in transverse direction pressure is significantly smaller.

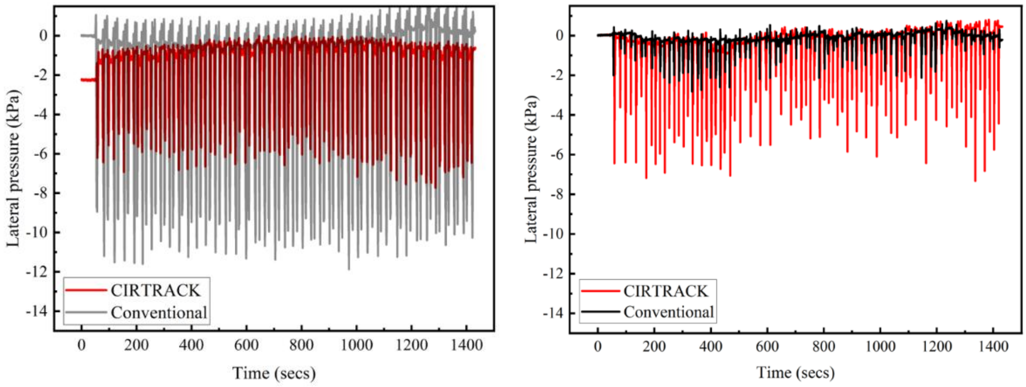

Figure 2: In field measured horizontal pressure in ballast in the longitudinal (left) and transverse (right) directions under 10 kN/axle traffic loading.

4.2 Sustainability

The investigation of reused ballast blended with tire-derived aggregates adds an important sustainability dimension to the proposed system. Reused ballast promotes the circular use of railway materials, while recycled rubber particles can enhance damping capacity and reduce ballast degradation. The most favorable performance was achieved for mixtures containing approximately 5% tire-derived aggregates by mass. At this content, the rubber particles increased energy dissipation and mitigated particle breakage without significantly compromising stiffness (Lenart and Karumanchi, 2025). However, the reduced shear strength of such reclaimed materials may lead to excessive lateral deformation and settlement when used in conventional ballasted track structures. By providing enhanced lateral confinement, the proposed CIRTRACK system enables the effective use of reclaimed ballast materials, including rubber-modified mixtures, under demanding railway traffic conditions while maintaining satisfactory track performance and stability.

5 CONCLUSIONS

Research showed that geosynthetic coupling enhances ballast confinement, reduces lateral deformation, and improves track stability under cyclic loading even in the case of reclaimed ballast material. Numerical analyses proved valuable for optimizing the geometry and mechanical characteristics of the system, while experimental testing confirmed its effectiveness in limiting settlement and maintaining elevated lateral pressure within the ballast layer.

6 ACKNOWLEDGEMENTS

This research was supported by the EU's Horizon Europe program, project LIAISON, grant No. 101103698, and by the Slovenian Research and Innovation Agency (ARIS) Program group P2-0273 and project L2-60150: BAST.

REFERENCES

Biabani, M.M., Ngo, N.T. and Indraratna, B., 2016. Performance evaluation of railway subballast stabilised with geocell based on pull-out testing. Geotextiles and Geomembranes, 44, 579–591. https://doi.org/10.1016/j.geotexmem.2016.03.006

Gong, H., Song, W., Huang, B., Shu, X., Han, B., Wu, H. et al., 2019. Direct shear properties of railway ballast mixed with tire-derived aggregates: Experimental and numerical investigations. Construction and Building Materials, 200, 465–473. https://doi.org/10.1016/j.conbuildmat.2018.11.284

Guo, Y., Xie, J., Fan, Z., Markine, V., Connolly, D.P. and Jing, G., 2022. Railway ballast material selection and evaluation: A review. Construction and Building Materials, 344, 128218. https://doi.org/10.1016/j.conbuildmat.2022.128218

Indraratna, B., Sun, Q. and Grant, J., 2017. Behaviour of subballast reinforced with used tyre and potential application in rail tracks. Transportation Geotechnics, 12, 26–36. https://doi.org/10.1016/j.trgeo.2017.08.006

Kachi, T., Kobayashi, M., Seki, M. and Koseki, J., 2010. Evaluation tests of ballasted track reinforced with geosynthetic bags. In: Proceedings of the 9th International Conference on Geosynthetics, Brazil, 1499–1502.

Lenart, S. and Karumanchi, S.R., 2025. Deformation properties and performance evaluation of reused ballast with waste tire-derived aggregates. Transportation Geotechnics, 52, 101586. https://doi.org/10.1016/j.trgeo.2025.101586

Lenart, S., Karumanchi, S.R. and Garcia Sanchez, D., 2026. Novel use of geosynthetics to increase the confinement of railway track ballast layer. Proceedings of the 13th International Conference on Geosynthetics (submitted).

Le Pen, L.M. and Powrie, W., 2011. Contribution of base, crib and shoulder ballast to the lateral sliding resistance of railway track: a geotechnical perspective. Proceedings of the Institution of Mechanical Engineers, Part F: Journal of Rail and Rapid Transit, 225(2), 113–128. https://doi.org/10.1177/0954409710397094

Leshchinsky, B. and Ling, H.I., 2013. Numerical modeling of behavior of railway ballasted structure with geocell confinement. Geotextiles and Geomembranes, 36, 33–43. https://doi.org/10.1016/j.geotexmem.2012.10.006

Prasad, K.V.S. and Hussaini, S.K.K., 2022. Review of different stabilization techniques adapted in ballasted tracks. Construction and Building Materials, 340, 127747. https://doi.org/10.1016/j.conbuildmat.2022.127747

IGS: Soil Reinforcement (TC-R):
https://www.geosyntheticssociety.org/council-committees/technical-committees/soil-reinforcement/

ISSMGE: Reinforced Fill Structures (TC-218):
https://www.issmge.org/committees/technical-committees/applications/reinforced-fill-structures